

# VISUOHAPTIC SIMULATION OF A BORESCOPE FOR AIRCRAFT ENGINE INSPECTION

---

A Dissertation  
Presented to  
the Graduate School of  
Clemson University

---

In Partial Fulfillment  
of the Requirements for the Degree of  
Doctor of Philosophy  
Computer Science

---

by  
Deepak S. Vembar  
December 2009

---

Accepted by:  
Andrew T. Duchowski, Committee Chair  
Robert M. Geist, III  
Anand K. Gramopadhye  
Donald H. House

# Abstract

Consisting of a long, fiberoptic probe containing a small CCD camera controlled by handheld articulation interface, a video borescope is used for remote visual inspection of hard to reach components in an aircraft. The knowledge and psychomotor skills, specifically the hand-eye coordination, required for effective inspection are hard to acquire through limited exposure to the borescope in aviation maintenance schools. Inexperienced aircraft maintenance technicians gain proficiency through repeated hands-on learning in the workplace along a steep learning curve while transitioning from the classroom to the workforce.

Using an iterative process combined with focused user evaluations, this dissertation details the design, implementation and evaluation of a novel visuohaptic simulator for training novice aircraft maintenance technicians in the task of engine inspection using a borescope. First, we describe the development of the visual components of the simulator, along with the acquisition and modeling of a representative model of a PT-6 aircraft engine. Subjective assessments with both expert and novice aircraft maintenance engineers evaluated the visual realism and the control interfaces of the simulator. In addition to visual feedback, probe contact feedback is provided through a specially designed custom haptic interface that simulates tip contact forces as the virtual probe intersects with the 3D model surfaces of the engine. Compared to other haptic interfaces, the custom design is unique in that it is inexpensive and uses a real borescope probe to simulate camera insertion and withdrawal. User evaluation of this simulator with probe tip feedback suggested a trend of improved performance with haptic feedback.

Next, we describe the development of a physically-based camera model for improved behavioral realism of the simulator. Unlike a point-based camera, the enhanced camera model simulates the interaction of the borescope probe, including multiple points of contact along the length of the probe. We present visual comparisons of a real probe's motion with the simulated probe model and develop a simple algorithm for computing the resultant contact forces. User evaluation comparing our custom haptic device with two commonly available haptic devices, the Phantom Omni and the Novint Falcon, suggests that the improved



camera model as well as probe contact feedback with the 3D engine model plays a significant role in the overall engine inspection process.

Finally, we present results from a skill transfer study comparing classroom-only instruction with both simulator and hands-on training. Students trained using the simulator and the video borescope completed engine inspection using the real video borescope significantly faster than students who received classroom-only training. The speed improvements can be attributed to reduced borescope probe maneuvering time within the engine and improved psychomotor skills due to training. Given the usual constraints of limited time and resources, simulator training may provide beneficial skills needed by novice aircraft maintenance technicians to augment classroom instruction, resulting in a faster transition into the aviation maintenance workforce.

# Acknowledgments

I greatly appreciate the advice and support of all those who helped me over the course of my graduate studies at Clemson. First and foremost, I would like to thank my advisor, Andrew Duchowski. Over the past six years, Dr. Duchowski has had a great influence on my research, helping me determine my dissertation topic and providing constructive feedback at every step of implementing and testing the borescope simulator. His experience and assistance in reviewing and editing my publications, very often at short notice, is greatly appreciated. I would also like to thank Anand Gramopadhye for providing useful feedback during the design of my human subject experiments. My time spent working with Dr. Duchowski and Dr. Gramopadhye will have a strong influence on my future for many years to come. I would also like to thank my committee members, Dr. Geist and Dr. House, for their feedback on methods to improve the visual fidelity and behavior of the borescope simulator.

This dissertation would not have been possible without the support and assistance from Carl Washburn, the Dean of Aircraft Maintenance Program at Greenville Technical College, the faculty and students in the AMT program. I would like to thank my fellow research group members, Sajay Sadasivan, Paris Stringfellow, Thashika Rupasinghe, Melissa Paul and Nathan Cournia who worked on various research projects with me, helping me understand complex ideas and putting up with endless arguments about user testing scenarios. I also thank the students, faculty and staff in the Industrial Engineering department, especially Sandra Holland, Mary Beth Kurz, Mark McElreath, Kapil Chalil and Inderneel Dabhade. Additional thanks to my fellow grad students at Clemson, especially David Braganza and Apoorva Kapadia, for providing useful distractions from research. I would also like to thank the engineering team at Hansen Medical, especially Chris Sewell, Federico Barbagli, Neal Tanner, Chris Carlson and Francois Conti for ideas in implementing the probe model.

This dissertation work was supported through two generous research grants from the National Science Foundation. Financial support to attend IEEE regional conference from the Graduate School at Clemson is gratefully acknowledged. I would also like to thank the anonymous reviewers at 3DUI and GI, for their

constructive criticism that helped improve the publications related to this dissertation.

Finally, I am forever grateful for the love and support of my mother, Rekha Vembar, my late father, Shashidhar Vembar, my sister and other family members.

# Table of Contents

<b>Title Page</b> . . . . .	<b>i</b>
<b>Abstract</b> . . . . .	<b>ii</b>
<b>Acknowledgments</b> . . . . .	<b>iv</b>
<b>List of Tables</b> . . . . .	<b>viii</b>
<b>List of Figures</b> . . . . .	<b>ix</b>
<b>1 Introduction</b> . . . . .	<b>1</b>
1.1 Motivation . . . . .	1
1.2 Contributions . . . . .	3
1.3 Dissertation Organization . . . . .	3
<b>2 Borescope Inspection: Overview</b> . . . . .	<b>5</b>
2.1 Comparison with Minimally Invasive Medical Procedures . . . . .	6
2.2 Inspection Process . . . . .	8
<b>3 Simulator Development</b> . . . . .	<b>12</b>
3.1 Prior Work . . . . .	12
3.2 Engine Model Acquisition . . . . .	14
3.3 Graphical Rendering and User Controls . . . . .	16
3.4 Experiment 1: Visual Fidelity Evaluation . . . . .	17
3.5 Experiment 2: Control Interfaces Evaluation . . . . .	22
<b>4 Development of a Haptic Interface</b> . . . . .	<b>28</b>
4.1 Prior Work . . . . .	28
4.2 Building the Haptic Box . . . . .	30
4.3 Experiment 3: User Evaluation of Haptic Box . . . . .	35
<b>5 Physically-based Probe Model</b> . . . . .	<b>43</b>
5.1 Prior work . . . . .	44
5.2 Implementation . . . . .	46
<b>6 Empirical Evaluation: Camera Model and Haptic Interfaces</b> . . . . .	<b>56</b>
6.1 Experiment 4: Evaluation of Camera Constraints . . . . .	56
6.2 Experiment 5: Haptic Interfaces Evaluation . . . . .	62
<b>7 Contact Detection and Response</b> . . . . .	<b>72</b>
7.1 Improving Intersection Response . . . . .	74
7.2 Multi-contact Force Feedback . . . . .	76

7.3	Experiment 6: Comparison of Probe Model . . . . .	78
<b>8</b>	<b>Evaluating Skills Transfer . . . . .</b>	<b>84</b>
8.1	Experiment 7: Inspection Performance Evaluation . . . . .	84
<b>9</b>	<b>Conclusion . . . . .</b>	<b>94</b>
	<b>Bibliography . . . . .</b>	<b>96</b>

# List of Tables

3.1	Subjective questionnaire for subjective evaluation of visual fidelity of the borescope simulator. Responses were on a 7-point Likert scale, with 1-Strongly disagree, 4-Neutral and 7-Strongly agree. . . . .	20
3.2	Key mapping for the three different interfaces . . . . .	24
3.3	Subjective questionnaire for subjective evaluation of the three control interfaces of the borescope simulator. Responses were on a 5-point Likert scale, with 1-Strongly disagree, 3-Neutral and 5-Strongly agree. . . . .	25
4.1	Components used in the Haptic feedback device. . . . .	31
4.2	Subjective questionnaire for evaluation of haptic interface. . . . .	40
6.1	Subjective questionnaire. . . . .	68

# List of Figures

2.1	Two different types of video borescopes: XL PRO™Plus VideoProbe from Everest, and The IPLEX Borescope from Olympus. . . . .	6
2.2	Cross-section of borescope tip. . . . .	7
2.3	Articulation of borescope tip. . . . .	7
2.4	Medical endoscope. . . . .	7
2.5	Close-up view of endoscope tip. . . . .	7
2.6	Inspection of aircraft components using the video borescope. . . . .	10
2.7	The video borescope’s articulating tip and the turbine inspection process. . . . .	10
3.1	Actual and modeled engine sections (left, right) of stator (top) and rotor blades (bottom). . .	15
3.2	Visual output from the actual borescope (left) and our simulator (right). . . . .	16
3.3	Orientation and translation control of the virtual camera with the directional pad and buttons (1 and 4) on the gamepad. . . . .	17
3.4	Visual output from the virtual borescope and user controls via the gamepad. . . . .	17
3.5	Inspection scenario (from left to right): top and side views inside the engine casing, with guide tube exit positioned just above the stator; braided textured cylinder illustrates the typical path of the simulated borescope through the stator to its position during turbine (rotor) blade inspection. Once in position, the task mainly consists of rotating the turbine to visually inspect each of its blades. Note that the user never sees this external viewpoint—the user’s only viewpoint is from the tip of the borescope. . . . .	19
3.6	Average participant responses to the Presence Questionnaire evaluating visual fidelity on a 7-point Likert scale, with 1-strongly disagree, 4-neutral and 7-strongly agree. . . . .	21
3.7	Output of the simulator with numbered arrows denoting direction of inspection. . . . .	24
3.8	Average time to task completion among the three control interfaces. . . . .	26
4.1	Top view of the feedback device with mouse and guide tube, with probe entry at left (the haptic component has been removed to show the guide tube into which the probe is inserted). . .	31
4.2	Haptic feedback interface with motors installed. . . . .	32
4.3	Sailing cam cleat with spring-loaded cams (Ronstan, Australia) prior to its refurbishment for the simulator (left); following its attachment to the servo motors (right). . . . .	32
4.4	Motor operation with the motorized cam cleat (direction of insertion is up). Note that once clamped, further insertion is prevented, however, retraction of the probe is still possible. . .	34
4.5	Experimental setup. . . . .	36
4.6	Speed comparison between conditions and subjects: Visual (V), Visual and Haptic (V+H). . .	39
4.7	Subjective impressions (average) regarding system use. Users’ responses were made on a 5-point Likert scale corresponding to agreement with the questionnaire statements (1:strongly disagree, ..., 5:strongly agree) listed in Table 4.2. . . . .	39
5.1	Representation of the linear chain of nodes used to model the borescope probe. Each adjacent pair of nodes is connected by a set of linear and angular springs. . . . .	47
5.2	Linear elongation due to spring between two adjacent nodes of the probe. . . . .	48

5.3	Angular response due to flexion and torsion, resulting in bending and articulation of the probe in planar space. . . . .	49
5.4	Single point contact with position of Haptic Interface Point (HIP) and proxy position. . . .	50
5.5	Simulation of probe model with multiple points of contact, calculated by taking into account the dynamic model of mass-spring system and point-proxy HIP forces. . . . .	51
5.6	Interaction of the virtual probe with a rigid surface. The point proxies constrain the nodes to the surface of the cube and cause deformation of the virtual probe. . . . .	53
5.7	Multiple points of contact of the probe nodes with the rigid object. . . . .	54
6.1	Visualization of the virtual borescope's articulation. This view is never seen by the user, instead, the user's viewpoint is from the probe's tip. . . . .	57
6.2	Actual borescope control (left) and gamepad with button mapping (right) used with borescope simulator. . . . .	58
6.3	Camera navigation through two sets of fixed stator blades (left and center) with the goal of positioning the probe camera at the engine rotor for inspection of 5 rotor blades (right, see Figure 6.4 for inspection details). . . . .	59
6.4	Visual inspection of rotor blade. Inspectors are trained to inspect the rotor in clockwise order, first inspecting the front face (left), then advancing the probe forward and rotating the probe tip to inspect the back face (right). Next, the entire rotor is rotated by pressing the turbine rotation gamepad button. Arrows are shown here for clarity, they were not presented to participants. . . . .	60
6.5	Mean completion times per camera interface. . . . .	61
6.6	Mean collisions per camera interface. . . . .	62
6.7	Operational evaluation of (from left to right) the Haptic box, Falcon and Phantom Omni interfaces with the borescope simulator. . . . .	64
6.8	Mean search times per interface. . . . .	66
6.9	Mean hits per interface. . . . .	66
6.10	Responses to subjective questionnaire. . . . .	68
7.1	Intersection of the probe with edges of objects leading to jitter in the position of the virtual camera. . . . .	73
7.2	Use of additional proxy nodes to improve intersection response. . . . .	75
7.3	Computation of forces along the probe length with multiple points of contact. . . . .	77
7.4	Top-view of apparatus designed to simulate feed and interaction of borescope probe with engine blade. . . . .	79
7.5	Starting position of the borescope probe in the experiment (left) and modeled simulation environment with the virtual probe (right). . . . .	79
7.6	Sliding intersection of the probe with the engine (left) and simulated results (right). . . . .	80
7.7	Contact detection along the body of the borescope probe (left) and simulated results (right). . . . .	81
7.8	Intersection response at 30° angle of incidence (left) and simulated results (right). . . . .	81
7.9	Intersection response with probe tip articulated to 60° (left) and simulated results (right). . . .	82
7.10	Intersection response with guide tube 3" from the blade (left) and simulated results (right). . .	82
8.1	Inspection of PT-6 aircraft engine using borescope (left) and operator view of the camera output on the screen (right). . . . .	86
8.2	Average time taken to insert, maneuver, inspect and withdraw the borescope from the test engine, grouped by type of training provided. . . . .	89
8.3	Time taken for simulated inspection and total number of virtual probe camera hits with the engine model evaluated at the end of training on day 1 and 2. . . . .	89
8.4	Average time taken for maneuvering the borescope through the engine between the stators. . .	91



# Chapter 1

## Introduction

In aircraft maintenance, visual inspection is an important part of non-destructive testing [4] accounting for almost 80% of planned maintenance inspection in large aircraft [14]. Due to minimal equipment costs, visual inspection is usually the quickest and most economical way to obtain a preliminary evaluation of the condition of an aircraft [13]. Regular visual inspection by experienced maintenance technicians ensures timely detection of critical defects and airworthiness of an aging aircraft fleet.

Visual inspection of easily accessible regions of an aircraft such as cargo bay and fuselage require simple equipment, such as a flashlight and magnifying glass. Enclosed components, such as an aircraft engine, present a challenge as the parts are not easily accessible without a complete teardown of the equipment. To enable a technician to inspect an area that is inaccessible by other means, a device known as a borescope is used. A borescope is an optical device consisting of a rigid or flexible tube with an eyepiece or video screen at one end and a miniaturized camera or lens system on the other end. The two components are linked together by a fiber optic cable which carries a video signal and serves to illuminate the engine component under inspection.

### 1.1 Motivation

Although borescopes have been in use by aircraft engine mechanics for many years, the training required to operate and master these tools is expensive and lacks standardization. While there are standards and regulations that govern aircraft maintenance in general, none provide detailed information on borescope training. The American Society for Nondestructive Testing (ASNT) is recognized for its leading role in main-

taining regulations for Non-Destructive Inspection (NDI) training. Currently, the ASNT only provides a brief introduction to borescopes in levels I and II of their visual testing curriculum [5, 6]. While the ASNT requires a written examination, a hands-on test, and experience to become qualified for NDI inspection, it does not provide any standards by which borescope inspectors can become qualified. The American Federal Aviation Association (FAA) engine certification program, which details individual engine certification requirements for aircraft engine technicians, only refers to engine manufacturers' instructions for borescope usage [63]. Although the FAA provides a general overview of borescope use, it lacks detail and standardization in the area of borescope inspection training. Technical colleges which provide training to students expecting to have careers in aircraft maintenance thus have varying guidelines and procedures to follow.

Current borescope inspection training in technical colleges is limited to a few courses on general engine and airframe inspection, with very little hands-on experience with the actual device. The costs of new generation video borescopes are prohibitively high for all but the largest of technical schools. On-the-job training at the workplace by shadowing an expert inspector is the only feasible option to obtaining experience working with the borescope. Aircraft maintenance technicians graduating from technical colleges face a steep learning curve while transitioning from the classroom to the workforce. An aging workforce of experienced inspectors combined with inexperience of new inspectors joining the aviation maintenance industry could cause maintenance errors with catastrophic results. There is a substantial need for improved training methods to augment classroom learning to provide basic skills in borescope usage.

Computer simulators have been used in a variety of fields, most notably in the medical community, to improve competency of novice participants and provide simulated task training. Medical simulators for pre-operative path planning [53], medical procedures such as laparoscopy [23], endoscopy [7] and mastoidectomy [1] have been developed and evaluated to examine their efficacy in training resident doctors in these complex operating procedures. Follow up studies of simulator trained participants have shown improvements in task performance in the simulator as well as the real world.

In keeping with the use of simulator training to augment classroom learning and improve task preparedness, this dissertation presents the development and user evaluation of a virtual borescope simulator with visual and haptic feedback to improve student outcomes from a representative aircraft maintenance school. Unlike unaided visual inspection, the borescope provides indirect visual feedback of the component under inspection through the camera output on the video screen and is a suitable candidate for realistic visual simulation.

## 1.2 Contributions

The primary contribution of the dissertation is the development of a novel simulator for training borescope inspection using visually realistic 3D models of engine components, along with quantitative metrics to evaluate the speed and accuracy parameters that are beneficial in providing feedback to novice users. We are unaware of any previous work specifically related to aviation inspection training using the borescope, except the hands-on learning with the actual device that is usually provided by borescope and engine manufacturers.

In addition to purely visual feedback, the second contribution is the development of a simple haptic interface for provision of borescope probe contact response to the users. Off-the-shelf solutions for providing haptic response are expensive, provide only single point contact response and are stylus-based. As the interaction with the simulation is through a pen-like manipulator, these devices are not very well suited for a task such as probe insertion.

Probe motion through an actual engine is an important skill that is hard to teach effectively in the classroom. We present a behaviorally realistic probe model building on prior work in multi-point collision detection and response, with particular emphasis on fast update rates needed for realistic haptic feedback. Integration of the probe model with the simulator provides novice users the camera articulation control training needed to prevent damage to the borescope probe tip. In addition, we develop a simple algorithm to calculate the contact forces along the length of the probe, and compare the interaction of the simulated probe with a real borescope probe.

The final contribution is a report on an evaluation of the simulator training with actual students in an aircraft maintenance program. There is a limited understanding of task performance and transfer effects of simulator training with real participants. Our evaluation study shows that the psychomotor skills needed to maneuver the borescope through the engine can be successfully taught to students through repeated exposure to the borescope simulator and that the performance improvement gained by this experience is not significantly different from hands-on training with the real borescope.

## 1.3 Dissertation Organization

The dissertation is organized as follows. We provide an introduction to the borescope inspection procedure, as it is used in engine overhaul, in Chapter 2. The development of the visual aspects of the sim-

ulator is presented in Chapter 3, along with results of the visual fidelity and user interface studies performed with experienced borescope inspectors. Chapter 4 outlines the development of a simple, cost-effective haptic interface suited to borescope inspection task along with results from user evaluations.

Improvements to the behavioral realism of the simulator by implementing a physically-based model of the borescope probe are detailed in Chapter 5. We present results evaluating the usability of this model in Sections 6.1 and 6.2. Improvements to the camera model are presented in Chapter 7, and we follow up with a comparison of the behavior of the real borescope probe in Section 7.3. We present the results from the skill transfer studies comparing the task performance of novice aircraft maintenance technicians trained on the simulator with those receiving training using the actual video borescope in Chapter 8, and conclude with a summary and directions for future work in Chapter 9.

## Chapter 2

# Borescope Inspection: Overview

Borescope inspection in the aviation field is an essential Non-Destructive Inspection (NDI) procedure used to examine aircraft components for defects. It is usually performed in an area or enclosure that is not easily accessible without a complete tear-down of the equipment. Inspection of an aircraft engine, for example, is a common borescope task performed to prevent potentially costly dismantling of the engine. Aircraft turbine engines have access ports that are specifically designed for borescopes. Borescopes are also used extensively in a variety of aviation maintenance procedures to determine the airworthiness of difficult-to-reach components.

Borescopes are long, tubular, precision optical instruments with built-in illumination, designed to allow visual inspection of internal surfaces or otherwise inaccessible areas. The tube, which can be rigid or flexible with a wide variety of lengths and diameters, provides the necessary optical connection between the viewing end and an objective lens at the distant, or distal tip of the borescope. Borescopes are available in different designs for a variety of standard applications and manufacturers also provide custom designs for specialized applications. In this document, a borescope is assumed to mean a video borescope: an instrument with a flexible fiber-optic probe that uses a video screen for image output as opposed to the optical borescope which uses an eyepiece instead.

A video borescope (Figure 2.1) consists of a base unit with an attached monitor, a flexible fiber-optic probe with a CCD camera and a hand-held interface for controlling the articulation of the probe tip. The base unit consists of a light source, a video processing unit to manipulate the video feed from the camera, and memory card slots for storing captured images. Similar devices, called endoscopes, have been used in the medical field for surgical path planning and minimally invasive surgical procedures.



**Figure 2.1:** Two different types of video borescopes: XL PRO™Plus VideoProbe from Everest, and The IPLEX Borescope from Olympus.

The probe consists of a magnifying CCD camera attached to the tip that transmits the images through the optical fibers to the base unit (Figure 2.2). Optic fiber is used to transmit light from the base unit to illuminate the internal components being inspected. The probe tip can be articulated with the control interface, and can rotate almost 180 degrees about its pivot. The entire probe is enclosed in a braided metallic sheath to prevent damage to the fragile optical fiber.

The control interface is a light, one-handed device possessing a mini-joystick that is used to control the articulation of the probe tip, as shown in Figure 2.3. Buttons on the interface allow the inspector to take screen captures of the video, record live video for off-line analysis, freeze the articulation of the probe, and compare the size of the defects encountered during the inspection process.

## 2.1 Comparison with Minimally Invasive Medical Procedures

Minimally invasive surgery such as endoscopy or colonoscopy use the endoscope (Figure 2.4) which is inserted into the human body to search for lesions and cancerous tumors. Conceptually, the borescope is similar to the medical endoscope, a long catheter with an integrated imaging device at its tip. The borescope

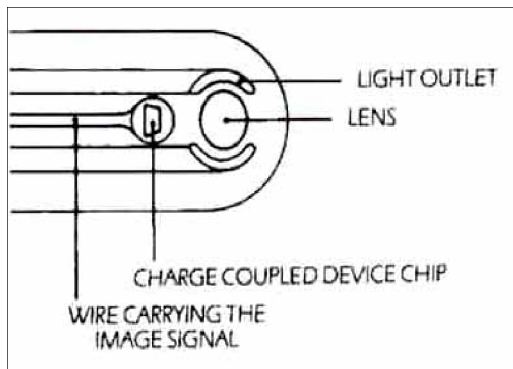


**Figure 2.2:** Cross-section of borescope tip.



**Figure 2.3:** Articulation of borescope tip.

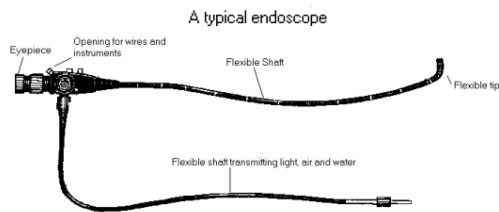


**Figure 2.4:** Medical endoscope.



**Figure 2.5:** Close-up view of endoscope tip.

has a slightly longer flexible probe with an articulating camera at its tip. In both the medical and the aviation fields, the devices are used primarily for visual search. The control interfaces for the endoscope and the borescope are somewhat similar. However, there are two major differences between the borescope and the endoscope.

First, the borescope is used only for visual search and display. The tip of the borescope contains just the CCD camera used for imaging and nothing else. The articulation controls rotate the camera about the central axis to obtain a better view of the area under inspection. In the endoscope, in addition to the camera, there are additional channels along the probe which allow for entry of medical instruments or manipulators. This not only allows the physician the option of visual inspection, but also enables to take biopsies and retrieve foreign objects from the body (Figure 2.5).

The second and more important difference is the force exerted on the probe when it is maneuvered during inspection. When using either the endoscope or the borescope, forces are exerted at multiple points

across the probe depending on the path followed by the device. The major difference between the two devices is the interaction of the tip with the operating environment. Interaction forces experienced by the endoscope stem from the flexible behavior of the probe as well as the forces exerted by the tissues of the human body. When the operator exerts large forces via the endoscope, the tip exerts these forces against tissue walls causing them to deform. This deformation produces an elastic force that is perceived by the operator.

In case of the borescope, contact of the probe with an engine's rigid surfaces plays an important role in determining the forces experienced by the operator. Unlike similar devices used in the medical field, the collision is between the semi-flexible probe and a rigid body. Hence there are no elastic forces exerting feedback on the borescope.

## **2.2 Inspection Process**

The borescope inspection procedure is an example of a visual search and discrimination task. The primary aim of the procedure is to look for engine component anomalies or defects. The search aspect of the task can be broken down into navigation of the borescope through the engine, articulation of the camera to acquire a useful field of view, and a visual search within the given field of view to locate defects. Once a defect is detected, the task shifts from search to discrimination. Based on prior experience or knowledge of standardized defect categories, the inspector has to decide whether the severity of the defect warrants corrective action.

The borescope inspection can either be performed by a single inspector who guides the borescope tip through the engine, or by two persons. In the latter case, the technician performing the inspection keeps the borescope stationary in a fixed position in which he has full view of the turbine, while the aide manually rotates the engine shaft, which in turn rotates the turbines. Although this solution is viable in case of small engines, it is not practical in case of wide-bodied aircraft.

The first step in the inspection process is to prepare the engine to be inspected. Manufacturers of engines usually provide detailed guidelines and a timeline for preventative engine inspection. As a first step, the engine maintenance technician removes the fuel injection manifold from the engine for easier access to the engine interior. Engine manufacturers usually provide guide tubes of different lengths and shapes, which provide an easy way to guide the probe of the borescope to the desired location in the engine and minimize probe damage while inserting the borescope through the engine. In a multi-stage engine, depending on the stage of the engine being inspected, the technician has to choose the correct guide tube to aid probe insertion.



Once the tip of the borescope is at the desired position within the engine, probe articulation is controlled by the handheld joystick control interface. The controls provide for 2-axis articulation control of the probe tip containing the camera. Probe insertion and withdrawal is performed very carefully to prevent tip damage due to excessive contact forces when the probe collides with engine components (Figure 2.6).

Experienced inspectors usually follow a systematic search strategy in the inspection procedure [63]. If they are inspecting a turbine, they first inspect the leading edge of the blade from the base of the blade to the tip, then follow along the front face of the blade to the trailing edge (see Figure 2.7). The trailing edge is then inspected from the tip to the base of the blade and back to the front of the blade. Thus the inspection procedure follows a systematic, circular motion by which the inspector can detect and identify defects. The inspector then moves to the next blade of the turbine and repeats the procedure. Once all the front faces of the blades are inspected, the inspector changes the orientation of the probe to face the back face of the blade and the same systematic search procedure is repeated. Any defects found during inspection are logged and the engine is dismantled for further repairs if necessary.

In addition to the visual feedback provided by the CCD images, the borescope inspector also feels force feedback when the probe collides with the engine surfaces. For simplicity, the forces experienced can be broken down into contact forces that act on the tip of the probe and sliding forces acting on the probe as it snakes through the engine. The angle of the probe tip's contact with the rigid surface plays an important role in determining the forces experienced by the inspector. Upon contact with a rigid surface, the tip can either slide, stop, or deform. When the angle of incidence between the tip and the contact surface is large, the tip will either slide along the surface unless it encounters further hindrance or it will stop and deform if its motion is impeded. When the angle of incidence of the borescope tip is almost perpendicular, the probe may deform if the force applied by the inspector is large. The probe's deformation will depend on the physical characteristics of the probe and the contact surface. If the force applied by the inspector is not as large (e.g., the inspector stopped pushing the probe due to visual feedback), no deformation will occur and the tip will stop.

To summarize, the main skills needed for borescope inspection are:

1. Probe feed. The probe's position and orientation is governed by its motion constrained within 2 degrees of freedom. It can be manually pushed into or pulled out of the engine, combined with its roll about its longitudinal axis. In/out translation of the probe determines its location within the engine, while its axial rotation determines the camera's attitude. Although the probe is flexible, the amount of bend is constrained by the bundle of fiber-optic cables and its braided sheath.



**Figure 2.6:** Inspection of aircraft components using the video borescope.

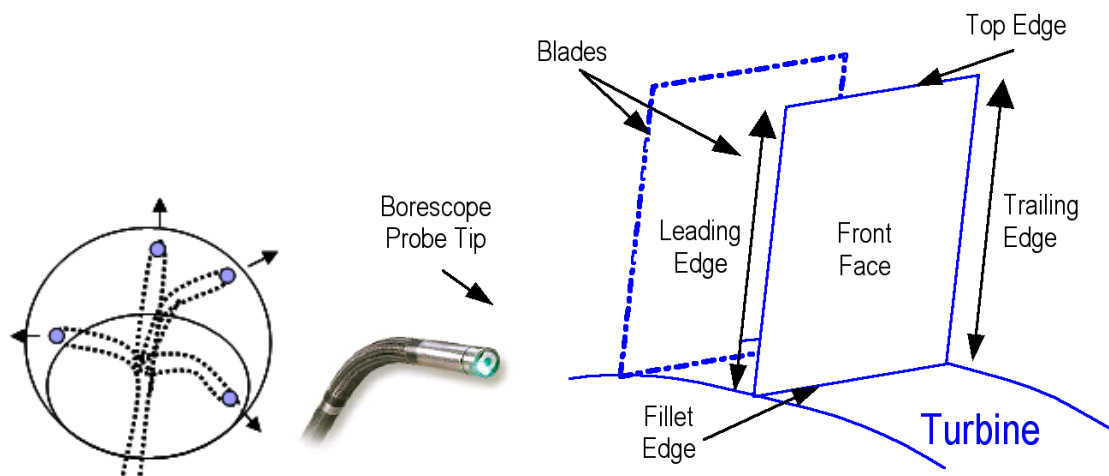


**Figure 2.7:** The video borescope's articulating tip and the turbine inspection process.

2. Camera articulation. The CCD camera's articulation is controlled by manual (hand-held) joystick controls. The operating region of the probe tip forms a partial sphere and has two degrees of articulation, yaw and pitch, about the local  $x$  and  $y$ -axes (see Figure 2.7).
3. Visual and force feedback. Visual feedback on the monitor is the borescope's primary form of feedback. Visual search for defects in the output from the borescope camera is the primary task of the engine inspector. Determination of defect severity and remedial action is usually performed in collusion with the engine manufacturer's recommendations.

In addition, the inspector also receives force feedback whenever the tip of the probe collides with the rigid engine components. The real probe may drag along the surface of the engine, it may stop, or it may become entangled in the blades. It is desirable to avoid damage to the probe tip as replacements are expensive and time consuming.

## Chapter 3

# Simulator Development

### 3.1 Prior Work

Virtual Reality (VR) simulators have been used for training novices in a wide spectrum of areas, ranging from flight training to surgical procedures. Interest in VR simulators can be traced back to the successful training of airline pilots. The simulators provide a realistic, real-time environment with the ability to provide instantaneous feedback on performance. The simulator usually consists of a 3D model rendered on the computer with which the users can interact in real-time using input devices ranging from a simple joystick to a more expensive 6 degree-of-freedom (DOF) mouse. The displays vary from a simple computer monitor to fully immersive head-mounted-displays.

Training sessions can be easily customized to suit individual needs and skill levels. Prior research has shown that the skills training obtained from the use of simulators is similar to those obtained from real-world experiences and that these skills successfully transfer to task performance [25, 62]. However, the fidelity of the VR simulation is crucial for the skills to transfer effectively from the virtual testbed to the real world.

The borescope is similar in design to the commonly used medical tools such as the endoscope. Both instruments are used to check for abnormalities by visual inspection. The skills and the hand-eye coordination needed to manipulate the articulating tip in both these devices are similar in nature. Past research has led to the development of desktop VR simulators for training doctors in bronchoscopy, colonoscopy, mastoidectomy, etc. [22, 19, 33, 48]. Virtual endoscopy consists of navigation of a virtual camera through a 3D reconstruction of a patient's anatomy enabling the exploration of the internal structures to assist in surgical planning [41].

Virtual exploration through patient-specific data can help the surgeon perform a diagnosis without having to operate on the patient. The data can also be used to train novice doctors in the correct procedures to be adopted for performing the operation. Virtual endoscopy can be used to screen, diagnose, evaluate and assist determination of surgical approach, and provide surveillance of certain malignancies.

The basic methodologies adopted in developing the various virtual endoscopy medical training simulators are similar. As the first step, high resolution data obtained from CT scans or MRI are used to reconstruct realistic, 3D models of the human anatomy. If needed, the operator can configure the 3D data with texture-mapping to introduce abnormalities such as tumours, lesions and polyps to the 3D models. Physically realistic effects such as soft tissue deformation and haptics can also be used to increase the sense of realism and presence in the simulator. The second and most important step is the user interaction with the virtual model. The participants can either use a “free-fly” model of camera or use a predetermined route to navigate through the model. Using a variety of input devices, the users interact with the virtual scene and perform pre-defined tasks which help determine the effectiveness of the simulator. The third step consists of assessing the benefits of training with the virtual simulator in the real world scenario. Process and performance measures such as the total time taken, tumours identified and missed as well as subjective questionnaires are used to evaluate the simulator.

Evaluation studies used to assess the realism of such simulators showed that participants felt that the virtual simulators strongly represented the real world environment. Ferlitsch et al. [21] observed that novices trained on such simulators performed their tasks faster and with fewer errors than those who did not have similar training. They also observed that there are distinct differences between the strategies adopted by expert doctors and novices when they were asked to use the simulator. It was also found that using real life props, such as a mannequin, and providing real time force feedback increased the sense of presence and realism of the virtual simulator [62]. Lamata et al. [33] attempted to provide baseline metrics for incorporating virtual simulators in training doctors in laparoscopy using virtual trainers. Although repeated training on the simulators have been found to improve the performance of novices, the transfer effects of training on virtual simulators and performance in the real world are not fully understood.

Visual inspection comprises a major proportion of the aircraft maintenance procedure. This is usually preformed by an aircraft maintenance technician, who is trained in the inspection procedures, identification and classification of defects. Most of the theoretical knowledge on the inspection procedures is gained from classroom teaching. On-the-job training by a more experienced inspector is used to bridge the gap from the academic setting to a more practical workplace environment. However, this transition from the class-

room to the workplace is not easy. Many novice inspectors face a steep learning curve because they lack the required hands-on experience required to make a smooth transition to the workplace.

The major limitation in providing more practical experience to students is the prohibitive costs associated with obtaining different types of aircraft to train the students. Computer-based training simulators have been used for enhancing the skill set of the novice inspectors. Due to advances in the commodity graphics market and the availability of faster and cheaper Graphics Processing Units (GPUs), the visual realism of the simulators has improved considerably. The training simulators vary in realism and degree of interaction, from a simple desktop point-and-click version to a fully immersive, virtual reality simulator. Although these simulators facilitate cost-effective, hands-on training in the classroom, it is to be noted that they are meant to merely augment, not replace, on-the-job training.

In the following section, we describe the development of the graphical simulator used to render and interact with 3D models of aircraft engine components.

## 3.2 Engine Model Acquisition

Before the development of the simulator, a detailed task analysis of the borescope inspection was carried out at Steven's Aviation and the Aircraft Maintenance School at Greenville Technical College in Greenville, South Carolina [63]. An expert inspector was video taped performing a mock engine inspection and his comments and observations recorded for later transcription and analysis.

The first step in developing the visual aspects of the borescope simulator was determining a representative aircraft engine for modeling. We settled on the Pratt and Whitney PT6 engine commonly found in turboprop aircraft. The PT6 engine is a two-shaft engine with a multi-stage compressor driven by a single-stage compressor turbine and an independent shaft coupling the power turbine to the propeller. We decided to concentrate on borescope inspection of the hot-section of the engine which is made up of two stages of turbines, a fixed stator and a movable rotor.

We modeled one stage of the hot section of the aircraft engine in Maya [47] and exported it as an Alias|Wavefront .obj file [3] with texture and material information. The 3D models are scaled representations of the actual engine. The environment consists of an enclosed stator and turbine modeled on the interior of a real engine as seen in Figure 3.1.



**Figure 3.1:** Actual and modeled engine sections (left, right) of stator (top) and rotor blades (bottom).

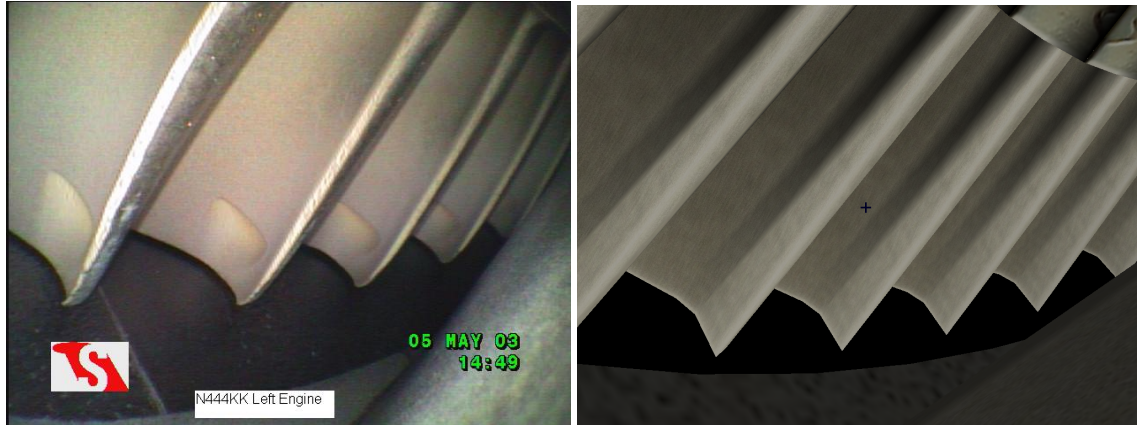


**Figure 3.2:** Visual output from the actual borescope (left) and our simulator (right).

### 3.3 Graphical Rendering and User Controls

For the first iteration of the simulator, based on informal discussions with experienced borescope inspectors, we developed a simple `.obj` viewer to render the engine model. The model is texture-mapped and lit to simulate the visual look and feel of an actual borescope camera image. Instead of developing a custom graphical renderer for the 3D models from scratch, we decided on using existing 3D APIs for developing the simulator. OpenSceneGraph (OSG),<sup>1</sup> is a commonly used open source API, written in C++ and built atop OpenGL [59, 73]. OSG has built in file importers which make it easy to import files created in 3D applications such as Maya and view them in a window viewport. In addition to rendering functionality, OSG also provides simple input handling for handling keyboard and mouse events. Figure 3.2 shows a screenshot from the simulator compared to an actual video borescope frame.

We implemented a simple camera model for the simulator. The camera is modeled as a point in 3D space. Unlike the real borescope camera, which is attached to the tip of the probe and is constrained in motion, the free moving camera is unconstrained and can move and rotate in 6-DOF space. Although this is not representative of the actual camera behavior, our aim, at this point in the study, was to rapidly produce a prototype that we could use for evaluation. One of the simplifications was in the camera behavior and control. Collision detection and response in this version of the simulator was intentionally kept simple. Axis-aligned bounding boxes (AABBs) were precomputed for the 3D engine models and ray-box collision detection and response implemented in the simulator to prevent penetration of the camera with the virtual models.

An off-the-shelf Logitech gamepad was used for camera control. User interaction with the simulator

<sup>1</sup><http://www.openscenegraph.org/>, last accessed 01/09.





**Figure 3.3:** Orientation and translation control of the virtual camera with the directional pad and buttons (1 and 4) on the gamepad.



**Figure 3.4:** Visual output from the virtual borescope and user controls via the gamepad.

was through the gamepad. Camera translation was mapped to button presses on the gamepad. Translation of the camera was always along the view-vector as seen on the display screen. The orientation of the camera was controlled by the directional pad of the gamepad. Figure 3.4 shows the visual output of the simulator and the control interface.

After development of the prototype borescope simulator, we evaluated the visual and behavioral realism of the simulator with experienced borescope inspectors. We were particularly interested in their subjective experience with the virtual prototype and their comments in using the gamepad to control the virtual camera in the simulator. In this stage of evaluation, we used a pristine engine model with no defects to remove the search aspect of the task. We also provided no force feedback to the users as we wanted to disambiguate the visual and the tactile feedback from the simulator. We performed two different evaluations of the simulator. First, we evaluated the visual fidelity of the simulator with experienced borescope inspectors to obtain their input in the iterative design of the simulator. On completion of this experiment, we evaluated commonly used interfaces used to control the probe articulation in the borescope such as gamepad, joystick and keypad.

### 3.4 Experiment 1: Visual Fidelity Evaluation

In this section, we present the results of subjective evaluation of the visual and behavioral realism of the simulator conducted by experienced borescope inspectors. The main aim of the experiment was to determine the perceived sense of presence and realism experienced by the participants using the virtual simulator.

The results presented in this section have been published as “Vembar, D et al., Design of a Virtual Borescope, in The Proceedings of HCII’05 Conference, 2005” [67].

### **3.4.1 Participants**

Eight participants (all male) were invited to evaluate the virtual borescope. All the participants were familiar with the video borescope and had extensive experience using the borescope for aircraft engine inspection. Each of the participants was either an aircraft maintenance technician or taught an aircraft maintenance course on engine and aircraft inspection. The participants were asked to interact with the desktop version of the borescope simulator and express their observations on the visual realism and correctness of the simulator. Their comments were recorded for later transcription. On completion of the experiment, the participants filled out a questionnaire evaluating the visual fidelity of the simulator.

### **3.4.2 Apparatus and Stimuli**

The experiment was carried out on a Pentium4, 2.6GHz computer, with 512MB RAM and a GeForce 5700Ultra graphics card. The frame rates were maintained above 30fps for an interactive, real-time experience. An off-the-shelf Gravis Eliminator Pro gamepad was used to control the camera position and orientation in the simulation. Unlike the actual borescope, where the tip has limited motion, the camera in the virtual borescope had no constraints and could rotate a full 360° about either axis. The camera orientation was controlled by the analog, 2-axis directional pad of the gamepad. Two buttons on the gamepad simulated the feed and withdrawal of the probe by moving the camera along the direction of the view vector. The experimental setup is shown in Figure 3.4.

Using the hot section of a Pratt and Whitney PT6 engine, 3D models of the turbine and stator were modeled. The 3D models of the engine blades along with the real blades are shown in Figure 3.1. The engine blades were combined together and enclosed in a sphere to simulate the experience of performing the inspection on an actual engine. This combined engine was imported and rendered using OSG. Collision detection was enabled in the simulator to prevent the participants from moving the camera through the engine blades. Depending on the angle of incidence at the collision point, the camera either slid along the surface of the engine or it stopped without any further motion, until the participant changed the position or the orientation of the camera. Unlike an actual engine, the 3D model was pristine, i.e., there were no defects on the engine blades such as cracks or corrosion.

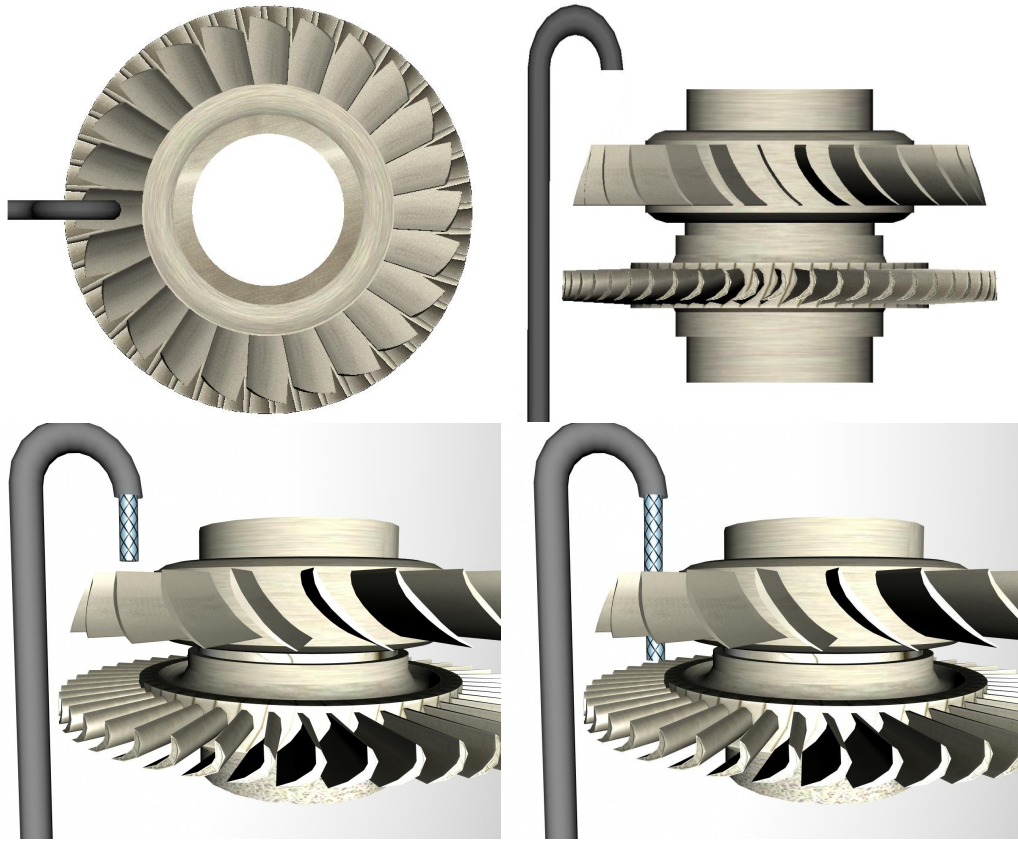


**Figure 3.5:** Inspection scenario (from left to right): top and side views inside the engine casing, with guide tube exit positioned just above the stator; braided textured cylinder illustrates the typical path of the simulated borescope through the stator to its position during turbine (rotor) blade inspection. Once in position, the task mainly consists of rotating the turbine to visually inspect each of its blades. Note that the user never sees this external viewpoint—the user’s only viewpoint is from the tip of the borescope.

Figure 3.5 shows a simulated view of the task performed by the participants. All the participants started at the same start position in the simulator. The task consisted of maneuvering the virtual camera through one set of stator blades and performing a simulated inspection of the rotor. The models were texture mapped with clean textures to remove any effect of visual search on fidelity evaluation.

### 3.4.3 Procedure

Before the experiment, the participants were asked to complete a demographic questionnaire which collected data related to their familiarity with the borescope and engine inspection procedures. The participants were then presented with the virtual borescope simulator. The participants were given a brief overview of using the gamepad to control the camera motion in the simulator. They were then asked to use the gamepad

- 
1. The environment was responsive to actions that I initiated.
  2. I was involved by the visual aspects of the environment.
  3. The interactions with the environment seemed natural.
  4. The mechanism which controlled movement through the environment seemed natural.
  5. The visual aspects of the virtual environment seemed consistent with my real-world experiences.
  6. I was able to anticipate what would happen next in response to the actions that I performed.
  7. I could examine objects from multiple viewpoints.
  8. Manipulating the borescope tip in the virtual environment seemed compelling.
  9. I was involved in the simulated borescope experience.
  10. The control mechanism was distracting.
  11. There was no delay between my actions and expected outcomes.
  12. I adjusted quickly to the virtual environment experience.
  13. I felt proficient in moving and interacting with the virtual environment at the end of the experience.
  14. The visual display quality interfered with performing the task.
  15. The control devices interfered with performing the task.
  16. I could concentrate on the task rather than on the mechanisms used to perform the task.
  17. The software is applicable for training borescope inspection of engines.
  18. I would personally prefer the environment for training of borescope inspection.
- 

**Table 3.1:** Subjective questionnaire for subjective evaluation of visual fidelity of the borescope simulator. Responses were on a 7-point Likert scale, with 1-Strongly disagree, 4-Neutral and 7-Strongly agree.

and navigate through the 3D models. The participants were given unlimited time to interact with the simulator. They were instructed to “think aloud” during their interactions with the simulator and comment on the visual fidelity and interaction experience in the simulator. Their observations and comments were recorded for later evaluation.

### 3.4.4 Design and Data Collected

On completion of the experiment, the participants were asked to fill out a modified version of the Witmer-Singer Presence Questionnaire [72], which evaluated the realism of the simulator on a seven-point Likert scale, ranging from strongly disagree to strongly agree, with four (4) being neutral. The questionnaire is shown in Table 3.1.

### 3.4.5 Results

The results were analyzed using SAS (v8.2). The Wilcoxon test was used to determine the deviation from the neutral point (4) on the Likert scale. The results are summarized in Figure 3.6. The results show a significant inclination ( $p < 0.05$ ) of the participants to agree with questions 1, 2, 3, 4, 6, 11, 12, 13, 16, 17 and 18 and disagree with questions 10 and 15. There was no significant deviation from the neutral value for the responses to questions 5, 7, 8, 9 and 14.

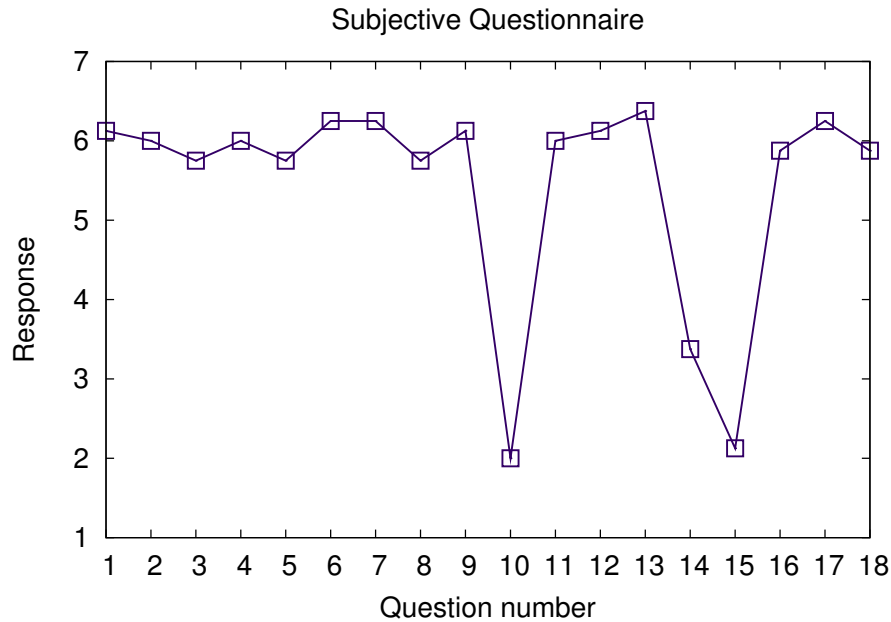


**Figure 3.6:** Average participant responses to the Presence Questionnaire evaluating visual fidelity on a 7-point Likert scale, with 1-strongly disagree, 4-neutral and 7-strongly agree.

### 3.4.6 Discussion

The results signify a high degree of presence experienced by the participants while using the simulator. The prototype of the virtual borescope was used for this study had a pristine model of the engine components. This was pointed out by the participants. The participants found the environment to be responsive and felt involved in its visual aspects. The participants reported that they experienced no delay in the simulator's response and were able to anticipate the response to their actions. The participants felt that they adjusted quickly to the virtual experience and could concentrate on the task without being distracted by the control mechanism involved. They found the interactions with the environment to be natural.

Interaction of the participant with the simulator was through a standard gamepad. The use of the gamepad and a desktop computer, instead of the joystick and the hand-held device, did not adversely affect the interaction in the virtual world. User responses indicate the gamepad did not distract the participants or hamper them in their interactions with the simulator (Q2, Q4, Q10, Q13, Q15 and Q16) . The participants were able to adjust to the virtual borescope and were adept at using it by the end of the task. The participants felt that the virtual borescope would be a useful medium of instruction in the classroom for providing training in engine inspection procedures.

The participants observed that the camera was unconstrained and pointed out that the articulating

tip of the actual borescope probe was limited in its ability to move very freely within the engine. Responses to Q17 and Q18 indicate that the participants consider the virtual simulator to be a useful tool for providing training in engine inspection using borescopes.

Results from this expert evaluation suggest that the visual aspects of the simulator are acceptable for use in training novice trainees in engine inspection. There were two observations that the experts suggested would improve the realism in the simulator. First, the participants noted that they were disconcerted by the lack of force feedback when there were intersections with the model. In the real world, when the probe tip hits the engine, the inspectors feel contact feedback which is an important component of the inspection process. Experts noted that provision of contact feedback would probably improve the behavioral fidelity of the simulator.

Second and more importantly, the experts noted that unlike the real borescope camera, they could move and rotate in full 3D space and perform loops about the engine blades. They felt that this was not possible with the real borescope due to the physical characteristics of the fiber optic probe. Due to the unconstrained motion of the camera, the participants noted that they were easily lost while interacting with the engine. They suggested implementing a constrained motion of the camera to compensate for this shortcoming in this version of the simulator.

### **3.5 Experiment 2: Control Interfaces Evaluation**

The most common form of interaction with a computer has been through the keyboard and the mouse. Though these devices are particularly suited for tasks such as text selection, typing or pointing tasks [43], they are ill-suited for specialized tasks such as 3D object selection, manipulation and other such tasks in a virtual environment. Although 2D input devices have been used to control objects in a 3D environment [16], well-designed interaction techniques using input devices with multiple degrees of freedom may sometimes provide superior performance to normal 2D input devices. Numerous studies have evaluated the efficiency of input devices such as the 3D spaceball and 6-DOF Flock of Birds (FOB) in interacting with object in virtual environments [44]. Although these devices afford extra levels of interaction and make it easier for the user to interact with the object, their prohibitive costs lead to their use only in specialized cases.

It is important here to differentiate between an interaction task and an interaction technique [29]. Interaction tasks are low-level primitive inputs required from the user. Examples of an interaction tasks include entering a block of text or selecting an option from a series of options. For each task, an appropriate

interaction technique must be selected, which is a way of using an input device to perform an interaction task. An interaction technique represents an abstraction of some common class of interactive task. In our case, the interaction task consists of probe manipulation and selection of defects in the engine model.

In this section, we present a feasibility study evaluating commonly available input interfaces similar to that used in the actual borescope for controlling probe tip articulation. We evaluated three common off-the-shelf input interfaces, a gamepad, a joystick and keyboard with the borescope simulator. The results presented in this section were published in “Sadasivan, S. et al., Evaluation of Interaction Devices for NDI Training in VR, in The Proceedings of the Human Factors and Ergonomics Society (HFES) Annual Conference, 2006”.

### **3.5.1 Participants**

A total of seven subjects (all male) participated in this study. The participants were either industry veterans with extensive borescope inspection experience or were instructors in the aircraft maintenance training school who had prior experience with using the borescope for engine inspection.

### **3.5.2 Apparatus and Stimuli**

The virtual borescope simulation was run on both a desktop and laptop. The desktop consisted of a 2.6Ghz Pentium4 processor, coupled with 1GB RAM and GeForce 5700Ultra video card. The laptop consisted of a PentiumM 1.6GHz processor with 512MB RAM and a GeForce 6800 video card. The simulators were run at interactive frame rates on all the machines.

The engine blades were modeled in Maya from the hot-section engine components of a PT-6 engine and exported as .obj files. Textures were applied to the model to denote the path to be followed in the task performed by the participants. We used OSG for rendering the engine blades on the screen. The participant was presented a camera-view of the engine on the computer screen. Unlike the actual borescope where the tip has limited motion, the camera in the virtual borescope had no constraints and could rotate a full 360° about either axis. A timer was implemented to record the user clicks as a way of measuring the time taken to move from one target to the next.

The position and orientation of the camera was controlled by specific keys in the input device, as outlined in Table 3.2. Figure 3.7 shows the visual output of the simulator, while Figure 3.3 shows the gamepad used to control the camera. Note the mini-joystick like interaction interface provided by attaching a push pin to the directional controller. This modification presented an interface similar to the control interface used in

Interface	Position	Orientation
Keyboard	W - Zoom in X - Zoom out	Arrow keys
Gamepad & mini-joystick	1 - Zoom in 4 - Zoom out	D-pad
Joystick	Trigger - Zoom in Hat - Zoom out	2-axis joystick

**Table 3.2:** Key mapping for the three different interfaces

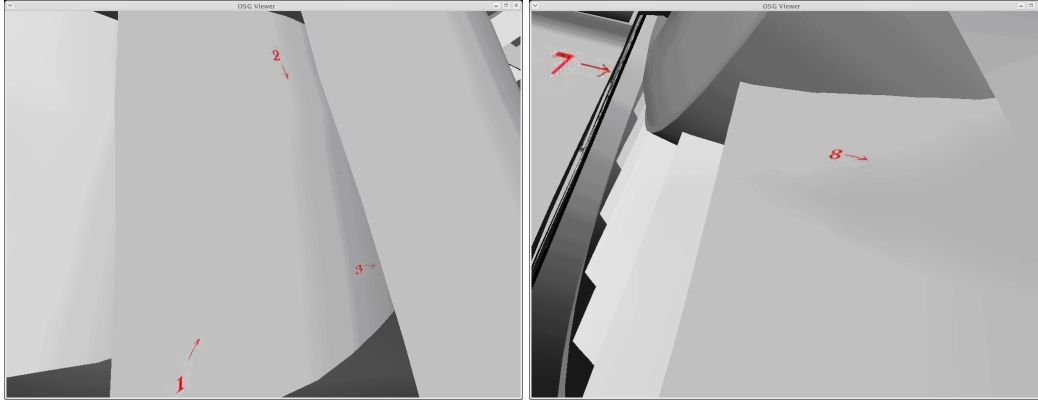


**Figure 3.7:** Output of the simulator with numbered arrows denoting direction of inspection.

the actual borescope.

### 3.5.3 Procedure

Before the start of the experiment, the participants were asked to complete a consent form and a demographic questionnaire, which collected data about their experience with borescope inspection and use of training simulators. The experiment consisted of two steps: familiarization phase and testing phase.

In the familiarization phase, the participants were provided training on the borescope inspection simulator and interaction with the environment using one of the input devices. On successful completion of this step, the participants were provided with a simple task scenario in which they were asked to follow a numbered path on the blades from points 1 through 10. To prevent searching among the targets, all the participants were familiarized with the path at the beginning of the experiment. Figure 3.4 shows the view of the virtual environment as seen by the participant on the screen.

When the target was acquired at the centre of the screen, the participants pressed the left mouse button to provide a timestamp of target acquisition. These were stored in a file, which was used for later analysis. After completion of the task, the participants filled out a subjective presence questionnaire [72],



---

1.	The interactions with the environment seemed natural.
2.	I was involved by the visual aspects of the environment.
3.	The mechanism which controlled movement through the environment seemed consistent with my real-world experiences in using the borescope.
4.	I was able to anticipate what would happen next in response to the actions that I performed.
5.	I could examine objects from multiple viewpoints.
6.	I was involved in the simulated inspection experience.
7.	The control mechanism was distracting.
8.	There was no delay between my actions and expected outcomes.
9.	I adjusted quickly to the virtual environment experience.
10.	I felt proficient in moving and interacting with the virtual environment at the end of the experience.
11.	I could effortlessly manipulate the interface for target selection in the virtual environment.
12.	The control device allowed me to follow the paths shown on the models with ease.
13.	The control device interfered with performing the task.
14.	I could concentrate on the task rather than on the mechanisms used to perform the task.
15.	I would personally prefer this interface for training using virtual borescope simulator.

---

**Table 3.3:** Subjective questionnaire for subjective evaluation of the three control interfaces of the borescope simulator. Responses were on a 5-point Likert scale, with 1-Strongly disagree, 3-Neutral and 5-Strongly agree.

concerning the input device they had just used in the task. This procedure of interface familiarization and user testing was repeated for the other two input interfaces, with the subjective questionnaire administered at the end of each test phase. On completion of all the three interfaces, the participants were informally debriefed and were asked to rank the interfaces they had used for training novice engine inspectors.

### 3.5.4 Design and Data Collected

We used a within-subjects, counterbalanced design to evaluate the three input interfaces. All of the participants were provided the same interfaces, but the order of the input interfaces was counterbalanced to prevent order and learning effects.

During the testing phase of the experiment, we recorded the time taken by the participants to move from one target to the other as well as the total time taken to complete the task. On completion of each phase of interface testing, the participants were asked to complete a subjective questionnaire. The responses to the questionnaires were on a 5-point Likert scale, with 1 being strongly disagree, 5 being strongly agree, and 3 being neutral. A majority of the questions in the questionnaire dealt with the perceived ease of use of the input device for navigation within the virtual environment as well as the interaction capabilities of the input devices (refer Table 3.3).

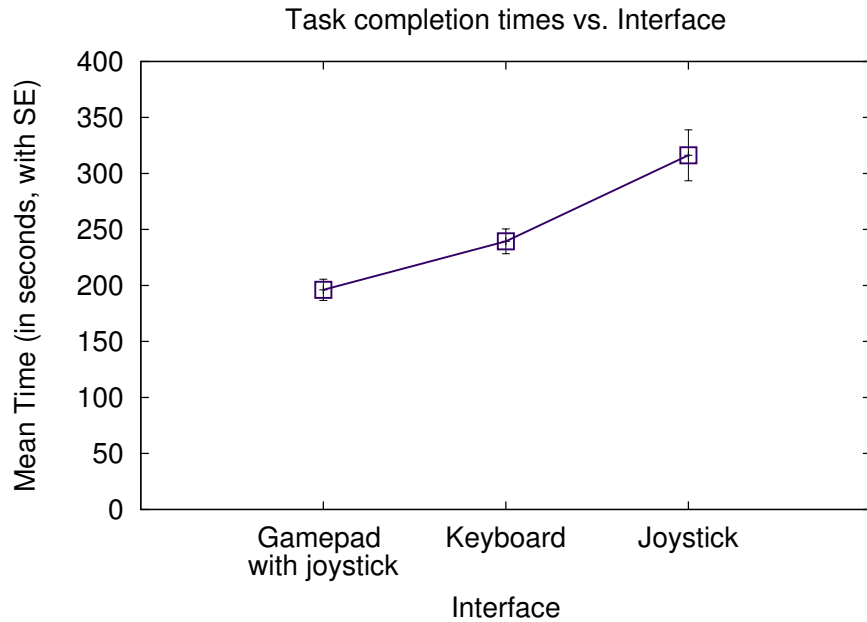


**Figure 3.8:** Average time to task completion among the three control interfaces.

### 3.5.5 Results

Figure 3.8 shows the mean times taken to complete the tasks by the participants computed from the data collected. The mean time taken by the participants using the gamepad was 196.14 seconds, while the mean time to complete the task using the keyboard and joystick was 239.4 and 316.2 seconds respectively. ANOVA revealed a significant difference in the three interfaces on the time taken for task completion ( $F(2,12) = 6.17, p < 0.01$ ). A pairwise t-test found that there was a significant difference between the gamepad with joystick and the other two interfaces ( $p < 0.05$ ). There was no significant difference between the keyboard and joystick.

### 3.5.6 Discussion

Wilcoxon analysis of the subjective data obtained from the questionnaire from the gamepad evaluation showed that the participants found the visual aspects and interaction with the environment to be consistent with their real world experience with borescopes. They also reported that they could examine the models from multiple viewpoints and were able to anticipate the results from their actions in the virtual environment. The participants' answers show that they adjusted quickly to the gamepad and felt proficient in moving and interacting with the virtual model.

The Wilcoxon rank sum test was used to analyze the combination of the data obtained from the questionnaires of the three input interfaces. When the gamepad was compared with the joystick, the responses indicated that the participants preferred the gamepad over the joystick (Q12) due to its quick responsiveness (Q1) and ability to anticipate what happened next in the visual output due to actions initiated by the user. Participants reported that the the gamepad was more natural in interacting with the simulator compared to the joystick (Q2), which they felt was more distracting and interfered with the task (Q5, Q10). The participants reported that they adjusted quickly to the virtual environment experience (Q6) and obtained proficiency in moving and interacting with the virtual environment more easily with the gamepad (Q7). Overall, the participants reported that they could concentrate more on the task with the gamepad (Q11) which they felt aided them better than the joystick in following a path (Q9).

The Wilcoxon rank sum test comparing the responses of the participants with the gamepad and the keyboard showed that the responses were significantly different ( $p < 0.05$ ) in only one question (Q12). The participants reported that they prefer providing virtual borescope inspection training to novice inspectors using the gamepad with the joystick rather than the keyboard. There were no other significant differences between the keyboard and gamepad.

Combined with the ease of use, minimal interference with the inspection task and faster proficiency in interacting with the simulator afforded by the gamepad compared to the joystick and the keyboard, we conclude that it is more suited for the virtual borescope control interface than the joystick or the keyboard.

## Chapter 4

# Development of a Haptic Interface

Since we were developing a training simulator that would be used in the classroom for training students, we wanted to find interfaces that are cheap, sturdy, and easy to maintain. Off-the-shelf devices such as the PHANToM [46] simulate contact forces with a high degree of realism, but are expensive and are not suitable for all applications. The primary requirements of the borescope interface are simulation of the probe feed to increase the behavioral realism of the simulator and provision of simple, synchronous force feedback to the user based on intersections of the virtual camera with the engine model.

To facilitate inspection training, we built a simple and cost effective haptic interface to provide tactile feedback of probe collisions with the engine model. Navigation of the borescope's articulating tip is simulated by feeding a real borescope's braided sheath through a newly constructed device providing haptic feedback in reaction to the tip's physical interaction with virtual objects (e.g., engine stator and turbine fan blades). In the next sections, we describe the design and operation of a novel motor-powered clamp that provides force feedback of the collision of the virtual borescope camera detected in virtual space. The design and evaluation of the Haptic box was published in "Vembar, D. et al., A Haptic Virtual Borescope for Visual Engine Inspection Training, in Proceedings of the IEEE Symposium on 3D User Interfaces, 2008" [66].

### 4.1 Prior Work

One of the simplest forms of haptic feedback is the interaction of a rigid body with a rigid manipulator. An analysis of human perception of interaction with a rigid surface revealed that the perception of encountering a rigid surface is not as strongly correlated to its stiffness as it is correlated to the initial

contact with the surface [55]. Furthermore, when using a haptic interface to simulate contact forces, Tan, et al. [9] showed that users have poor force direction discrimination resolution. This suggests that although users can perceive the magnitude of the force, they are unable to perceive the direction of the simulated force with the same resolution. In the presence of multiple input modalities including visual, auditory, and haptic, intermodal integration may be a key psychological mechanism contributing to the sense of presence in the virtual environment. While it is reasonable to assume that the simulator with the highest haptic fidelity will be perceived by the user as the “most real” interface, psychophysical testing with human subjects is needed to reveal the minimum performance requirements of the hardware interface to be used in the simulator.

Training simulators have mainly been visual in nature. However, haptic devices such as SenseAble Technologies’ PHANToM have made it easy to incorporate force feedback into virtual models. Prior studies have shown that haptic feedback plays an important role in improving performance [68], augmenting the skills transfer in novice trainees, and that early exposure to force feedback in the simulator improves performance [64]. Recent studies of haptic interfaces have focused on the use of the PHANToM when used in assembly tasks where a hand-held object is being manipulated (e.g., *peg-in-hole* task) [28, 40, 24]. O’Malley and Upperman have discussed human performance in size identification and size discrimination tasks with the PHANToM [50].

There are multiple instances of custom interfaces developed for honing endoscopy skills. Korner and Manner [31] developed a simple haptic interface, where the physician moves the flexible endoscope within a pipe. Haptic feedback modeled the complex interaction of the forces experienced by the probe tip and the endoscope. Samur et al. [57] developed a compact and portable haptic interface to provide position and orientation data acquisition as well as force feedback for linear and rotational motion of a colonoscope inserted into the device. Maillard et al. [45] developed a modified version of the clinical colonoscope to measure tip rotation by its use of switches, maintaining aesthetic and functional similarity to its real counterpart. This colonoscope was integrated with their simulator to provide a visual and haptic simulation of the colonoscopy procedure.

Among the commercial solutions available for medical simulators, Immersion Technologies’ Accutouch endoscopy simulator provides authentic visual as well as haptic feedback for training. Similarly, Simbionix developed the GIMentor where a mannequin is used to train doctors in both upper and lower endoscopic procedures. Both simulators incorporate deformable anatomic models to provide realistic feedback and provide a safe environment to practice operating procedures to reduce the learning curve for novice doctors.

Evaluative studies have been performed with medical simulators to determine the benefits and ease of transition to the operating room by novice doctors. Novice doctors who had exposure to laparoscopic simulator training made fewer errors than doctors who did not have simulator training, though the task completion times were not significantly different between the two groups [62]. Koch et al. [30] performed subjective evaluation with the GIMentor endoscopic simulator to determine if it is possible to distinguish between novice and expert doctors based on their simulator performance. Subjective evaluation of performance showed that the visuo-haptic simulation offered a realistic representation of the colonoscopy procedure and that differences in skill levels can be gauged based on performance in simulated tasks. Sedlack et al. [60, 61] evaluated first-year residents' performance on actual patients following training on the Accutouch colonoscopy simulator. The addition of simulator training in the curriculum was found to enhance early performance and decrease task completion rates compared with traditionally trained doctors. The authors noted that simulator training provides a "measurable advantage in the early stages of training by accelerating the process of attaining proficiency in basic colonoscopy skills".

Wagner et al. [69] examined the effects of force feedback in a blunt dissection task. The results showed that force feedback: (1) improved performance over visual feedback alone by reducing the overall forces applied; (2) reduced errors due to accidental incursions into surrounding tissue; and (3) served to reduce the mental workload of the participants in the study.

In the case of the borescope, the inspection task differs from the peg-in-hole assembly task in that the user does not have the benefit of seeing the borescope (e.g., peg), rather, the user *is* the peg, as it were, and sees the virtual environment from the peg tip's point of view. As a first step toward developing a haptic force feedback device for the borescope, we developed a simple OFF/ON haptic device using a cheap off-the-shelf motor kit. The custom research-quality haptic device is suitable for the borescope inspection task since it allows inspectors to physically insert the probe into a simulated engine just as they would in the real situation. The design of the haptic box is presented in the next section.

## **4.2 Building the Haptic Box**

### **4.2.1 Design and Construction**

Figure 4.1 shows a top-down view of the haptic box designed to address the main requirements of the simulator. The first stage of the device consists of an entry point that guides the probe beneath an optical

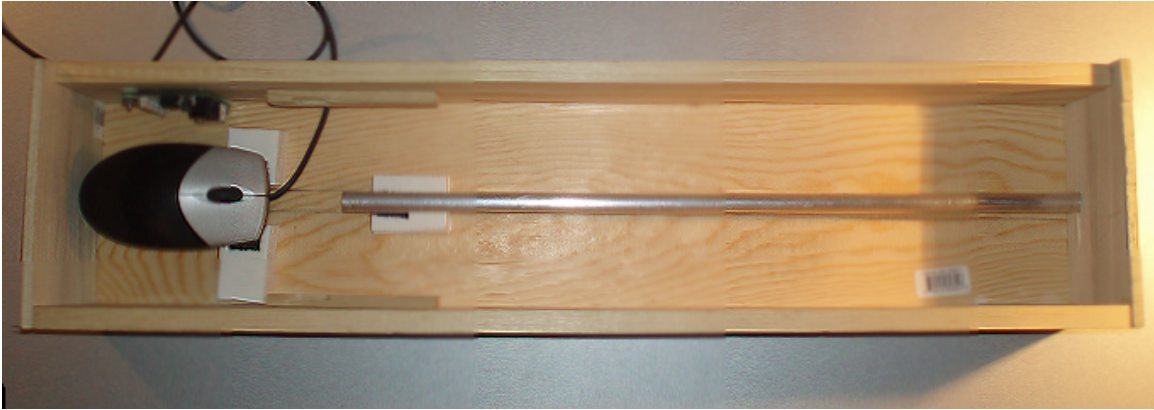


**Figure 4.1:** Top view of the feedback device with mouse and guide tube, with probe entry at left (the haptic component has been removed to show the guide tube into which the probe is inserted).

Component	Quantity	Cost
Model wood planks	6	\$20
Optical computer mouse	1	\$15
Phidgets Interface Kit	1	\$75
USB Servo Motors kit	2	\$70
Cam cleats	2	n/c
Borescope probe	1	n/c
Total Cost		\$180

**Table 4.1:** Components used in the Haptic feedback device.

mouse, as the probe enters the box from the left side (the haptic component has been removed to show the guide tube into which the probe is inserted). The dimensions of the wooden enclosure are 6"× 6"× 24". The aluminum guide tube is 1 cm in diameter and runs through the entire length of the box, ensuring that the probe follows a predefined path within the enclosure. The box was designed for a borescope probe 8 mm in diameter, but can be used for any probe thickness by changing the guide tube's diameter.

The second stage of the haptic box contains the force feedback device consisting of two servo motors attached to two serrated cams obtained from a cam cleat formerly used in its original sailing application (Figure 4.3). A cam cleat is normally used to maintain sail tension by preventing a sailing control line (e.g., main sheet) from backing up through the cleat. In its present configuration, it is used in the reverse, preventing a line (the borescope probe) from being inserted forward. To allow computer-controlled operation of the cam cleat, its springs were removed and its cams made operable via attachment to the two servo motors. Table 4.1 details the total costs associated with construction of the haptic box.

The main components of the haptic box are:

1. Optical mouse. The mouse provides the measurement of probe feed (mouse  $\Delta y$ ) and probe twist (mouse

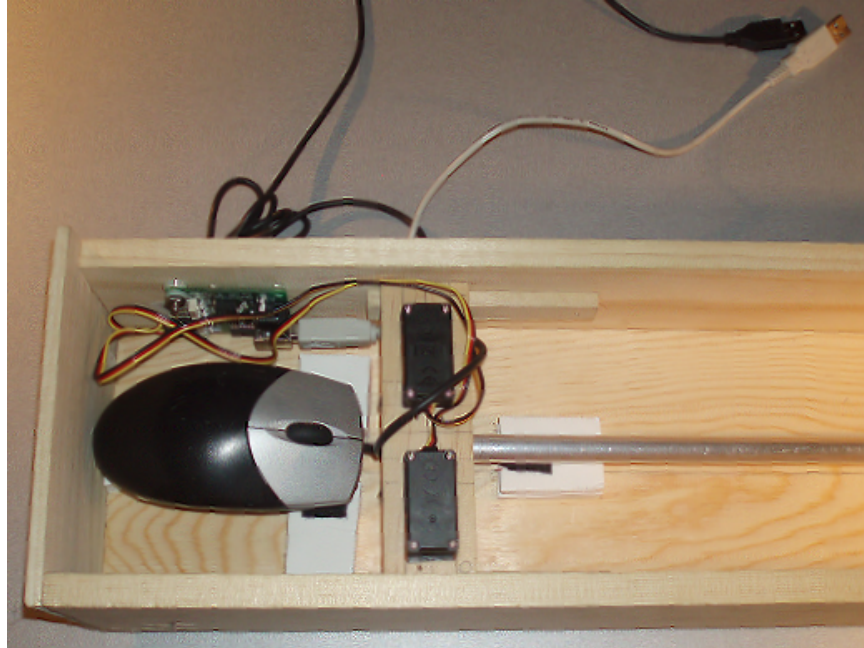


**Figure 4.2:** Haptic feedback interface with motors installed.

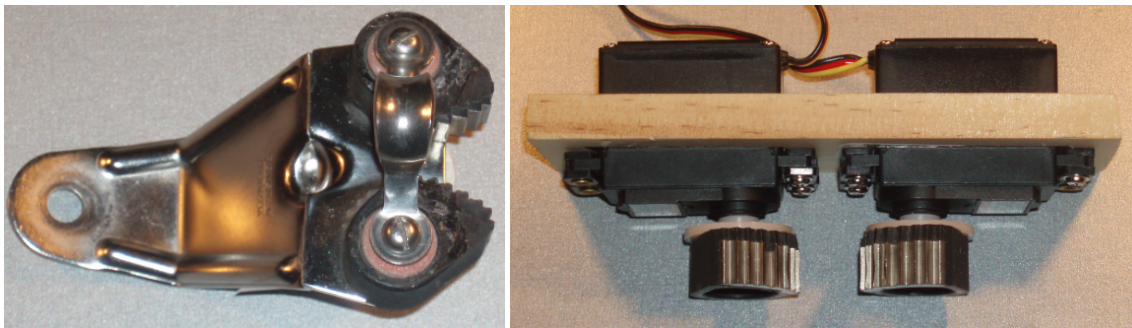


**Figure 4.3:** Sailing cam cleat with spring-loaded cams (Ronstan, Australia) prior to its refurbishment for the simulator (left); following its attachment to the servo motors (right).



$\Delta x$ ) as it passes through the guide tube. A 4'' section of the tube is glued to the underbelly of the mouse with a small notch cut out to allow the optical sensor of the mouse to detect motion as the probe moves through the tube. A scaling factor, calculated from the physical diameter of the probe and the relative  $\Delta x$  changes in the mouse coordinates, is used to provide accurate visual feedback when the user twists the probe (e.g., with the probe approx. 2.5 cm in circumference, mapping to 350 pixels when using the mouse, one complete rotation ( $2\pi = 350$  pixels) of each pixel change is about 0.018 radians, the camera roll scaling factor is therefore set to 0.02).

2. Servo motors and the Phidgets [26] interface kit (Figure 4.3). Two servo motors mounted on a wooden platform are the primary force feedback interface. The motors are mounted such that the probe passes midway between the two motors after it exits the guide tube in the first stage. The servos operate at 50 Hz with an accuracy of  $0.1^\circ$ . An interface kit mounted along the inside wall of the enclosure controls both the servos. The interface kit is connected to the computer through USB and allows the simulation program to read and set the values of the motors.
3. Cam cleats. The re-configured cam cleats are glued to the servo motors with the help of attachments that were provided in the motor kit.
4. Aluminum tube and probe. A 1 cm diameter aluminum tube is used along the base of the box to guide the probe through the box. The length of the guide tube beyond the motors is approximately 18''. The guide tubes were cut to size and placed in the box such that the probe is always in the guide tube, except when it passes through the cam cleat. The probe used was that of a real but inoperative optical borescope.

#### 4.2.2 Operation

The operation of the haptic box can be divided into two related functions: probe feed measurement provided by the optical mouse and active force feedback provided by the Phidgets interface unit. In the first stage of the interface, the borescope probe passes underneath the optical mouse. The braided cable enclosing the optical fibers of the borescope provides a sufficiently rough surface to enable the optical sensors of the mouse to detect motion. The guide tube attached to the base of the mouse constrains the motion of the probe such that the optical sensors can pick up slight changes in the probe's translation and twist.

The translation and rotation of the camera are controlled by the relative change in the mouse coordinates obtained from the first stage of the haptic box, which in turn is controlled by the participant

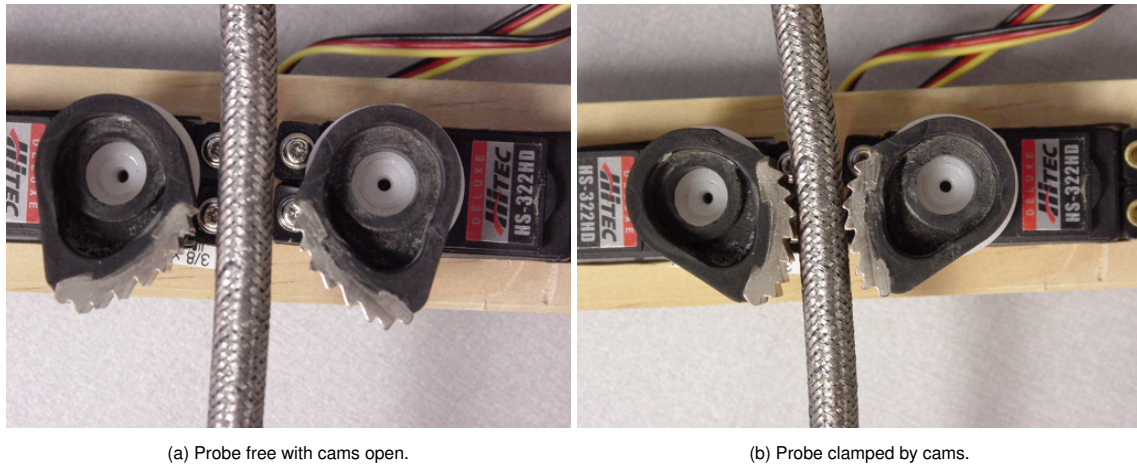


**Figure 4.4:** Motor operation with the motorized cam cleat (direction of insertion is up). Note that once clamped, further insertion is prevented, however, retraction of the probe is still possible.

inserting or withdrawing an actual borescope probe into a guide tube fixed within the haptic box. A scaling factor is used to map the relative change in mouse coordinates to the physical parameters of the probe used in the study. The translation of the camera is always along the view vector, either forward when the user pushes the probe into the haptic box or in reverse when the probe is withdrawn.

A simple collision response is implemented in the simulator. At every frame, changes in camera position and orientation are checked with the bounding sphere of the nearest component in the virtual model. The camera is updated only if there are no penetrations of the surrounding model. Note that this does not take into consideration the angle of incidence of the camera with the intersecting surface. In the real borescope, the behavior of the probe is dependent not only on the angle of contact with the surface, but also the force applied by the user and the location of the probe tip.

The interaction of the motors with the simulation is more involved. The cam cleat was specifically chosen because of its serrated cams. Figure 4.4 depicts the two stages of the motor operation. In Figure 4.4 (a), the position of the two motors is such that the cams are open and the probe is free to pass through (in both forward and reverse directions). Figure 4.4 (b) shows the position of the two motors that results in the cams clamping shut on the probe. The force applied to the probe by the cams is just sufficient to prevent the probe from moving in the forward direction but provides no hindrance to translation in the reverse direction. The serrated metal cams grip the probe's sheath and provide a slip-free hold on the probe.

The servo motors are controlled with the Phidget motor interface board. This board is connected to the computer through the USB interface and is integrated into the virtual borescope simulator. When there

is no intersection of the virtual camera with the model geometry, the servo motors are programmed to open the cams to allow free motion of the probe. When the simulation detects intersection between the virtual camera and the model geometry, the motors rotate the cams shut. Note that we use only one pair of motors to simulate force feedback in only one (the forward) direction.

Note that haptic feedback is currently provided only when the camera intersects the model geometry in the forward direction. Intersections of the camera when the probe is being withdrawn from the haptic box do not result in any force feedback, although this is somewhat important in the actual task. The borescope tip may break if the articulated camera tip catches on a surface during extraction. The reason for the lack of force feedback in our simulator during extraction is twofold. First, the majority of probe maneuvering takes place when the participant starts the inspection procedure. Once the probe is positioned within the space between the two stator blades and the simulated engine inspection has begun, the primary motion is forward probe feed into the box accompanied by camera articulation. Second, in the actual task, the inspector has the option to reset camera articulation by pressing a “home” or reset button. This reduces the chances of probe entanglement and tip breakage when being withdrawn. We felt that the most important probe contact forces that needed to be simulated were forces in the forward direction.

### **4.3 Experiment 3: User Evaluation of Haptic Box**

The purpose of the empirical evaluation was to gage the effectiveness of the haptic force feedback provided by the haptic box. We hypothesized that haptic feedback would provide a measurable effect in simulator usage. We were also interested in users’ subjective impressions of the device.

#### **4.3.1 Participants**

Eight participants (all male) were recruited to evaluate the virtual borescope and the force feedback device. All participants were familiar with optical borescope inspection and had prior experience in aircraft engine inspection (average experience was about 6 years). The aims of the experiment were explained to all participants and informed consent and demographic data collected prior to its commencement. All participants were right-handed and were seated during the testing phase of the experiment (Figure 4.5).

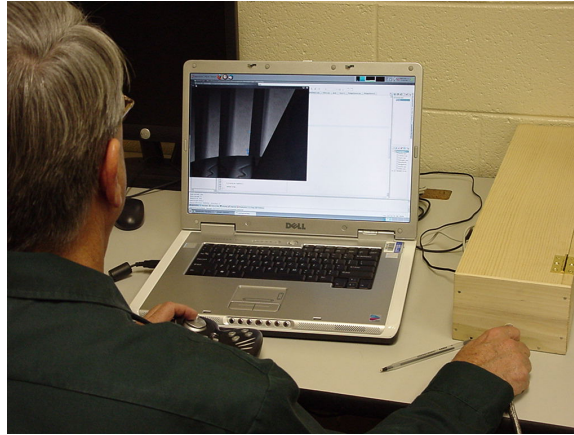


**Figure 4.5:** Experimental setup.

### 4.3.2 Apparatus and Stimuli

The simulator was run on a Dell 9300 laptop, equipped with 2 GB RAM and a GeForce 6800 video card. The simulator's visual output was presented in a 1024×768 window on the 17" screen on the laptop. The simulator maintained an interactive frame rate (60 fps) throughout the experiment. The laptop was placed on the table directly in front of the participant.

The haptic box was placed about 6" to the right of the laptop so that the participants used their dominant hand for the probe feed, and their non-dominant hand to control the gamepad. An old borescope probe, approximately 6 feet in length was manually inserted by the volunteers into the haptic box during the experiment. To simulate the rotation of the turbine, one of the gamepad buttons was mapped to modify the scene graph to rotate the turbine (in the real task, turbine rotation is usually performed manually by the inspector or by an accomplice). The participant could visually observe the turbine rotating when the button was pressed. The button was selected such that the participant could control the manipulation of the virtual camera with one hand on the gamepad.

In both test conditions, participants used the gamepad and the probe feed to control the orientation and translation of the virtual camera. The visual feedback that the participants received was the same in both conditions. The only difference was the feedback that the participants received when the software detected intersection of the virtual camera with the engine model geometry. In the visual only condition ( $V$ ), the only indicator of camera intersection was visual, i.e., the simulator would not update the display until the participant either changed the position of the camera by moving the probe through the haptic box or changed the orientation of the camera. In the visual and haptic condition ( $V+H$ ), intersections of the virtual camera

with the model in the forward direction resulted in the motors engaging the cam cleat to clamp on the probe. The forces on the probe were calibrated such that it would not move in the forward direction but could be pulled out easily. The clamps disengaged when the participant either pulled out the probe or changed the orientation of the virtual camera and there was no penetration of the camera with the model.

Due to the use of the servo motors to control the force feedback, it was observed that engaging and disengaging of the cam cleats was accompanied by an audible noise from the motor. Prior research has shown that auditory cues can influence task performance, either when separate from visual cues or when used concurrently with visual feedback [74]. To prevent the participant from using these auditory cues, the device was completely enclosed to dampen the motor noise. To further mask the cam cleat's motor noise, a dummy motor was placed in the haptic box which randomly changed its position and emitted a sound similar to the motors controlling the cam cleats. Participants were informed that the noise was the probe feed device working. The participants were intentionally kept unaware of the contents of the box.

### **4.3.3 Procedure**

To begin, participants filled out a brief inspection experience questionnaire. They were then seated in front of the test computer and were instructed on the use of the gamepad to control the orientation of the virtual camera and the probe feed to control the position of the camera. The starting position of all the participants was the same. Participants were instructed to maneuver the camera through the first stage of the stator and start the inspection of the rotor, as they would normally do in the real task

Instead of defects in the model of the engine blades, visual markers in the form of a numbered sequence were used to guide the inspection process. The participants were instructed to first inspect the leading edge of the blade and then the trailing edge. On completion of one face, they were asked to change the orientation of the camera to inspect the back face of the next blade. Once they had completed inspection of one blade, participants were asked to move onto the next blade by pressing the gamepad button to turn the rotor and repeat the inspection process.

In the first phase, participants were provided training with the visual stimulus and the haptic box. This phase was untimed and allowed familiarization of the control interfaces. Once users were proficient in using the interfaces, they were asked to inspect the first 5 marked blades on the rotor under one of *V* or *V+H* conditions. On completion of this first task, participants were given post-test and workload questionnaires to complete. After a brief familiarization phase with the second interface, participants performed the same inspection process with the second interface. Participants then filled out a second questionnaire followed by

a post-test debriefing.

#### 4.3.4 Design and Data Collected

A within-subjects design was used for this experiment due to the limited pool of experienced borescope inspectors. We tested the simulator under two conditions: visual only condition ( $V$ ) and combined visual and haptic condition ( $V+H$ ). Haptic feedback constituted the independent variable. Time taken to complete inspection of the virtual model served as the dependent variable. The alternating order of the two conditions was balanced evenly between subjects so that half started with the visual only condition first while the other half started with the combined condition.

We collected subjective data in the form of questionnaire responses and performance data in terms of time taken to complete each of the tasks. The questionnaire was divided into three sections: visual realism, interface evaluation, and perceived workload. The visual and interface related questions were derived from Witmer and Singer's presence questionnaire [72], while the workload section was derived from the NASA TLX questionnaire [27]. The responses for all the questions were on a 5-point Likert scale, with 1 indicating strong disagreement, 5 strong agreement, and 3 neutral.

#### 4.3.5 Results

Performance data collected was time taken for completion of the task. The data was analyzed using SAS v9.2. The average time taken for completion of the task with both visual and haptic feedback ( $V+H$  treatment condition; mean time = 280.75 s) was shorter than the average time taken to complete the task with only visual feedback ( $V$  condition; mean time = 306.50 s), although not significantly so ( $F(1,7) = 0.58$ ,  $p = 0.47$ , n.s.), according to a repeated measures one-way ANOVA. An ANOVA performed on the completion times with the participants as the blocking factor revealed the participant as a significant main effect ( $F(7,7) = 5.56$ ,  $p < 0.05$ ), as shown in Figure 4.6, indicating significant variability between subjects.

Friedman's test performed on the subjective data found significant difference in only one of the questionnaire responses (Q11;  $\chi^2(1, N = 8) = 3.84$ ,  $p < 0.05$ , see Table 4.2). Figure 4.7 shows the average responses to the questions provided by the participants. In the post-test debriefing, 6 out of 8 participants preferred the simulator with force feedback, one had no preference for either condition while the last had no comments.

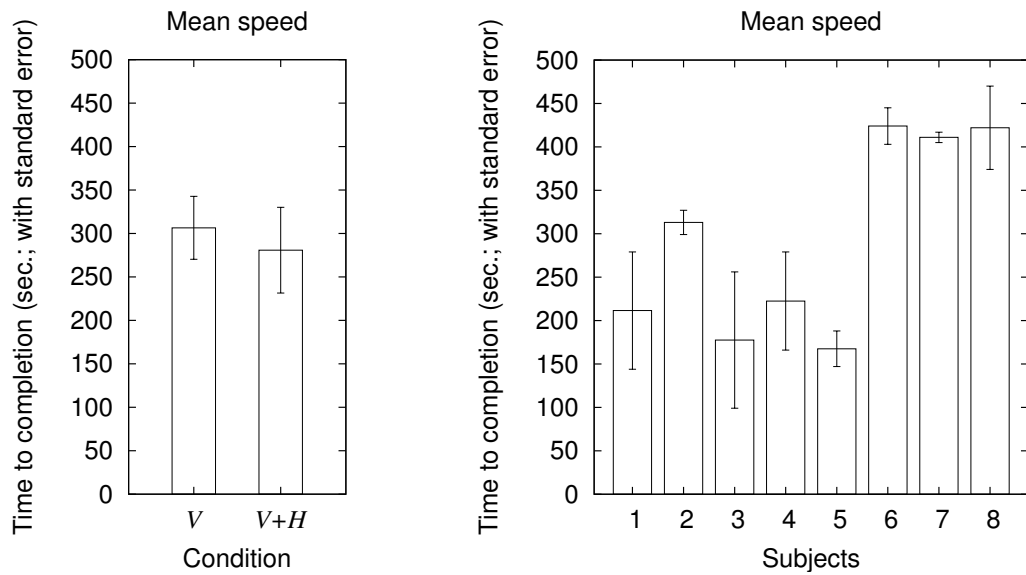


**Figure 4.6:** Speed comparison between conditions and subjects: Visual (V), Visual and Haptic (V+H).

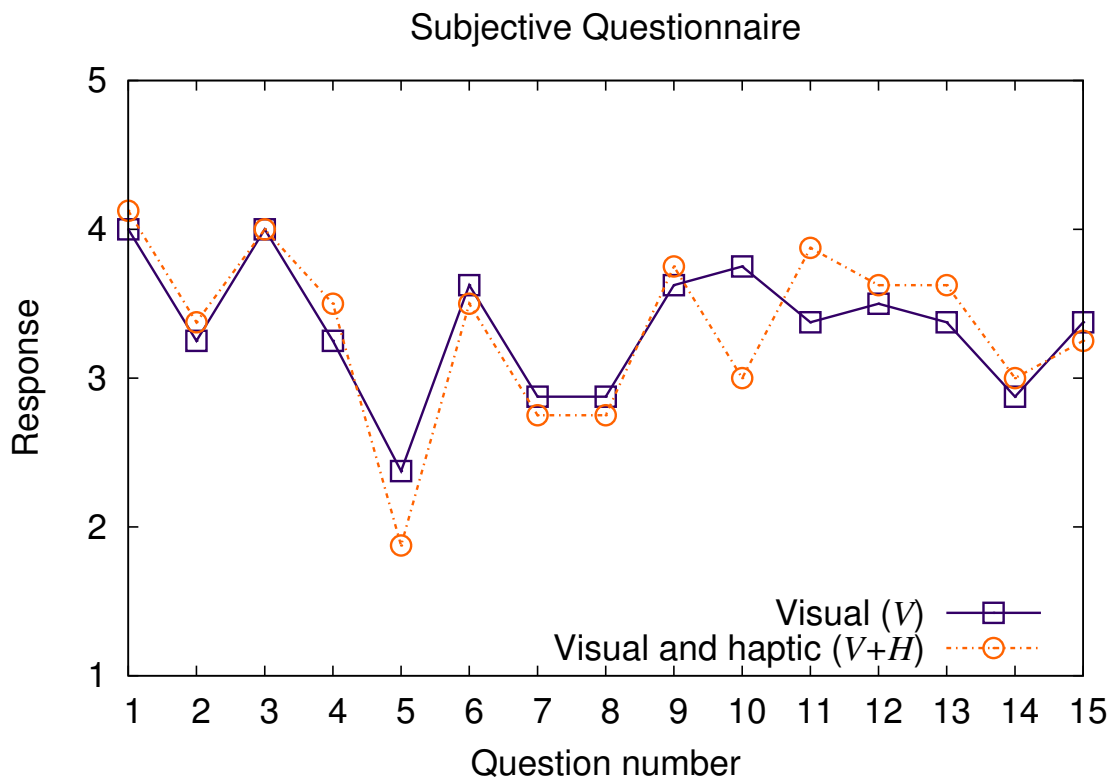


**Figure 4.7:** Subjective impressions (average) regarding system use. Users' responses were made on a 5-point Likert scale corresponding to agreement with the questionnaire statements (1:strongly disagree, ..., 5:strongly agree) listed in Table 4.2.

Visual section	
1.	I was involved by the visual aspects of the environment.
2.	The visual aspects of the virtual environment seemed consistent with my real-world experiences.
3.	I could examine objects from multiple viewpoints.
4.	There was no delay between my actions and expected outcomes.
5.	The visual display quality interfered with performing the task.
Control and workload interface section	
6.	The interactions with the environment seemed natural.
7.	The mechanism which controlled movement through the environment seemed intuitive.
8.	The control mechanism and/or control device was distracting.
9.	Manipulating the borescope tip in the virtual environment seemed compelling.
10.	I could concentrate on the task rather than on the mechanisms used to perform the task.
11.	The mental and perceptual activity required (e.g., thinking, deciding, calculating, remembering, looking, searching, etc.) was very high.
12.	The physical activity required (e.g., pushing, pulling, turning, controlling, activating, etc.) was very high.
13.	I had to work (mentally and physically) very hard to accomplish my level of performance.
14.	I felt frustrated (discouraged, irritated, stressed and annoyed versus gratified, content, relaxed and complacent) during the task.
15.	I think I was successful in accomplishing the goals of the task.

**Table 4.2:** Subjective questionnaire for evaluation of haptic interface.

### 4.3.6 Discussion

Results indicate no significant effect of haptics on performance. The data suggest a trend of participants completing the task faster with haptic feedback, but the significant variability among subjects may be masking its effect on performance. The results, although inconclusive, are in line with previous studies suggesting that haptic feedback improves performance (mean time to task completion) [64, 68]. Lack of significance in our performance analysis may be due to the inspectors' inexperience with a video borescope or the simplicity of our chosen task, as explained below.

Participants in our study were experienced borescope inspectors, but their inspection experience was mainly with the optical borescope and not the video borescope we are simulating. Of the 8 participants, only 2 had prior experience with the video borescope, while the remaining 6 had limited to no previous experience. Unlike its video counterpart, the optical borescope has simpler probe articulation controls and an eyepiece for visual feedback from the probe's tip that is much smaller than the video borescope's screen. We suspect that participants paid more attention to the visual output due to its novelty, i.e., its larger field of view and higher resolution than what they were accustomed to. Furthermore, because vision tends to dominate touch (particularly when in conflict [54]), and because the inspection task is inherently visual, it may be that haptic feedback was simply ignored under present experimental conditions (e.g., the task lacked a sufficiently compelling tactile component to begin with).

Engine inspection is a repetitive process, where the inspector first maneuvers the probe through the



guide tube past numerous internal components of the aircraft engine. Once the blades to be inspected are in the borescope camera's field-of-view, the interaction is limited to the articulation of the probe tip and hence the camera. Instead of translating the probe, the inspector rotates the blades to inspect the rest of the engine. Tactile feedback is not needed for this task, rather, it is only needed when the inspector is maneuvering the probe into and out of the engine—we conjecture this is when tactile response is most important for avoiding damage to the borescope camera. In our experiment, participants were given a very simple scenario where they navigated through just one set of stator blades and performed a limited inspection of 5 blades of the turbine rotor. As the inspection was performed mainly by changing the orientation of the camera through the gamepad controls, haptic feedback was of little use during the actual visual inspection process.

In case of visual feedback with no haptics ( $V$ ), the only cues presented to the participant were visual where the camera stops on intersection. Irrespective of the amount of probe fed into the box, there is no change in the visual stimulus. In the case of the combined ( $V+H$ ) condition, the probe feed is stopped whenever there is intersection with the model. Thus in addition to the visual feedback, the participant also receives haptic feedback which prevents them from pushing the probe into the box any further. We believe the provision of both forms of feedback led to a faster mental registration of the model intersection and hence faster response to the stimulus.

The responses of the participants to the questionnaire revealed that they perceived the visual stimulus to be somewhat similar to that of the actual task (Q2). Since the visual stimulus was the same in both experimental conditions, no significant difference conditions was detected (none was expected). Participants reported that they were involved in the task by the visual output of the simulator (Q1) and that they could examine the objects from multiple viewpoints (Q3). From the remaining responses concerning visual realism (Q4 & Q5), we can infer that the interaction delay and visual display characteristics of the simulator did not significantly alter the perception of the inspection process. During the post-test debriefing, participants commented on the visual realism of the simulator, stating that it conveyed the engine inspection process accurately.

In the interface evaluation part of the questionnaire, participants noted that the interaction with the environment seemed somewhat natural (Q6). In the debrief some commented that they became “as lost in this as the real thing” and most noted that they had trouble getting used to the single-handed gamepad interface (although their response regarding the intuitiveness of the control (Q7) was neutral). Unlike the real control interface, we chose to use an off-the-shelf gamepad, which is normally manipulated by both hands. Since participants had to use their dominant hand to control the probe feed, they had to use their non-dominant hand

to balance and control the gamepad. Also, most of the participants had experience with the optical borescope where the control interface is simpler than the video borescope's. In this experiment, since the gamepad was used equally in both conditions, we can infer that it did not have any effect on performance. The neutral response to the question concerning distraction of the control (Q8) supports this reasoning.

The workload effects portion of the questionnaire compared the experience of using the virtual simulator under the two conditions. Participants reported that the mental and perceptual activity required for the inspection task was significantly higher with the haptic force feedback than without (Q11). This suggests that participants may have found the provision of haptic feedback extraneous in this particular task. Given the simplistic nature of the task, and the limited opportunity for interaction of the probe tip with the model surfaces, we believe that vision dominated the test scenario. The addition of haptic feedback may have distracted participants (hampered their concentration; Q10) and required marginally greater perceived mental and physical effort (Q12 & Q13). This increase in workload can be attributed to participants having to concentrate not only on the visual feedback, but also the force feedback received from the haptic box. In other words, the combined visual and haptic form of feedback was found to be more engaging than visual feedback alone. Overall the participants reported that the workload was similar to their experience in the actual task.

Most participants reported in the debrief that the simulated representation of the engine interior was visually realistic. However, they found the unconstrained articulation of the camera not to be as realistic as the actual optical borescope's. They reported that unlike the actual borescope, they could perform a full rotation of the camera. Participants also mentioned that the control interface took practice getting used to, but once they had experience using the articulation controls, they felt proficient in using the gamepad. At the end of the experiment, most participants noted that they preferred the provision of haptic response over the purely visual interface. Some noted that the combined interface "feels like the real thing" and "you need to have some force when the borescope hits the engine". Overall they reported positive experience with the haptic interface and one suggested that, for training purposes, intensive training with the visual only condition for familiarization with the control interface followed by simulator experience with haptic feedback would provide the best learning opportunity.

## Chapter 5

# Physically-based Probe Model

In a training simulation, two requirements must be fulfilled: the simulation must be realistic, and it must function in real time. During preliminary evaluation of the visual and behavioral realism of the borescope simulator, one common complaint was that the camera motion and articulation were very different from the real borescope. As we had implemented the camera as a point in space, with full 360° articulation about the three axes, participants reported that they got lost while navigating the engine model. As probe control and articulation is an essential skill for successful engine inspection, we decided on improving the model of the articulating probe tip to increase the behavioral realism of the simulator.

While graphics rendering focuses on the visual appearance of the model, haptic rendering simulates provision of force feedback and computes appropriate force/torque sensations for the human operator to feel the geometry, surface and material properties of the object. There are two major points of asymmetry between haptic and graphics rendering: collision detection and rate of dynamic simulation. Unlike graphic rendering which only needs to model object deformation to “look” realistic, haptic rendering has to be built upon a more accurate physics-based model. Also, the real-time update rate in graphics rendering is around 30-60 frames per second, while smooth haptic rendering requires an update rate of almost 1 KHz.

In haptic interface design, the deciding factor in choosing the best collision algorithm is the speed of calculation to determine whether a collision has occurred. Inter and intra-object collisions play an important role in the overall behavior of the interacting objects in a simulation. The choice of the contact model, single point versus multi-point contact detection and external forces such as static and dynamic friction influence the post-impact motion of the interacting objects. Quick changes in haptic forces when objects intersect can cause artificial growth of energy and lead to instabilities of the simulation [58].

Modeling and simulation of the borescope probe interaction is a challenging problem. Prior work in the medical simulation community has led to development of fast, scalable, multi-object, multi-point collision simulation and response algorithms [8]. In the following sections, we present work related to graphic and haptic simulation of deformable models and the constraints that have to be satisfied for believable interaction. We conclude by presenting our implementation of a mass-spring damper model of the borescope probe that provides fast response for both graphic and haptic rendering.

## 5.1 Prior work

Intersections of the borescope probe with the engine can occur at multiple points along the inserted length. Probe deformations occur due to collisions with the engine, and the amount of deformation is dependent on the position within the engine, force applied at the point of incidence as well as the angle of incidence of the probe at the point of contact. Unlike medical procedures, which use a catheter, such as vascular and cardio-thoracic surgery, interaction of the borescope probe with the engine consists of a semi-flexible body interacting with a rigid body. Instead of computing elastic and deformation forces experienced by the catheter due to the soft tissues, computation of deformations can be limited to the interaction of the semi-flexible probe with the rigid body.

Prior work, especially in radiology and vascular surgery [11, 12, 20, 42, 49], has resulted in visual and behaviorally realistic models for simulating catheters, guidewires and surgical threads. Deformable objects have been simulated using physically-based mass-spring models following Newtonian Laws of motion. The catheter or surgical thread is modeled as a linear system of point masses connected by linear and torsional springs between two adjacent points. Using explicit or implicit numerical integration, the velocities and positions of each point mass is computed over the duration of the simulation. Since collision detection is computationally expensive, methods are such as bounding spheres, axis-aligned bounding boxes (AABBs) or bounding volume hierarchies (BVHs) are used to speedup collision testing.

Dawson et al. [19] developed a catheter simulation based on a multi-body system composed of a set of rigid bodies and joints. Although the discrete model was a good approximation of a catheter, it required many small links to represent the catheter with a high degree of flexibility. Pai [52] proposed modeling one-dimensional deformable objects as Cosserat rods, with all possible deformations of a one-dimensional object to overcome the limitations of physical models such as mass-spring methods. However, contact handling with such a model is difficult for catheter navigation, where collisions occur continuously along the length

of the device. Brown et al. [15] presented a physical simulation model called Follow The Leader (FTL), where selected nodes are first moved by grasping them with an external manipulator, say a haptic device, with the other nodes moving to maintain the original inter-point distance. Alderliesten et al. [2] developed a simulation of the guidewire insertion into the vascular system. The discrete representation consisted of incompressible rigid segments simulating the guidewire, with Hooke's law used to model the bending and interaction of the guidewire with the vasculature. Wang et al. [70] implemented a physics-based simulation of a thread model, which took into account Newton's laws of motion as well as properties of real threads such as stretching, compression, bending and twisting. The model was integrated into an interventional radiology simulator, with real-time contact detection, self-collision and haptic feedback [71]. Kubiak et al. [32] present a real-time simulation of thread dynamics with all the relevant aspects of the physics model of the thread, including stiffness, bending, torsion and self-collision, and output forces for haptic feedback. Explicit numerical integration using the Verlet integrator led to a stable, controllable and computationally light simulation.

The main advantage of mass-spring methods is that they are fast, easy to implement and, with appropriate collision detection algorithms, can support haptic rates exceeding 1 KHz. However, the stability of the system depends to a great extent on the simulation parameters chosen. Simulation of interactions of rigid objects with large stiffness requires a small timestep for numerical stability, which in turn affects the interactive rates of the simulation. Biological materials, such as tissues, exhibit non-linear elasticity and are not at all homogeneous, so choosing realistic simulation parameters for the spring constants is time consuming.

Finite element models (FEMs) have been proposed as a solution to the difficulties with simplified physically-based systems. In mass-spring systems, the object is represented as a set of discrete point masses connected by springs. The initial formulation is discrete and any deformations of the model changes the level of potential energy in the model. By contrast, FEMs provide a continuous formulation that relates the model deformation to energy. FEMs compute deformation over the entire volume instead of at discrete points, and hence are more accurate than mass-spring systems, but at the expense of added computational complexity.

Contin et al. [18] developed a real-time model for deformation of devices such as catheters and guidewires during navigation inside complex vascular networks. The simulation is based on a static finite element representation and provides for collision response with a large number of contact points. Based on this approach, Lenoir et al. [38] used a composite model to realistically simulate a catheter/guidewire system, to perform operations such as stent placement in a simulated environment [39], and to simulate deformations

produced by the guidewire as it moved through a catheter at about 45 Hz for a catheter consisting of 100 nodes.

In addition to the graphical simulation of deformable objects, Laycock and Day [36, 37, 35, 34] have presented multiple algorithms to model the interactions of a deformable tool with a rigid body. The deformable tool, in this case an elastic rod, is modeled as linear chain of 6-DOF nodes and its behavior calculated using FEM analysis. Translational and rotational properties as well as realistic deformation of the beam elements were implemented. However, the simulation performance degraded as the number of nodes increased, due to the computational complexity of increased collision detection required for the additional nodes.

Our implementation probe model is based on Globular Elastic Models (GEM) [17] used to simulate deformable objects, but instead of computing the medial axis transform, the borescope probe is modeled as a discrete linear chain of point mass nodes  $(p_0, \dots, p_n)$  with damped linear and angular springs connecting adjacent nodes. We describe the model in the following section.

## 5.2 Implementation

Successful implementation of a physically based probe model requires fast detection of collisions, computation of interacting forces from internal mass-spring model of the simulation as well as external forces due to the point-proxy model, and collision response from the computed forces. We implemented a hybrid probe model combining the deformation modeling of a linear mass-spring system, and collision detection and response through a chain of point-proxy nodes.

### 5.2.1 Conceptual model

Figure 5.1 shows a diagrammatic representation of the borescope probe model. The foremost nodes control articulation of the virtual probe. Rotational torques can be directly applied to the foremost node, which is used to calculate the final position of the trailing nodes in the model through dynamic simulation of the whole mass-spring system. The nodes abaft the lead nodes do not directly control the articulation of the tip, but simulate the connected linear length of the probe. Aft nodes in the guide tube serve as anchor nodes and do not take part in the control of the tip articulation.

Linear elongation springs between adjacent nodes provide axial compression and elongation, and angular springs simulate flexion and torsion of the probe. The behavior of linear and angular springs is based

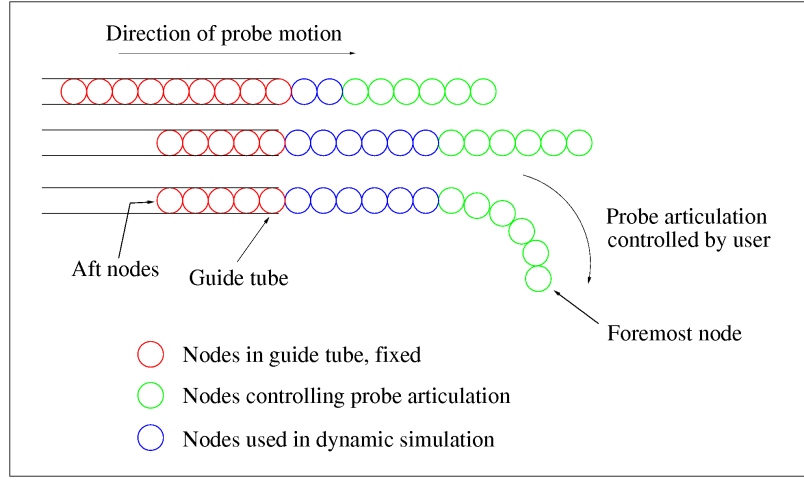


**Figure 5.1:** Representation of the linear chain of nodes used to model the borescope probe. Each adjacent pair of nodes is connected by a set of linear and angular springs.

on Hooke's Law. The rest length between two adjacent nodes,  $l_r$ , is a predefined constant (see Figure 5.2). To simulate bending curvature, the rest length between the adjacent nodes should be small. The linear elongation and compression forces experienced by the nodes connected by axial spring is given by:

$$\mathbf{F} = -k_e \Delta l \quad (5.1)$$

where  $\mathbf{F}$  is the restoring force exerted by the spring,  $k_e$  is the spring linear constant, and  $\Delta l = l - l_r$  is the amount of elongation or compression from rest length,  $l_r$ .

Similarly, the angular torques experienced by the probe due to flexion about the  $y$  and  $z$ -axes (see Figure 5.3) cause articulation of the probe. Four angular springs are used to control the orientation of the nodes about the center line. Torques due to flexion are computed as:

$$\tau = -k_f \Delta \theta \quad (5.2)$$

where  $\tau$  is the computed angular torque due to flexion,  $k_f$  is the angular spring constant, and  $\Delta \theta$  is the change in the angular orientation from its rest orientation. Torsion between adjacent nodes is due to a single angular spring about the centerline adjacent nodes. Torsion is computed similar to the flexion and is applied at the center of the two nodes.

Although the parameters of the spring constants are important, prior work has used heuristic methods to determine the values. In our case, axial compression and torsion about the longitudinal axis ( $x$ -axis) is

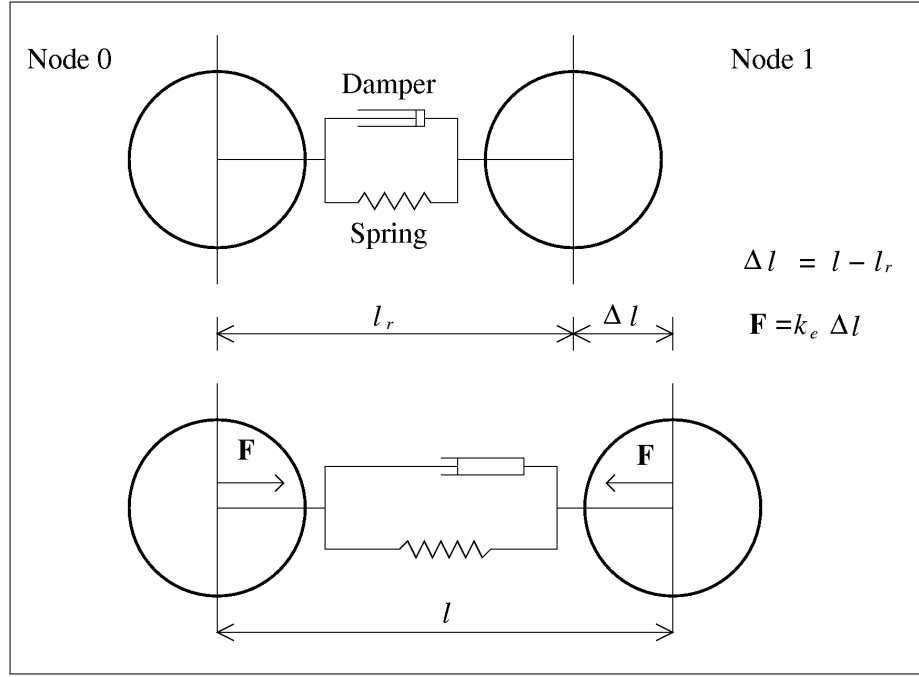


**Figure 5.2:** Linear elongation due to spring between two adjacent nodes of the probe.

significantly smaller compared to the flexion about the  $y$  and  $z$ -axes. This can be modeled by using large values of spring constants for elongation and torsion, but smaller values for flexion.

In addition to computing the internal forces due to the elongation, flexion and torsion of the springs connecting the nodes, damping forces were also computed and applied to stabilize the mass-spring system and prevent oscillations. The system was critically damped, with the damping constant computed for each spring as:

$$\mathbf{d} = 2 \sqrt{km} \quad (5.3)$$

where  $\mathbf{d}$  is the computed damping constant,  $k$  is the spring constant, and  $m$  is the mass of the node. Damping forces were computed for each of the three springs acting on the node. Unlike computing the forces on a per-node basis, the damping forces were computed on a per-link basis, and applied to each of the nodes connected to the springs, but in opposite direction to the application of the spring forces.



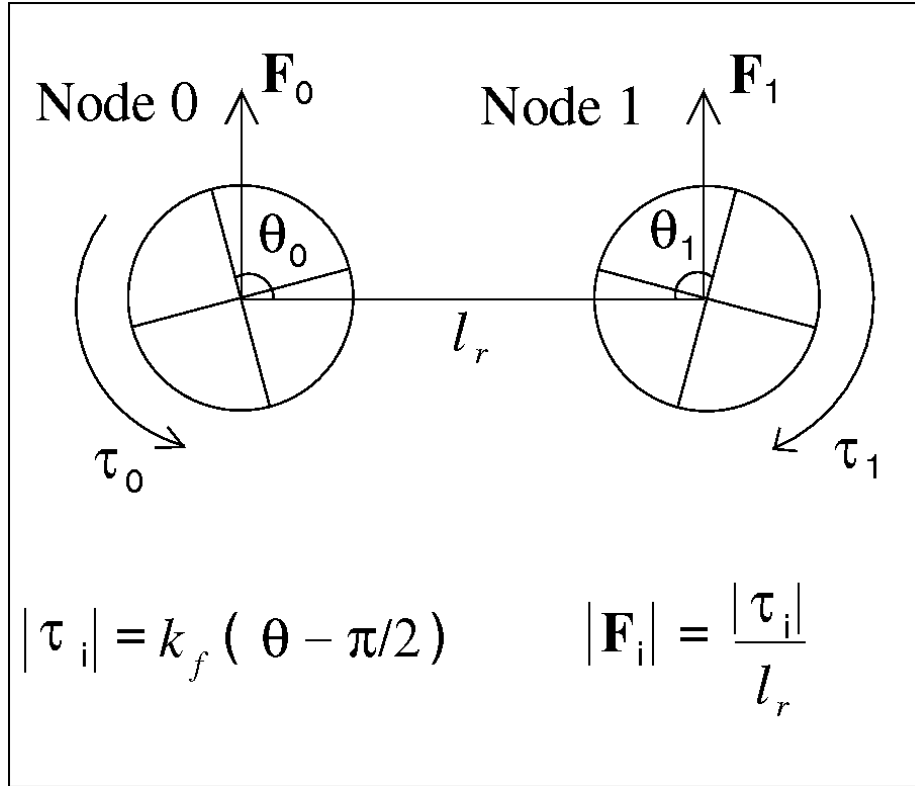


**Figure 5.3:** Angular response due to flexion and torsion, resulting in bending and articulation of the probe in planar space.

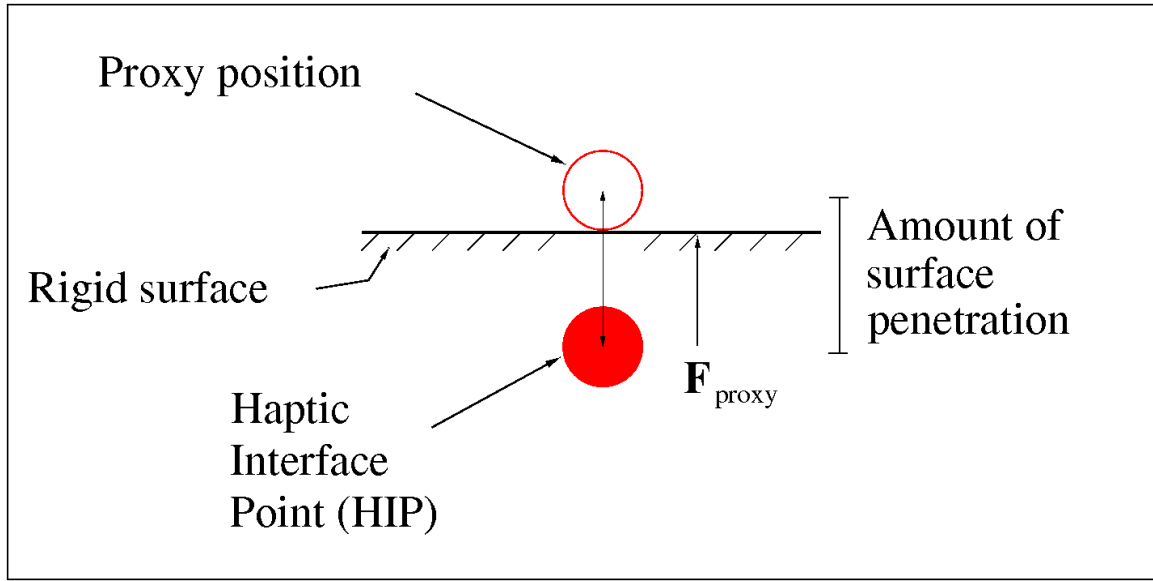


**Figure 5.4:** Single point contact with position of Haptic Interface Point (HIP) and proxy position.

### 5.2.2 Collision detection and response

Haptic rendering is the process of computing a reaction force for a given position of the haptic interface in the virtual world. Unlike visual stimulus, human estimation of spatial dimensions through haptic exploration has a larger threshold for error. In single point haptic interaction, the haptic device allows the user to interact with the objects in the virtual world. To prevent the haptic interface point (HIP) from penetrating into the objects, Zilles et al. [75] proposed the “God-object” and Ruspini et al. [56] the “virtual proxy” models, where the visual representation of the HIP in the scene, the proxy, is constrained to the surface of the object it is in contact with, as opposed to penetrating the object (see Figure 5.4). The proxy point is constrained to lie on the surface of the object, and represents the position of the HIP in the scene if the object were infinitely stiff.

The contact point of the HIP and objects in the scene can be obtained through simple geometric methods and the proxy-point force algorithm used to compute the haptic interaction forces. The most commonly used function to compute the feedback force is based on the penalty method, where the force exerted due to penetration of the HIP into the model is:

$$\mathbf{F} = -k\delta$$

where  $\mathbf{F}$ , the reaction force, is computed as a function of  $k$ , the spring constant (usually a large number for

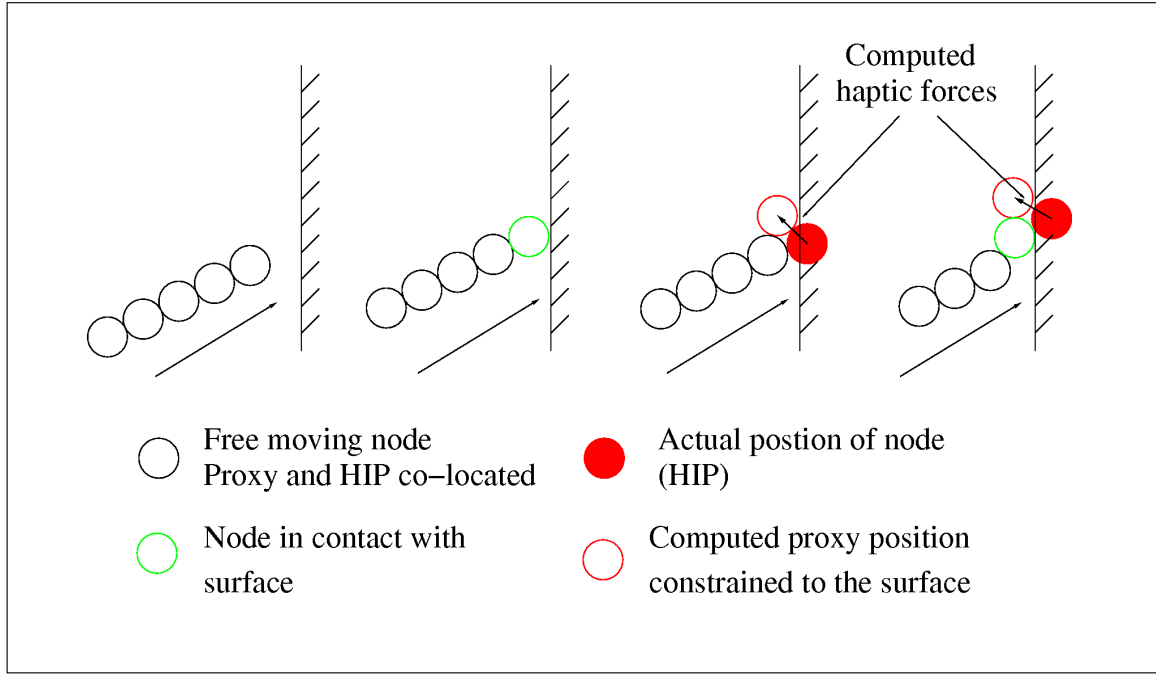


**Figure 5.5:** Simulation of probe model with multiple points of contact, calculated by taking into account the dynamic model of mass-spring system and point-proxy HIP forces.

stiff objects), and  $\delta$  is the linear distance between the HIP and the proxy point.

We extended the single point-proxy method to multiple contact points to model the interaction of the borescope probe. In addition to the linear chain of point masses as described earlier, each node is associated with a proxy node. The proxy node is used for probe visualization by constraining its position to the surface of the intersecting object. The proxy node also serves to exert an unbalanced external force based on the penalty method, which is applied to the node as an external force and used in the position calculation.

Figure 5.5 depicts the interaction of the simulated probe consisting of 5 nodes colliding with a rigid wall. The arrow at the bottom of the figure depicts the direction of motion of the probe. In the left figure, the probe is free to move and there is no intersection with the wall. On detecting intersection (middle figures), at the point of contact, both the actual and the proxy position of the node are co-located. As long as there is no further motion of the probe, the force exerted at the contact proxy position is zero. In the right-most frame, we see that the probe has advanced further along the direction of motion. The actual position of the leading node is inside the wall, but the computed position of the proxy node (depicted as a red circle) is constrained to the surface of the object. External forces computed by the proxy-point algorithm are added to the position of the node (filled circle) and the dynamic simulation of the probe computed. As long as the actual and the

proxy position of the node are different, a linear spring force is exerted.

### 5.2.3 Dynamic Simulation

In the simulation of the probe, we had to consider the interaction of the user with the borescope probe. There are two basic actions that the user performs during borescope inspection: insertion of the probe into the engine and tip articulation using the hand-held interface. We simulated the virtual probe as it emerges from the guide tube in the virtual model of the engine. A gamepad is used to directly control the articulation of the virtual probe by applying an unbalanced torque to the foremost node of the probe tip. Simulation of the probe takes into consideration both the internal forces acting on the nodes due to the mass-spring system as well as the external forces that arise due to node contact with objects in the scene.

The main steps in the dynamic simulation of the probe model are:

1. Clear internal forces and torques: At the beginning of the simulation, each node starts at equilibrium state where there are no internal unbalanced forces. There may be external forces such as the contact forces that arise from the probe proxy as it collides with the models in the environment or external unbalanced articulating torques applied to the foremost node of the virtual probe.
2. Calculate per-node and per-link forces and torques: The internal forces due to elongation, flexion and torsion springs used to connect the adjacent nodes in the mass spring system are computed at each step in the simulation and stored in the state space of the nodes they affect.
3. Numerical integration: Once forces and torques are computed, they are used to compute the next position and orientation of the node. We used a simple Euler solver to numerically integrate the new position and orientation of the node.
4. The newly computed position and orientation are used to render the updated node and checked for collision with the virtual objects in the scene to prevent interpenetration.

Figure 5.6 depicts the motion and interaction of the virtual probe with a cube. The series of figures shows the motion of the probe as it approaches and interacts with the rigid surface of the cube. For simplicity, we have stripped away the outer sheath of the probe to show the interaction of the nodes in the system. Figure 5.7 depicts the interaction of multiple nodes as they interact with the surface. Although there are multiple points of contact with the cube, the probe is constrained to the surface due to the proxy points.

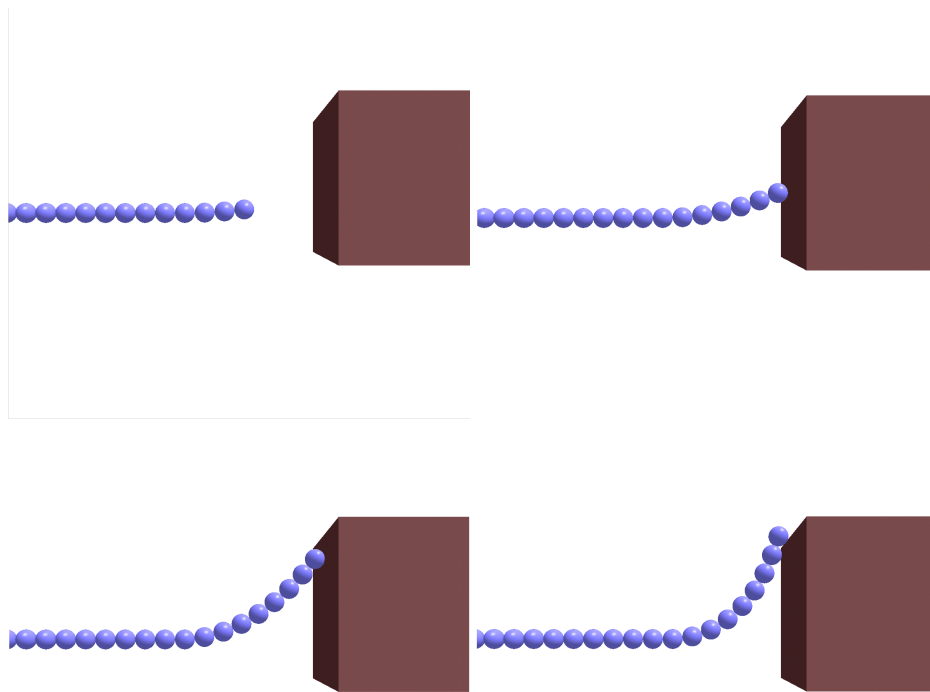


**Figure 5.6:** Interaction of the virtual probe with a rigid surface. The point proxies constrain the nodes to the surface of the cube and cause deformation of the virtual probe.

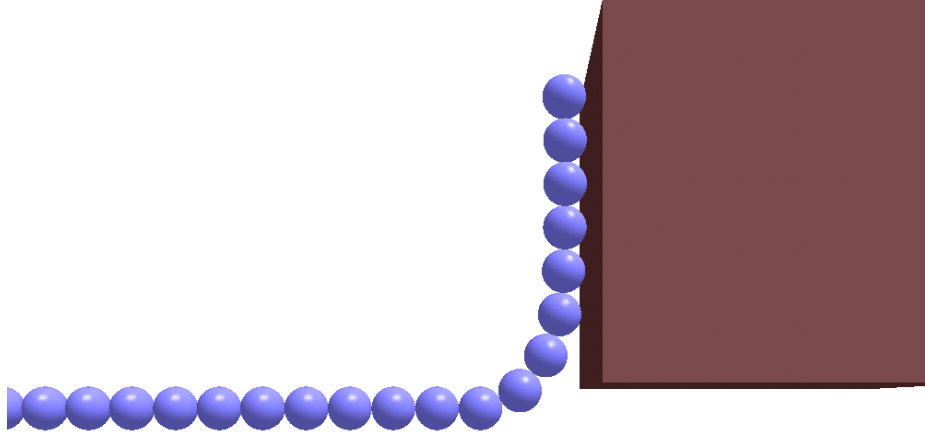


**Figure 5.7:** Multiple points of contact of the probe nodes with the rigid object.

#### 5.2.4 Implementation of the numeric solver

Simple Newtonian motion can be represented by the equation:

$$\mathbf{F} = m\ddot{\mathbf{x}} \qquad \tau = m\alpha \qquad (5.4)$$

where  $\mathbf{F}$  and  $\tau$  are the sum total of all the forces and torques acting on the node and  $m$  is the mass of the node.

Explicit numerical methods e.g., Euler solver, can be used for the numerical integration of the mass-spring systems. In our simulation, each node in the probe is expressed as a state vector,  $[\mathbf{x}, \dot{\mathbf{x}}, \ddot{\mathbf{x}}, \theta, \omega, \alpha]$ , where the terms  $(\mathbf{x}, \dot{\mathbf{x}}, \ddot{\mathbf{x}})$  represent the position, velocity and the linear acceleration, while  $(\theta, \omega, \alpha)$  represent the orientation, angular velocity and angular acceleration, respectively. We follow Euler's method in computing the values of the simulation at successive time steps.

Assuming that the forces and the torques acting on a node can be calculated at the beginning of the timestep  $n + 1$ , we can compute the instantaneous linear and angular acceleration as:

$$\ddot{\mathbf{x}}_{n+1} = \frac{\mathbf{F}}{m} \quad \alpha_{n+1} = \frac{\tau}{m} \quad (5.5)$$

The velocities and position/orientation at timestep  $n + 1$  can be computed through simple numerical integration of the ordinary differential equations.

$$\dot{\mathbf{x}}_{n+1} = \dot{\mathbf{x}}_n + \ddot{\mathbf{x}}_{n+1} \Delta t \quad \omega_{n+1} = \omega_n + \alpha_{n+1} \Delta t \quad (5.6)$$

$$\mathbf{x}_{n+1} = \mathbf{x}_n + \dot{\mathbf{x}}_{n+1} \Delta t \quad \theta_{n+1} = \theta_n + \omega_{n+1} \Delta t \quad (5.7)$$

The position and orientation of the node at timestep  $n + 1$  is stored and used to compute the proxy positions of the node at timestep  $n + 2$  by checking for collision with the virtual objects in the scene. A limitation of explicit methods is that simulation time step, damping and stiffness constants play an important part in the simulation. Incorrect values of the simulation parameters lead to instability in the system.

## Chapter 6

# Empirical Evaluation: Camera Model and Haptic Interfaces

In this chapter, we provide the results from user evaluation of the improved camera model as well as the integration of probe tip feedback in addition to the camera model. The results presented in this section have been published as “Vembar, D et al., Improving Simulated Borescope Inspection with Constrained Camera Motion and Haptic Feedback, in The Proceedings of Graphics Interface, 2009” [65].

### 6.1 Experiment 4: Evaluation of Camera Constraints

The purpose of this experiment was to evaluate the behavioral realism of the virtual borescope simulator’s camera model. In prior evaluation, experienced inspectors commented that the behavior of an unconstrained camera was disconcerting when using the borescope simulator. Because they could perform a full 360° rotation of the camera, they noted that they lost their sense of position and orientation within the virtual environment.

The present camera model’s rotation was constrained and tested against full 360° rotation. In both test conditions, participants used the gamepad to control the orientation and translation of the virtual camera. The difference between the two camera conditions was the amount of camera articulation and the corresponding visual output from the simulator. In the unconstrained condition, the virtual camera was allowed to rotate a full 360° about its axis. The camera was modeled as a point in 3D space with 6-DOF position and





**Figure 6.1:** Visualization of the virtual borescope's articulation. This view is never seen by the user, instead, the user's viewpoint is from the probe's tip.

orientation control.

In the constrained camera condition, as shown in Figure 6.1, the camera was simulated as a point at the tip of an articulating probe. The probe was modeled as a linear chain of point masses, with angular and torsional springs attached between the masses as described before. Camera articulation was limited to the surface of a sphere subtending a maximum angle of  $180^\circ$  about the center. Collision detection was implemented in both conditions to prevent the camera from penetrating engine model surfaces.

No tactile feedback was provided in this experiment, since the aim was to disambiguate the effect of camera fidelity from haptic feedback.

### 6.1.1 Participants

Five participants (all male) were recruited. All participants were instructors in the aircraft maintenance program and were familiar with using the borescope for engine inspection. Average experience of participants with optical borescope inspection was about 8 years, with three participants having about one year of experience with the video borescope. Participants also had prior experience with the borescope inspection training simulator. All participants were right-handed and were seated during the experiment.

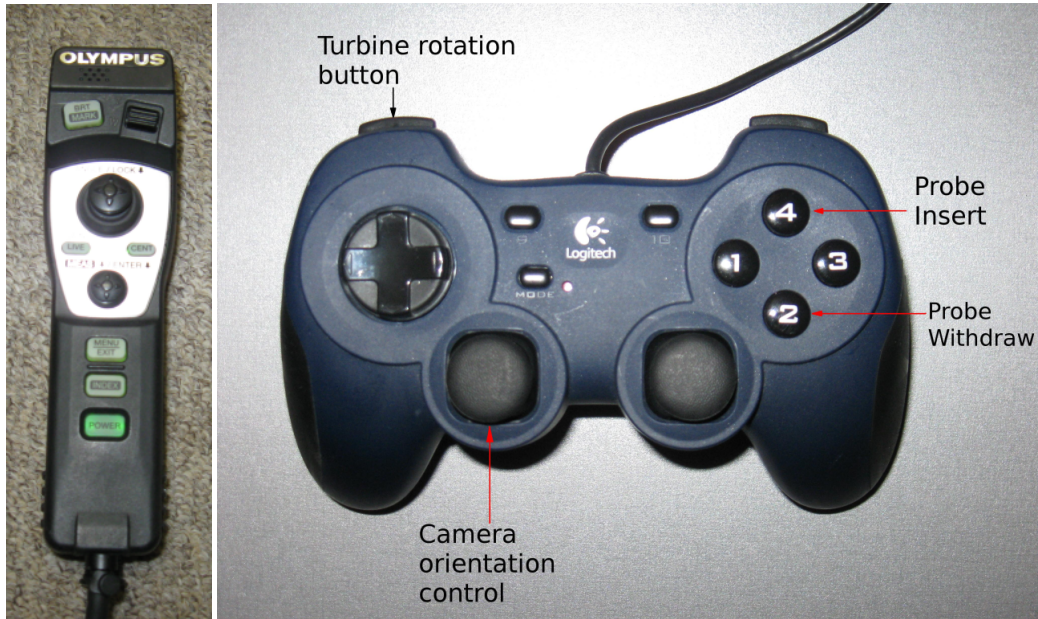


**Figure 6.2:** Actual borescope control (left) and gamepad with button mapping (right) used with borescope simulator.

### 6.1.2 Apparatus and Stimuli

The borescope simulator was run on a Dell Inspiron 9300 laptop, equipped with 2 GB RAM and a GeForce 6800 video card. The simulator's visual output was presented in a 1280×1024 window on the 17" laptop screen. The simulator maintained an interactive frame rate (60 fps) throughout the experiment. The laptop was placed on the table directly in front of the participant.

The visual stimulus consisted of a polygonal model of the hot section of a PT-6 engine, drafted in Maya and exported as an .obj file with texture and material information. The fixed section (stator) was modeled as two fixed rings of blades and the turbine (rotor) was modeled as one moving set of blades. The engine components were rendered using a custom viewer written with OpenSceneGraph [51].

An off-the-shelf gamepad (Logitech Dual-Action) was used to control both the position and orientation of the virtual camera (see Figure 6.2). The 4-way analog stick of the gamepad was mapped to control camera orientation with buttons 4 and 2 mapped to camera insertion and withdrawal, respectively. To simulate the rotation of the turbine, one of the gamepad buttons was mapped to modify the scene graph to rotate the turbine. The participant could visually observe the turbine rotating when the button was pressed. The gamepad controls were designed to simulate two-handed control of the camera, where the dominant hand controls the camera translation and the non-dominant hand controls camera orientation, similar to the real

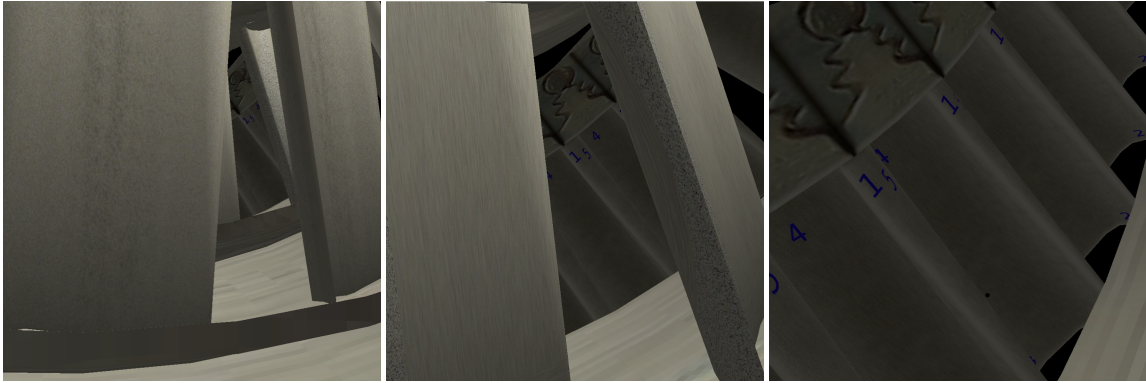


**Figure 6.3:** Camera navigation through two sets of fixed stator blades (left and center) with the goal of positioning the probe camera at the engine rotor for inspection of 5 rotor blades (right, see Figure 6.4 for inspection details).

operation of the video borescope.

### 6.1.3 Procedure

The aim of the experiment was explained to all participants and informed consent and demographic data collected prior to commencement of the test. They were then seated in front of the test computer and were instructed on the use of the gamepad to control the position and orientation of the virtual camera. The starting position of the borescope camera in the engine model was the same for all participants. Participants were instructed to maneuver the camera through the two sets of stator blades and complete inspection of 5 blades in the rotor, as they would normally do in a real inspection task (see Figure 6.3).

Instead of modeling engine blade defects, visual markers, in the form of a numbered sequence, were used to guide the inspection process (see Figure 6.4). The front face of the blades displayed the number sequence 1–4 simulating inspection of the blade commencing with inspection of its leading edge. The back face displayed the number sequence 5–8 simulating its inspection commencing with the trailing edge. Participants were asked to inspect the front face of the rotor blade first, followed by maneuvering the camera to inspect the back face. Once they had completed inspection of one blade, participants were asked to move on to the next blade by pressing the gamepad button to advance the rotor and repeat the inspection process. The start and end blades on the rotor were colored red to distinguish them from other blades.

In the pre-test phase, participants were provided training with the gamepad and the borescope simulator. Once they were proficient in using the gamepad to control the camera, they were asked to inspect five blades between the two marked blades of the rotor using one of the camera conditions. The participants

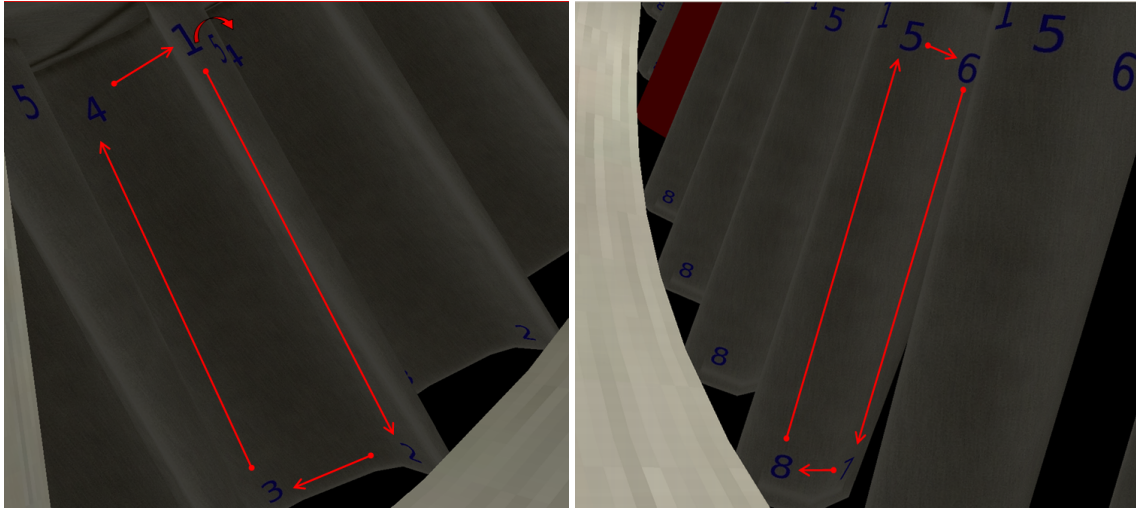


**Figure 6.4:** Visual inspection of rotor blade. Inspectors are trained to inspect the rotor in clockwise order, first inspecting the front face (left), then advancing the probe forward and rotating the probe tip to inspect the back face (right). Next, the entire rotor is rotated by pressing the turbine rotation gamepad button. Arrows are shown here for clarity, they were not presented to participants.

were unaware of the camera condition they were currently using. On completion of the first task, participants were given a brief rest period. After a brief familiarization phase with the second camera condition, participants performed the same inspection process. On completion of both phases, participants then filled out a preference questionnaire followed by post-test debriefing.

#### 6.1.4 Design and Data Collected

A within-subjects experimental design was used due to the limited pool of experienced borescope inspectors. The alternating order of the two conditions was balanced between participants so that half started with the unconstrained camera first while the other half started with the constrained camera. The camera condition served as the independent variable, with the participant acting as the blocking factor. Performance measures collected were time taken to complete the task and the number of collisions of the virtual camera with the virtual environment surfaces. At the end of the test procedure, the participants were asked to rank the two camera conditions in order of preference (1: most preferred, 2: least preferred), based on their experience interacting with the simulator.

The constrained camera was expected to yield shorter task completion times, fewer collisions, and was expected to be preferred by participants as it is thought to be more physically representative of the physical video borescope camera.

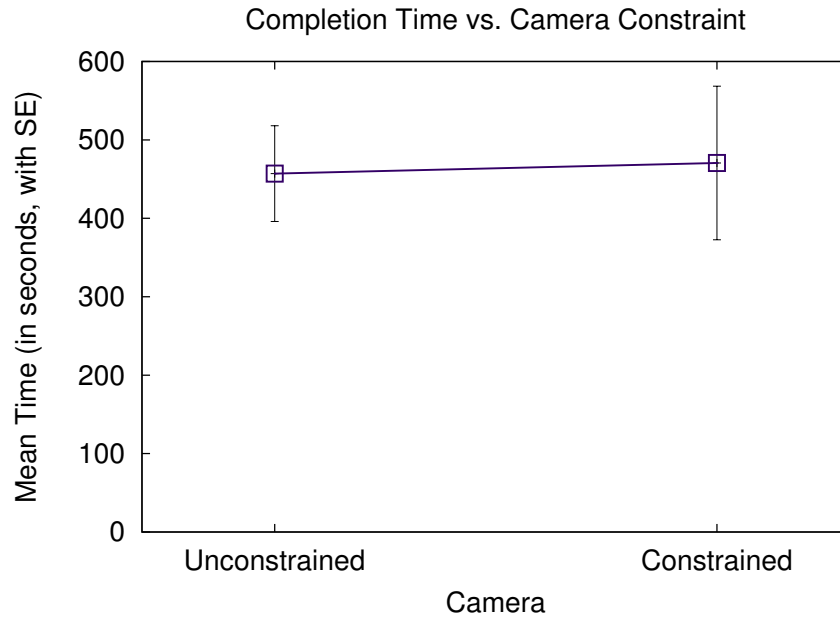


**Figure 6.5:** Mean completion times per camera interface.

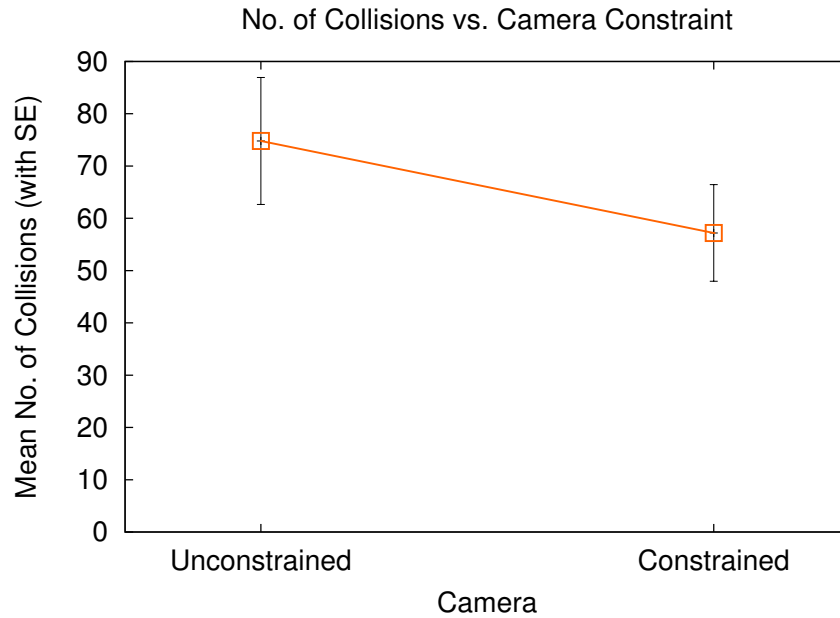
### 6.1.5 Results

Figure 6.5 shows the mean task completion time while Figure 6.6 shows the average number of collisions of the virtual camera with the engine model for the five participants. Task completion time with the unconstrained camera (457 s) appears faster than with the constrained camera (471 s), but not significantly so (repeated measures one-way ANOVA using R [10] shows no significant difference in task completion times;  $F(1,4) = 0.09$ ,  $p = 0.79$ , n.s.). The average number of collisions of the virtual camera with the engine model with the unconstrained camera (74.8 collisions) was significantly larger than with the constrained camera (57.2 collisions;  $F(1,4) = 28.26$ ,  $p < 0.01$ ). In post-test debriefing, 4 out of 5 participants preferred the constrained camera; only one preferred the unconstrained camera.

### 6.1.6 Discussion

One of the desired skills that experienced borescope inspectors would like novice trainees to adopt is the manipulation of the camera using the articulation controls. Since replacement probes are expensive, care should be taken to prevent damage to the probe. An experienced inspector can determine when the borescope probe is entangled within the aircraft engine and takes remedial steps to prevent the tip from suffering damage.

Ideally, users of the physical borescope should minimize the number of collisions of the borescope



**Figure 6.6:** Mean collisions per camera interface.

and engine components. This desirable outcome should be evident in the training simulator as well. Results indicate that participants made significantly fewer collisions with the constrained camera model than with the unconstrained model. The limitations on the camera movement could have helped keep the number of collisions small by limiting the number of needed corrections of camera position and orientation.

Despite limiting feedback to a visual-only display, a majority of the users preferred the constrained camera condition. During post-test debriefing, participants revealed that the visual output of the simulated engine model was consistent with their real world experiences. However, they noted that the interaction with the simulator was very dissimilar from the actual inspection process. They felt that without bi-manual articulation control and probe feed, the simulator “felt like a video game” and the lack of collisions response was “unrealistic”. Evaluation of force feedback with the constrained model of the camera was the goal of the next experiment.

## 6.2 Experiment 5: Haptic Interfaces Evaluation

In this experiment, in addition to visual feedback, the effect of tactile feedback was evaluated. Tactile feedback is produced when the tip of the probe collides with surfaces in the virtual environment. Camera rotation was constrained as in Experiment 4. In addition to a custom haptic device, off-the-shelf products

were evaluated for haptic feedback, including Novint's Falcon and SenseAble Technologies' Phantom Omni.

Forces exerted by the bending and twisting of the probe through the virtual environment (engine model) are calculated through the interaction of the mass-spring system used to model the probe. Though it is easy to compute the forces at discrete intervals along the length of the probe, it is difficult to represent the net effect of these forces through a single point-based interface like the Falcon. Since the interfaces used were limited to maximum 3-DOF force feedback lacking torsional response, tactile feedback was limited to the representation of only the forces experienced at the tip where the camera is located.

### **6.2.1 Participants**

Sixteen students enrolled in an aircraft maintenance program (all male with average age of 25 years) took part in this study. All had completed at least two semesters of engine inspection related coursework. Additionally, participants had at least two hours of hands-on engine inspection experience using a video borescope as part of the training curriculum. All participants were right-handed and were seated during the testing phase of the experiment.

### **6.2.2 Apparatus and Stimuli**

The borescope simulator was run on both laptop and desktop computers. The same laptop was used to drive the Haptic box as in the previous experiment. The desktop, a standard PC, was used to alternatively drive the Falcon or Omni. The PC was equipped with a PentiumD 2.4GHz processor, 4GB RAM, and a GeForce 7600GT video card. Visual output was presented in a 1024×768 window on a 19" LCD monitor placed in front of the participant. Despite the different computers used, care was taken to ensure similarity of the display window.

Rotor rotation and camera orientation were controlled by the gamepad as in Experiment 4. Mimicking interaction with an actual video borescope, participants were asked to control the orientation of the camera with their non-dominant hand, while using their dominant hand to simulate probe feed. The four conditions evaluated were: (1) Haptic box without force feedback, (2) Haptic box with force feedback, (3) the Falcon, and (4) the Phantom Omni.

The Haptic box without feedback served as the control condition. The major difference between conditions was the provision of tactile feedback and the manner of probe insertion. With the Haptic box, the position of the virtual camera is related to the position of an actual borescope probe within the box (the probe





**Figure 6.7:** Operational evaluation of (from left to right) the Haptic box, Falcon and Phantom Omni interfaces with the borescope simulator.

itself is inactive, its body acts as the physical element manipulated by the user). When software detects collision of the camera tip with a surface, a sailing cam cleat clamps the probe preventing further advancement. The user must either change camera orientation (via gamepad buttons) or position by withdrawing the probe. For the control condition with no force feedback, the cam cleat clamp is inoperative.

Falcon and Omni operation is described by either rest or active state. In rest state, the device is constrained to the center of the workspace with spring forces continually compensating for gravity (simply put, the device manipulator is suspended and does not drop to the desktop when not in use). Simulation of probe feed requires a button press on the device to advance the virtual camera. In this active state, the change in the  $x$ -axis position of the device is mapped to insertion or withdrawal of the virtual camera. Forces calculated by the interaction of the probe tip with the virtual environment surfaces are calculated at 1000 Hz and fed back to the device.

### 6.2.3 Procedure

The aim of the experiment was explained to all participants and informed consent and demographic data collected prior to commencement of the test. They were then seated in front of the test computer and were shown how to use the gamepad to control camera orientation and the haptic interface to control camera position (see Figure 6.7). The inspection task assigned to participants was the same as in the first experiment (inspection of numbered markers on the front and back faces of five rotor blades).

With each variant of the interface, participants performed a self-paced familiarization task to acquaint themselves with the gamepad and haptic device. Following performance of the inspection task, participants completed a modified presence questionnaire (Table 6.1) before moving on to the next interface.



## 6.2.4 Design and Data Collected

A within-subjects random complete block experimental design was used in this experiment. A 4×4 Latin square was used to determine the order of the treatment conditions presented to the user, to minimize learning and order effects. The interface condition served as the independent variable, with the participant as the blocking factor.

Performance measures collected were time taken to complete the inspection task and the number of collisions of the virtual camera with the virtual environment. Subjective data collected at the end of each treatment condition was in the form of a tailored Witmer-Singer presence questionnaire [72]. Responses to the questionnaire were on a 7-point Likert scale, with 1 being most negative, 4 neutral, and 7 most positive. On completion of all the four treatment conditions, the participant completed a subjective preference questionnaire which ranked the four interfaces with 1 indicating highest preference, 4 indicating lowest.

It was hypothesized that the Haptic box with no force feedback would be the least preferred device, followed by the two off-the-shelf haptic interfaces, then by the Haptic box with force feedback ranked as the most preferred interface. Only the condition with no force feedback was expected to yield both a significantly higher task completion time and the highest number of camera collisions.

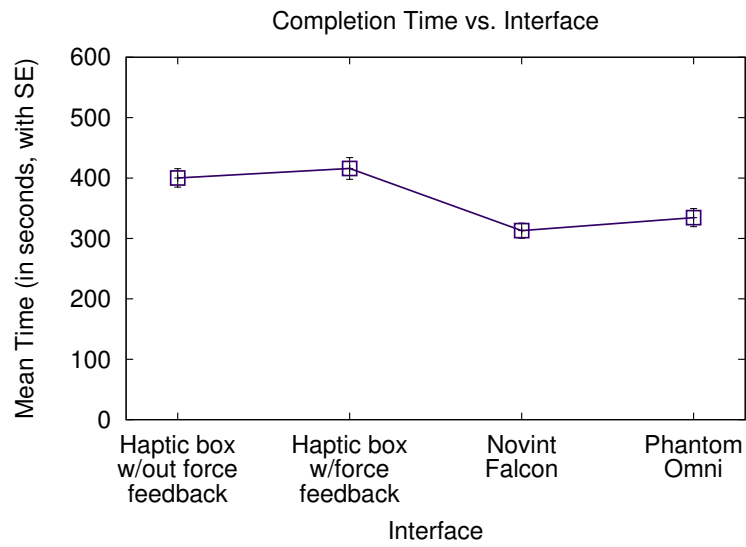
## 6.2.5 Results

Figure 6.8 shows the mean completion times for all conditions. According to a repeated measures one-way ANOVA on task completion, the Haptic box, with or without feedback, yielded significantly slower performance than either of the two commercial devices ( $F(3,45) = 5.09$ ,  $p < 0.01$ ).

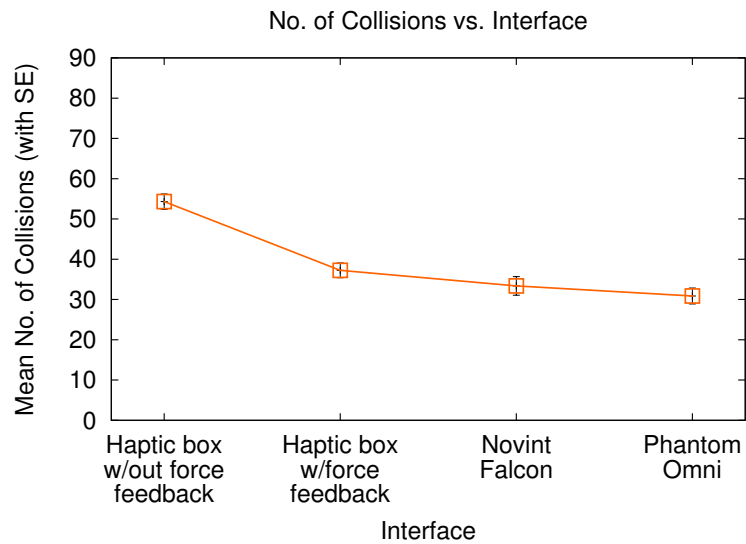
Pairwise t-tests (with Bonferroni correction) reveals no significant difference between operation of the Haptic box, with or without haptic feedback. No significant difference was observed between the operation of the Omni and the Falcon. However, significant differences in time to completion were detected between the Haptic box and the each of the other two devices ( $p < 0.01$  for all pairings except the Haptic box without feedback and the Omni, where  $p < 0.05$ ).

Figure 6.9 shows the average number of collisions of the virtual camera with the virtual environment (about 54 collisions with no force feedback and about 33 collisions, on average, with force feedback). Repeated measures one-way ANOVA shows the main effect of interface is significant ( $F(3,45) = 31.44$ ,  $p < 0.01$ ).

Pairwise t-tests (with Bonferroni correction) reveal significant differences between the Haptic box



**Figure 6.8:** Mean search times per interface.



**Figure 6.9:** Mean hits per interface.

(without force feedback) and all other conditions ( $p < 0.01$  for every pairing). No other significant differences were observed.

The subjective questionnaire data collected at the end of each treatment condition was evaluated using non-parametric repeated measures ANOVA (Friedman's test), revealing a significant difference in response only to Question 21 pertaining to concentration ( $\chi^2(3, n = 15) = 8.37, p < 0.05$ , see Table 6.1). The mean responses of the participants to each of the 21 questions with the 4 treatment conditions is plotted in Figure 6.10. An analysis of means to determine which interface was different showed that the participants preferred the three tactile feedback conditions over the control condition.

Friedman's analysis of the preference ranking of interfaces revealed significant difference among the four treatment conditions ( $\chi^2(3, n = 15) = 14.85, p < 0.01$ ). Non-parametric equivalent of Tukey's test to determine difference in means revealed that there were no significant difference between the three tactile feedback conditions, but each was different from the control condition, which was the least preferred by the participants.

## 6.2.6 Discussion

Task completion results indicate that participants consistently performed inspection faster with the Falcon or the Omni, compared to the custom Haptic box. The difference is likely due to the better build quality of the commercial interfaces. In particular, the choice of the probe feed measurement implementation and the simplicity of the force feedback offered by the Haptic box may have had an effect on the task completion times, as explained below.

Camera translation and rotation is measured by the Haptic box's use of an optical mouse to detect changes in translation and rotation of the actual borescope probe as it is inserted or withdrawn. The haptic feedback is provided by the cam cleat upon detection of camera collision within the environment. The braided cable enclosing the optical fibers of the physical borescope provides a sufficiently rough surface to enable the optical sensors of the mouse to detect motion, however, the sensed positional/rotational change is inexact compared to the 6-DOF measurements obtained from the Omni at high refresh rates (1000 Hz).

Borescope inspectors rely on tactile feedback when maneuvering the probe through the engine compartment. This feedback is important when the inspector is inserting or withdrawing the probe from the engine. Results indicate that provision of simple feedback of tip collision has a significant effect on the number of collisions with the engine model (accuracy). On average, the control condition yielded 66% more collisions than the conditions affording tactile feedback. Our results support earlier findings with surgical

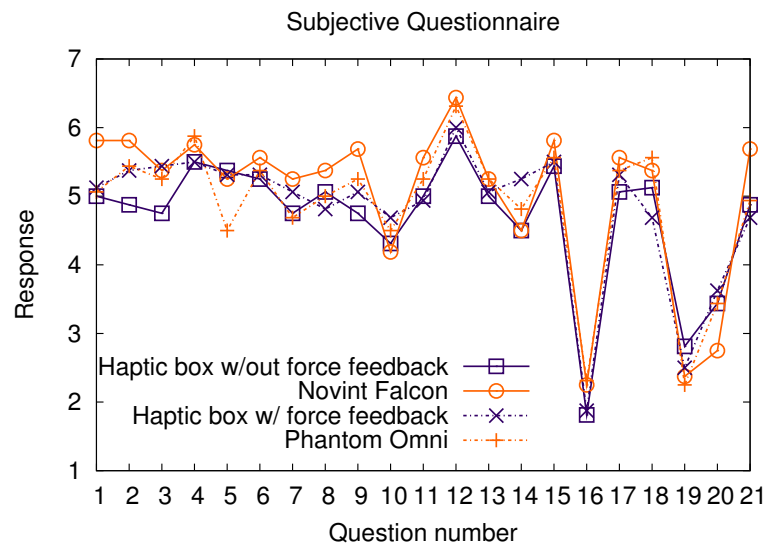


**Figure 6.10:** Responses to subjective questionnaire.

Witmer-Singer Presence Questionnaire	
1.	How much were you able to control events?
2.	How responsive was the environment to actions that you initiated (or performed)?
3.	How natural did your interactions with the environment seem?
4.	How much did the visual aspects of the environment involve you?
5.	How natural was the mechanism which controlled movement through the environment?
6.	How compelling was your sense of objects moving through space?
7.	How much did your experiences in the virtual environment seem consistent with your real-world experiences?
8.	Were you able to anticipate what would happen next in response to the actions that you performed?
9.	How completely were you able to actively survey or search the environment using vision?
10.	How well could you actively survey or search the virtual environment using touch?
11.	How compelling was your sense of moving around inside the virtual environment?
12.	How closely were you able to examine objects?
13.	How well could you examine objects from multiple viewpoints?
14.	How well could you move or manipulate objects in the virtual environment?
15.	How involved were you in the virtual environment experience?
16.	How much delay did you experience between your actions and expected outcomes?
17.	How quickly did you adjust to the virtual environment experience?
18.	How proficient in moving and interacting with the virtual environment did you feel at the end of the experience?
19.	How much did the visual display quality interfere or distract you from performing assigned tasks or required activities?
20.	How much did the control devices interfere with the performance of assigned tasks or with other activities?
21.	How well could you concentrate on the assigned tasks rather than on the mechanisms used to perform those tasks ?

**Table 6.1:** Subjective questionnaire.

simulators [68], where integration of visual feedback from the LCD monitor and tactile feedback from haptic interfaces had the desired effect of reducing camera-surface collisions during the test procedure.

Subjective responses to the presence questionnaire revealed that there were no significant differences in the visual stimulus presented to the users (as expected). Participants reported the visual stimulus afforded them sufficient ability to interact with the engine model to examine the turbine blades from multiple viewpoints (Q4, Q12 and Q13). They noted that there was minimal delay between the response of the visual stimulus to their actions with the treatment interfaces (Q16) and the environment felt sufficiently responsive to their actions (Q2). Response to Q19 suggests that the visual display quality did not have a detrimental effect on performance.

Participants responded neutrally to the effect of the control interfaces on user interaction (Q20). They noted that their interaction with the control interface and the environment seemed somewhat natural (Q3).

Participants felt that the Omni was less natural to interact with than the other three interfaces (Q5), though not significantly so. The possible reasons for this effect are two-fold. First, participants were instructed to grip the Omni stylus as they would the actual borescope probe using their whole hand and palm for insertion. It was later observed that while they started their interaction with the Omni stylus in the prescribed way, they later switched to holding the stylus like a pen as they found it uncomfortable manipulating the Omni while seated. Second, the roll of the Omni was mapped to camera roll. To simulate the rotation of the virtual camera about its axis, participants were instructed to activate the camera first (by pressing and holding the button on the stylus), and then to manually rotate the stylus until they obtained the desired view. It is reasonable to assume that this dual action created greater cognitive workload resulting in lower scores for this question (Q5). In contrast, neither the Falcon nor the Haptic box required multiple steps for users to memorize.

Overall, participants reported that they adjusted quickly to the virtual environment (Q17) and felt that they had gained proficiency in using the interfaces by the end of the experiment (Q18). Participants felt they could concentrate on the task better with the Falcon, compared to the other three treatment conditions (Q21). The response to Q20 (control devices interfering with the task) suggests that participants perceived the Falcon to be the easiest to use among the four interfaces to control.

During post-test debriefing, participants gave high marks to the visual fidelity of the simulator. One participant noted that “it looks like the real thing”. The haptic box with force feedback was well liked by some users, with one user suggesting that it was “very life-like and just like the real thing” but another noting

that it was “crude and jerky”. The Falcon and the Omni drew positive responses due to their ease of use. Users also had positive comments on the auto-centering of the Falcon and Omni manipulators whenever either was inactive.

Post-test preference data suggests participants preferred the haptic conditions significantly over the control condition with no tactile feedback. No significant differences between the three haptic conditions were noted, suggesting the provision of tactile feedback alone led to improved user performance in the reduction of collisions rather than the type of haptic interface.

Comparison of the Haptic box with force feedback to the commercially available devices shows similarity in terms of detected collisions. Although task completion with the Haptic box was significantly longer than with either the Falcon or the Omni, participants expressed an affinity toward the Haptic box for its insertion of an actual probe into the box. This is likely due to its highest degree of similarity to the look and feel of the actual task. The performance afforded with the Falcon is notable in light of its relatively low cost and ready availability. Given the traditional constraints of time and resources, the Falcon is a viable alternative to custom interface design, with minimal trade-off in performance.

It is important to note that haptic feedback was provided only when the virtual camera intersected model geometry in the forward direction. One reason for this design decision was due to the limited force feedback response of the devices being used. The Haptic box is limited to 1-DOF feedback (translation along the probe’s axis only). The Phantom Omni and the Falcon offer 3-DOF force feedback along each of the three coordinate axes. Torques generated when the probe twists within the engine, though calculated, cannot be presented to the end user. The prohibitive costs associated with acquiring 6-DOF devices to provide torsional response in the simulator outweigh the benefits of affordability of tools needed by technical colleges in training their students in engine inspection procedures.

Instead of performing large movements of the borescope tip once it has reached the desired blades in the engine, an experienced inspector performs a repeated set of fine motions with the articulation controls to inspect the blades. Instead of translating the probe repeatedly into the engine, the inspector usually calls on an accomplice to manually rotate the engine thus rotating the turbine under inspection. This helps in keeping the borescope at a fixed location, avoids pitfalls of losing orientation and position within the engine, and prevents accidental damage to the probe tip due to excessive manipulation of the probe. Button clicks on the gamepad essentially simulated a “virtual accomplice”.

The use of sequential numbers instead of models of defects (e.g., by texture maps) may seem somewhat odd for the inspection task. After all, the main aim of borescope inspection is to visually determine if

anomalies in the engine are defects and if so, recommend corrective action. However, in this study the focus was on the skills required to control the virtual camera, not on the ability to detect defects. By removing the search component of the task, differences between participants' skill levels were equalized.

## Chapter 7

# Contact Detection and Response

In the previous chapter, we described the development of a physically-based camera model using a link of masses connected to its adjacent neighbors with springs. Each of the masses in the system has a finite diameter equal to the size of the borescope probe being simulated. The camera model takes into account the behavior of the real borescope, including the articulating tip containing the camera. Similar to the real borescope, the articulation in the virtual borescope is controlled by the 2-axis controls on the gamepad.

Using proxy nodes of same diameter at each of the masses in the link, a penalty-based method was adopted to calculate the force feedback along the length of the probe. In the penalty method, the difference in the position of the actual and the proxy node is used to calculate the magnitude of the force feedback. The direction of the force is usually along the normal of the intersecting surface. Although the probe model allows for multi-point collision detection, one of the limitations of the prior implementation of force feedback was that it was limited to just the tip of the virtual probe.

In this chapter, we describe further enhancements to the probe model to account for jitter when the virtual probe intersects with the edges of engine blades. We present a simple algorithm for calculating the forces rendered on the haptic device when there are multiple intersections along the length of the probe. Finally, we compare the deformation produced by a real borescope interacting with an engine blade and simulate the same deformation with the virtual probe.



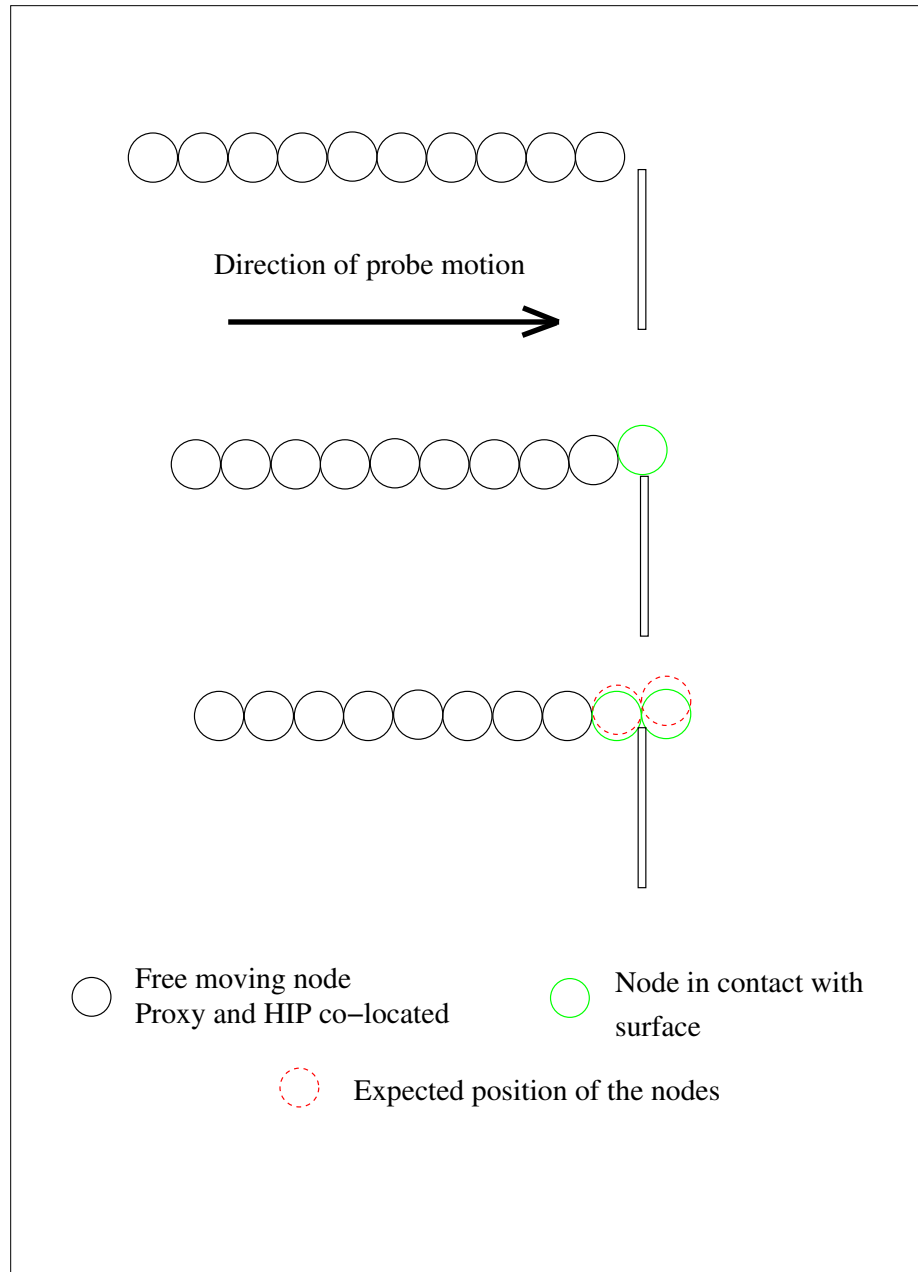


**Figure 7.1:** Intersection of the probe with edges of objects leading to jitter in the position of the virtual camera.

## 7.1 Improving Intersection Response

Consider the case of the probe approaching the blade to be inspected represented by the rectangular object shown in Figure 7.1. The direction of motion of the virtual probe is from left to right. Prior to intersection of the probe with the blade, both the proxy and the node are co-located. In the middle image, the tip of the borescope has just intersected with the edge of the blade. The proxy position of the node, depicted by the green circle, is visually constrained to never penetrate the surface of the virtual model. Due to this, the proxy is displaced from the original direction of motion.

The last image depicts the probe that has moved a little bit further such that the edge of the blade is now resting between the two proxy nodes. The nodes in red depict the expected position of the nodes if the virtual probe was modeled as a continuous cylinder with collision detection along the surface. The error between the expected position and the computed position of the nodes occurs due to the discontinuities in the proxy nodes used to simulate the surface of the the probe. This error in the position of the nodes does not play a dominant role when the distance between the camera and the intersecting edge is small. However as the probe is moved further along the edge of the blade and the trailing nodes move across the edge, there will be repeated jitter of the virtual camera at the tip of the probe.

To prevent repeated oscillations of the camera, a second set of proxy nodes were used in the virtual probe for improved collision detection. In addition to the proxy nodes co-located with the center of the point masses, extra nodes were placed exactly halfway between the centers of adjacent nodes in the virtual probe. These nodes were used only for collision detection along the length of the probe. Figure 7.2 shows the diagrammatic representation of these nodes, represented by the dashed lines. As the virtual probe intersects with the edge, the proxy nodes detect collision between 3D model and the probe and reduce the jitter of the probe tip. Errors in the expected and computed positions of the probe tip are reduced due to the use of additional proxy nodes.

However, additional proxy nodes increase the total number of intersection tests that need to be performed with the virtual probe. We used a hierarchical axis-aligned bounding box (AABB) for detecting collisions of the virtual probe with the engine model. In the borescope simulator, the time taken to compute the intersections of the probe with the increased number proxy nodes was negligible compared to the improved response of the virtual probe through reduced camera jitter.

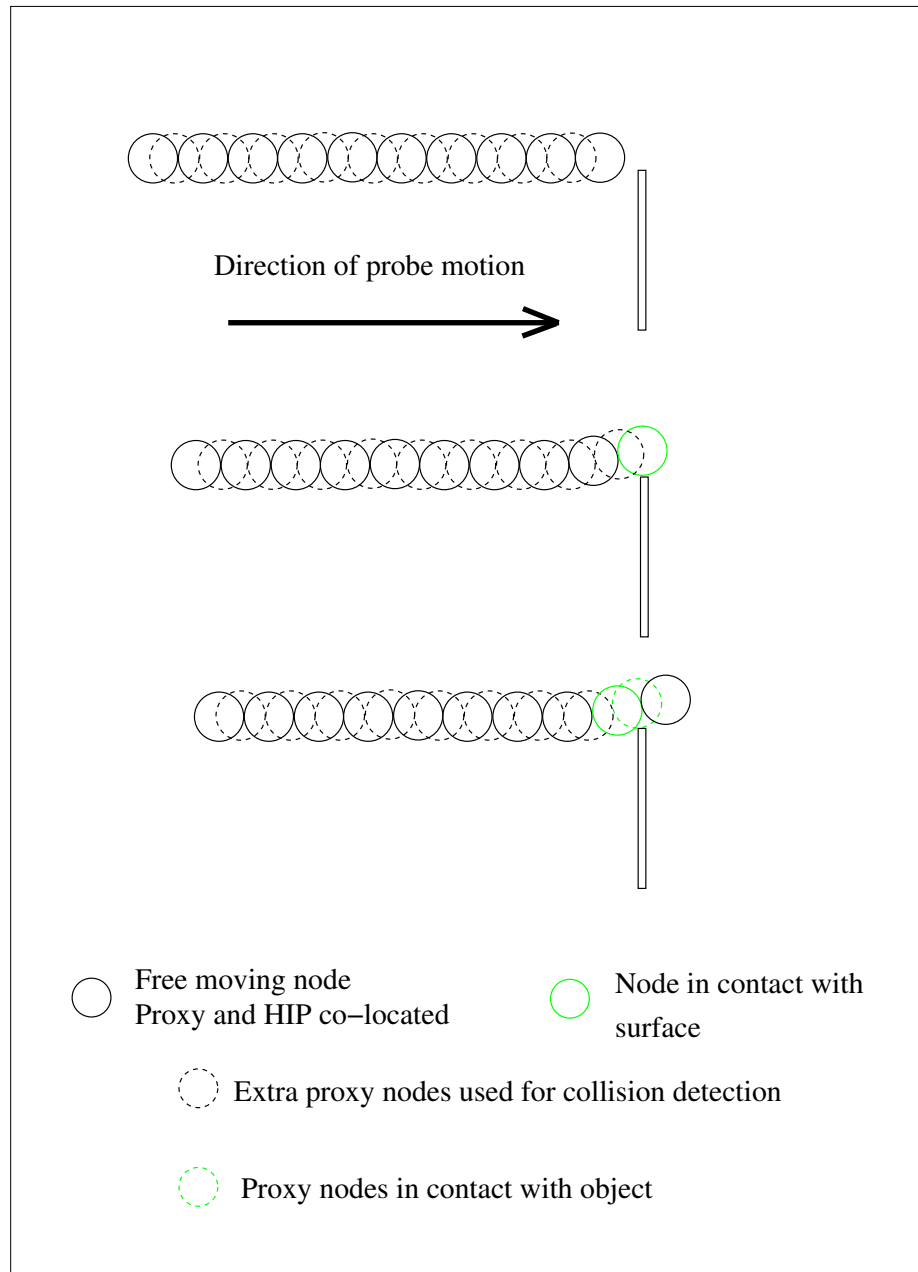


**Figure 7.2:** Use of additional proxy nodes to improve intersection response.

## 7.2 Multi-contact Force Feedback

In prior versions of the simulator, force feedback was limited to direct contact of the tip of the virtual borescope with the engine models. Although direct force feedback is important in preventing damage to the tip of the real borescope, experienced inspectors also rely on the feedback obtained from intersections of the engine along the length of the probe. This feedback, though not as direct as tip feedback, helps the technician guide the borescope through the engine. Representing multiple points of contact in the virtual borescope simulator using a haptic interface such as the Falcon is challenging, as the device provides only a single resultant force, effectively simulating a single point of contact.

To simulate feedback from multiple points of contact using the haptic interface, we developed a simple algorithm that computes the resultant force based on the total number of nodes of the virtual probe in contact with the 3D model of the engine. There are three common cases when the virtual probe interacts with a surface as shown in Figure 7.3 that have to be considered when developing the algorithm to determine the resultant force.

In the first case, consider the interaction of the probe with the surface (topmost image). The foremost node of the probe is in contact with the surface. With a single node in contact, the force feedback is limited to a single force acting on the node as shown in the figure. The force and the direction of action of the force can be represented easily with a 3-DOF force feedback device such as the Falcon.

In the second case, both the foremost node and abaft nodes are in contact with the surface (middle image in Figure 7.3). The collision detection algorithm and the proxy nodes constrain the nodes along the surface. When the virtual probe moves from the left to the right towards the surface, more nodes of the virtual probe come into contact with the surface. Representation of the force feedback by the haptic device has to now take into consideration the force feedback on the leading node as well as the feedback on the node adjacent to it that is in contact with the surface.

Finally, consider the last image in Figure 7.3. The leading node has progressed beyond the edge of the surface and is no longer in contact with the surface. However, nodes in the probe abaft the leading node are still in contact with the surface. The force algorithm has to take into consideration the resultant force of all the nodes in contact with the surface, as well as compute the resultant direction of application of the force.

For computing the resultant single force to be rendered by the haptic device, a linear combination of all the forces experienced by the virtual probe was calculated. The total force is computed as the force

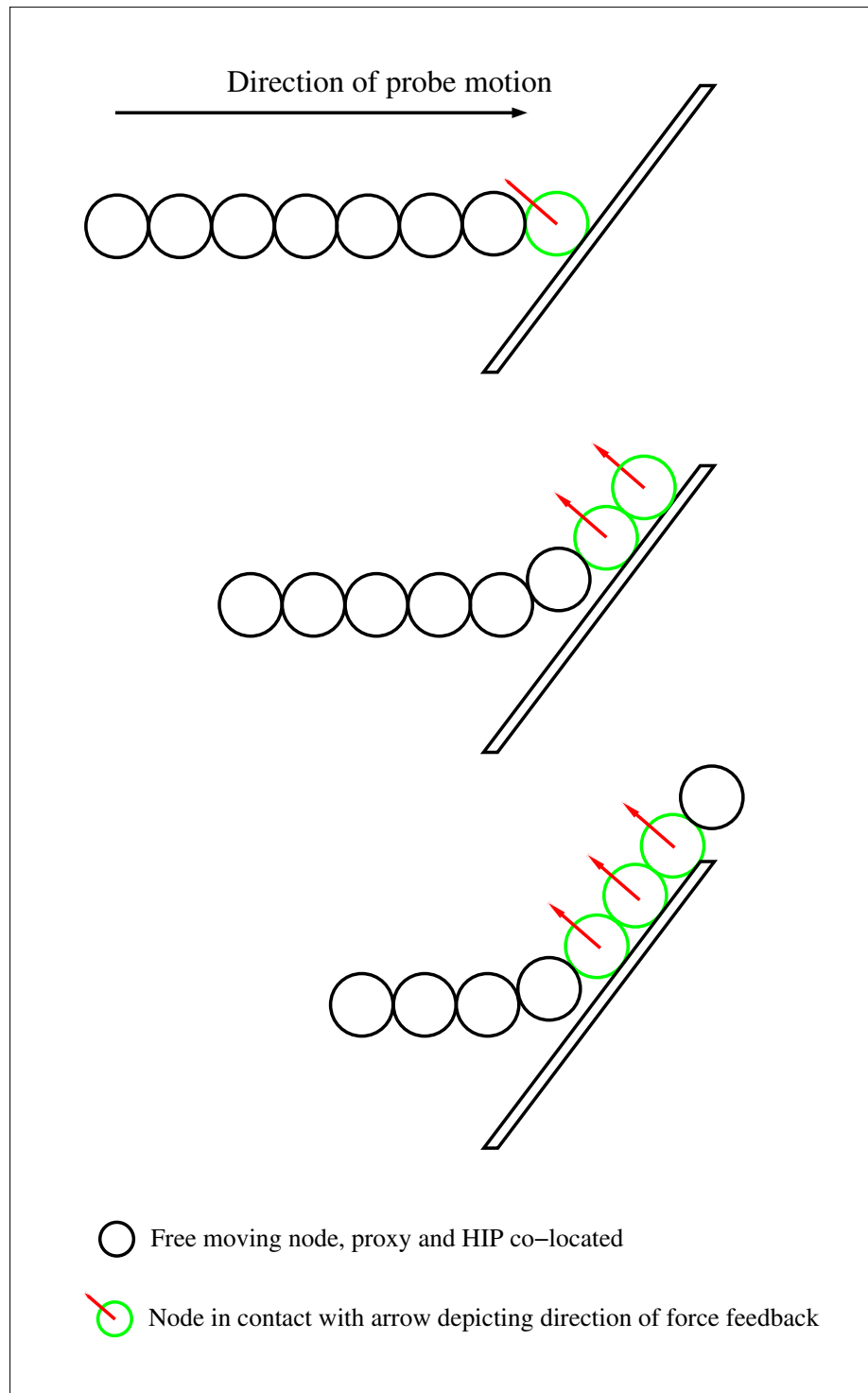


**Figure 7.3:** Computation of forces along the probe length with multiple points of contact.

experienced by the foremost node and the clamped linear sum of the other nodes in contact with the engine model. Assuming  $n$  nodes of the borescope are in contact with the surface, the total force  $F_{total}$  is calculated as:

$$F_{total} = F_{tip} + \max(0, \min(F_{max}, \sum_{i=0}^n F_i))$$

where  $F_{tip}$  is the total force experienced by the tip node,  $F_i$  is the force experienced by the  $i^{th}$  node in contact with the surface, and  $F_{max}$  is maximum contribution towards the total force.

The Novint Falcon has a maximum continuous force output of 2lbs or 8N. The contribution of the total force  $F_{total}$  was thus limited to 8N, with the contribution of foremost node clamped at 6N and the contribution of the other nodes clamped at 2N.

## 7.3 Experiment 6: Comparison of Probe Model

In the previous section, we described iterative improvements to the probe model to provide both multi-point contact detection of intersections as well as calculation of the resultant force feedback. In this section, we provide empirical evaluation of the interaction of the borescope probe with a single engine blade and compare the visual results with the simulated version of the same task with our probe model. Unlike visual confirmation of the virtual probe behavior, comparison of the force feedback between the real and the virtual borescope is considerably harder to measure and is beyond the scope of this dissertation.

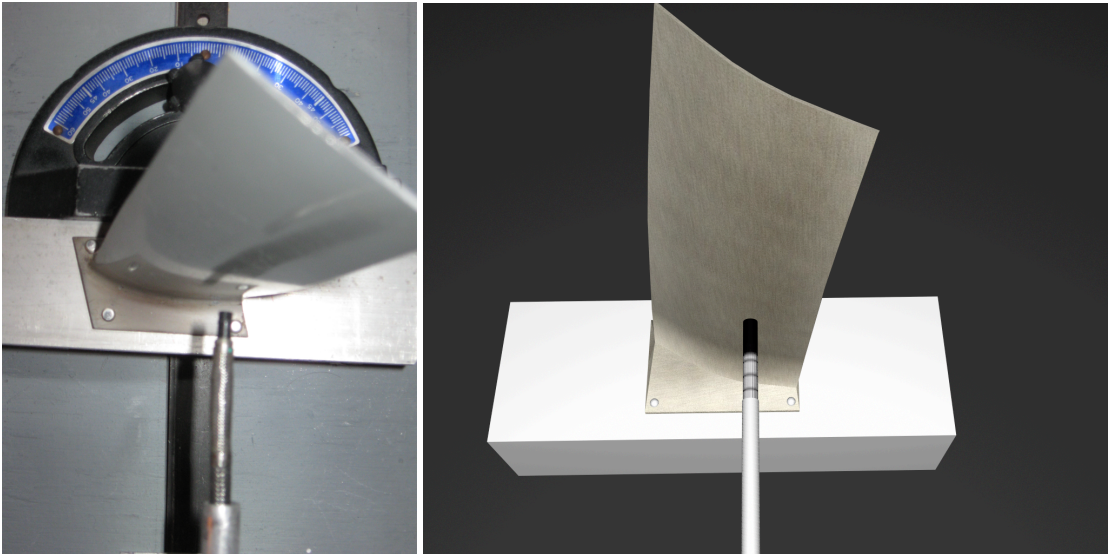
### 7.3.1 Apparatus

Figure 7.4 shows a top-down view of a prototype measurement device designed to simulate the interaction of the borescope probe with the engine blades. The apparatus consists of a single engine blade mounted on a platform that swivels about its axis providing  $120^\circ$  of rotation. By manually setting different angles of the platform, we can observe the response of the probe as it intersects with the blade at different angles of incidence.

A hollow aluminum tube is mounted at the bottom of the device as shown in the figure and simulates the guide tube used in borescope inspection. The borescope probe is inserted into this tube and guided to intersect with the engine blade. The distance between the guide tube and the blade is manually adjusted by moving the tube closer to or further away from the blade. An unused optical borescope with the probe



**Figure 7.4:** Top-view of apparatus designed to simulate feed and interaction of borescope probe with engine blade.



**Figure 7.5:** Starting position of the borescope probe in the experiment (left) and modeled simulation environment with the virtual probe (right).

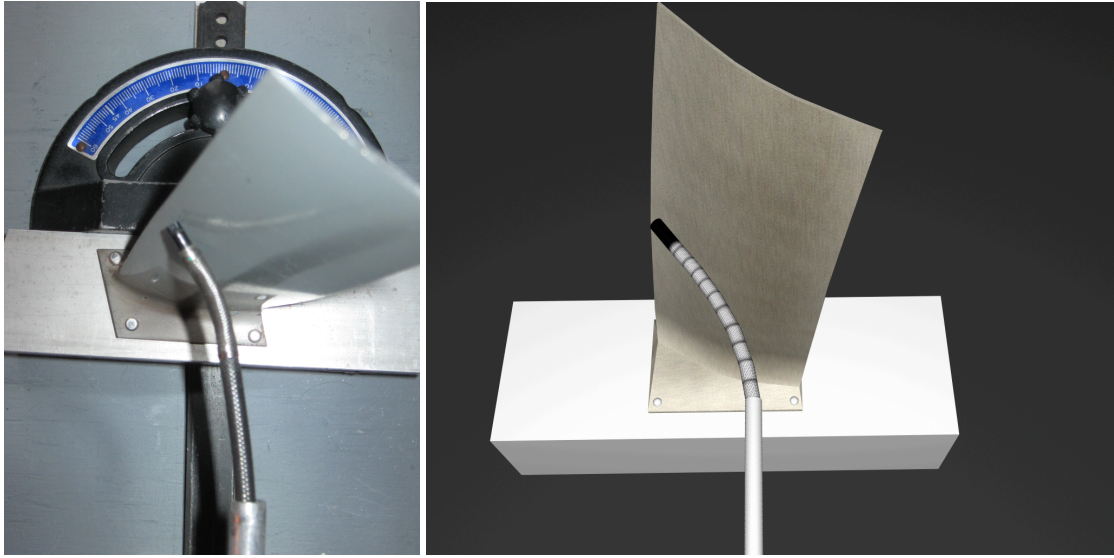


**Figure 7.6:** Sliding intersection of the probe with the engine (left) and simulated results (right).

diameter of 5mm was used in this evaluation.

### 7.3.2 Stimulus and Experiment

The engine blade used in the evaluation was modeled in Maya and exported as an `.obj` file, with texture, material and lighting information. A custom graphical viewer was written to import and render the model of the engine blade. The borescope probe was simulated using the model described in the prior section, with extra proxy nodes and full multi-point contact detection and feedback. Since the focus of this evaluation was visual comparison of the intersection response between the real and virtual borescope probes, haptic feedback was not provided.

The experiment consisted of visual comparisons of the probe deformation during intersection with the engine blade. The measurements consisted of visual confirmation of the virtual probe behavior compared to the real borescope probe and observations of deviant behavior. Three angles of incidence ( $0^\circ$ ,  $30^\circ$  and  $50^\circ$ ), two different distances between the guide tube and the blade (1" and 3") and two different angles of borescope tip articulation (straight and  $60^\circ$ ) were evaluated and behavior of the virtual borescope probe visually confirmed for correctness.



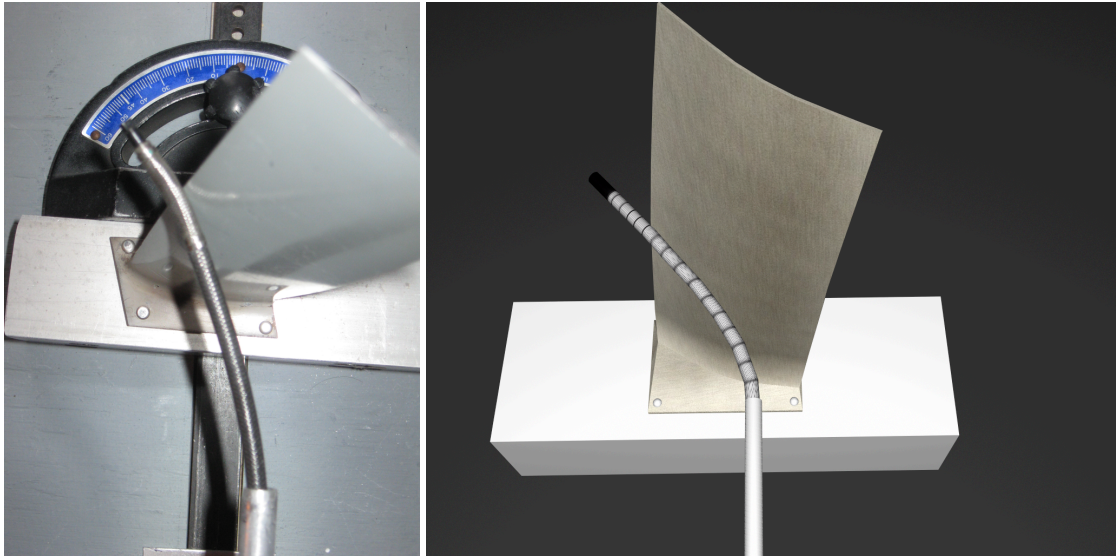


**Figure 7.7:** Contact detection along the body of the borescope probe (left) and simulated results (right).

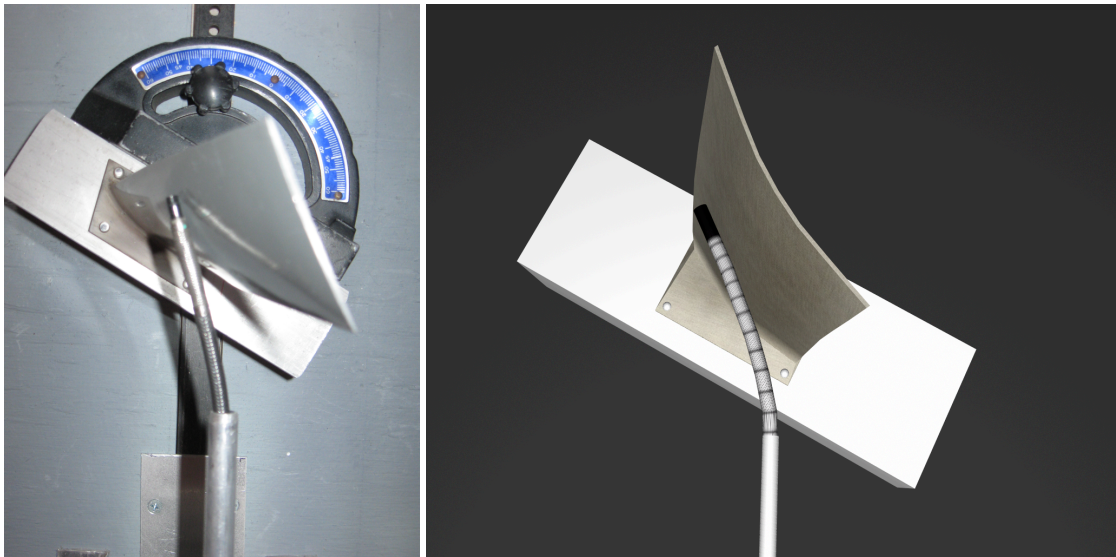


**Figure 7.8:** Intersection response at 30° angle of incidence (left) and simulated results (right).

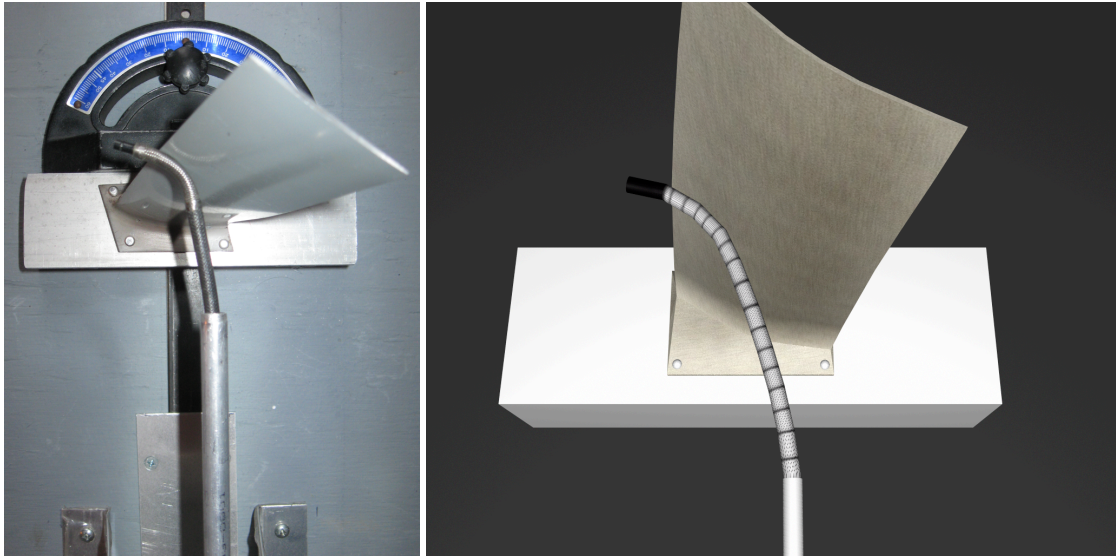


**Figure 7.9:** Intersection response with probe tip articulated to 60° (left) and simulated results (right).

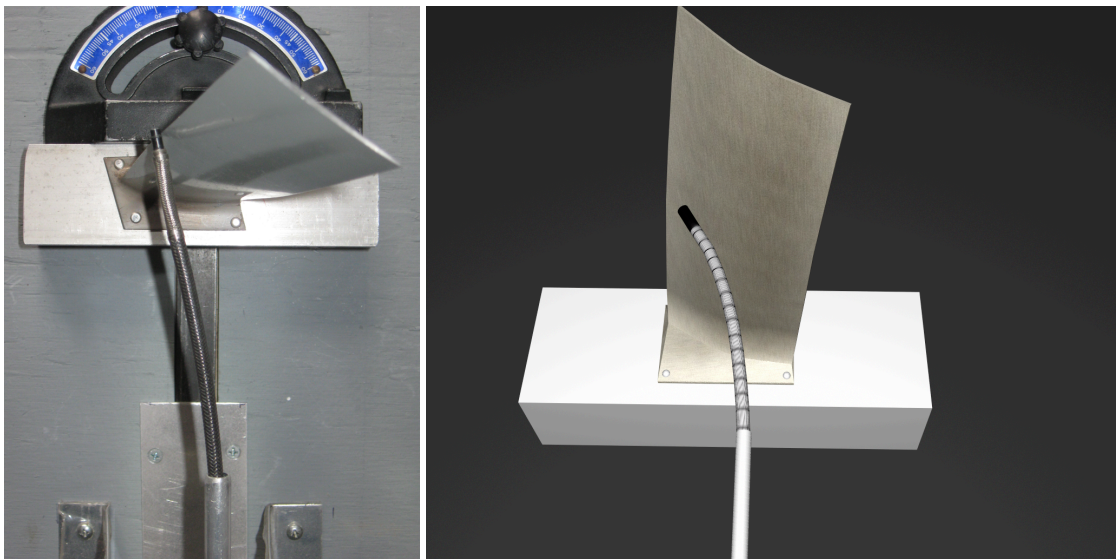


**Figure 7.10:** Intersection response with guide tube 3" from the blade (left) and simulated results (right).

### 7.3.3 Results and Discussion

In this section, we present a subset of the empirical evaluations carried out with different values of the angles of incidence, probe distance and tip articulation angles. Figure 7.5 through Figure 7.7 presents the behavior of the real probe (left) and the behavior of the virtual probe at  $0^\circ$  angle of incidence with the probe distance 1" from the blade. Figure 7.5 shows the output of the virtual probe as it emerges from the guide tube and before it intersects with the 3D blade model. In Figure 7.6, the tip of the virtual probe has intersected with the blade model and is sliding along the surface of the blade. Note that the behavior of the virtual and the real borescopes are similar in appearance. Figure 7.7 shows the behavior of the probe as the tip extends beyond the surface of the engine blade. Due to the use of the enhanced probe model and multi-point collision response, the nodes of the virtual probe intersect with the engine and are constrained to the surface of the engine providing a haptic response.

Figures 7.8 and 7.9 shows the behavior of the real and virtual probes as they interact with the blade at a  $30^\circ$  angle and the tip articulated to  $60^\circ$  respectively. Similar results are obtained from the virtual borescope model for both the cases. Finally, Figure 7.10 shows the behavior of the probe when the distance between the guide tube and the point of intersection is 3". This case simulates the behavior of the borescope as it maneuvers within the engine from one position to the other. In all cases, the behavior of the virtual probe was observed to be a good approximation to the real borescope interaction.

## Chapter 8

# Evaluating Skills Transfer

In the preceding chapters, we have presented the development and evaluation of the virtual borescope simulator with 3D models of engine components and off-the-shelf haptic devices to provide probe contact feedback. The development of the simulator was intended to enhance classroom instruction by providing hands-on training in a replicated simulation of the inspection task. The prior evaluations of the virtual borescope to determine the visual control and haptic fidelity of the simulator was restricted to evaluation of pre- and post-training metrics on the simulator. While literature evaluating the effectiveness of simulator training suggests a trend of simulator performance being a good predictor of real world performance, we wanted to determine if simulator training would be comparable to real world training with the actual device.

### 8.1 Experiment 7: Inspection Performance Evaluation

In this section we present the evaluation of three different training systems: classroom-only training, borescope simulator training with force feedback, and hands-on training with the real video borescope. We examine their influence on engine inspection by novice aircraft maintenance technicians. We were interested in comparing classroom-only instruction, with an emphasis on theoretical knowledge, with hands-on learning with the virtual borescope simulator. Specifically, we wanted to compare the skills transfer, if any, of simulator training to performance in the real world and draw inferences on the use of simulator training as an augmented aid to classroom instruction.

### **8.1.1 Participants**

Twenty six students enrolled in the aircraft maintenance program at Greenville Technical college took part in this study. The participants were divided into three groups, with one group with eight participants and the other two groups each with nine participants. All the students had completed at least two semesters of general aviation inspection related coursework and were familiar with the theoretical background on engine inspection. The participants had limited hands-on experience with the video borescope having observed its use by the classroom instructor. A few of the participants had experience with the optical borescope, but that was limited to a few hours of use.

### **8.1.2 Apparatus and Stimuli**

The students were divided into three groups based on the training they received.

1. Control group. Participants in this group received no hands-on training other than theoretical knowledge through classroom lessons.
2. Virtual borescope group. Participants in this group received two 45-minute training sessions on the virtual borescope simulator, followed by a 10-minute evaluation with the simulator to determine their proficiency with user controls and inspection procedures. The training sessions were spread over two days to prevent fatigue.
3. Video borescope training. Participants received two 45-minute training sessions through hands-on operation of a real video borescope on an aircraft engine.

Students in the simulator group received inspection training on the virtual borescope simulator. The simulator was run on a desktop PC, equipped with a PentiumD 2.4GHz processor, 4GB RAM, and a GeForce 9800GT video card. The output of the simulator was presented on a 19" LCD monitor placed in front of the participant in a 1024×768 window. The visual stimulus provided to the participants consisted of a polygonal model of the PT-6 engine, modeled and textured in Maya, and exported as an `.obj` file. The rendering of the engine components and the haptic feedback calculations was handled by CHAI libraries, an open-source API for graphical and haptic rendering. The camera articulation of the virtual probe was controlled by an off-the-shelf gamepad, similar to prior experiments. The Novint Falcon was used both for controlling the amount of virtual probe insertion into the 3D engine as well as to provide force feedback of the contact forces experienced by the virtual probe.



**Figure 8.1:** Inspection of PT-6 aircraft engine using borescope (left) and operator view of the camera output on the screen (right).

The students in the hands-on training group received inspection training using the Olympus video borescope. A representative engine of a PT6 aircraft was dismantled to expose the hot section components consisting of the stator and rotor, as shown in Figure 8.1. A guide tube was inserted into the fuel injection manifold at the top of the engine casing to allow easy insertion of the borescope into the engine and facilitate inspection of the rotor. An experienced borescope inspector was present to provide instruction and guidance on the best practices while inspecting using the borescope.

### 8.1.3 Procedure

At the beginning of the experiment, the participants filled out a demographic questionnaire on their experience with training simulators and the video borescope. The experiment was carried out over three days to prevent fatigue and avoid influencing the results of the experimental evaluation.

On day 1, the control group received no training on the simulator or the actual engine. The simulator group was provided training with the virtual borescope, with a focus on familiarizing the participants with the articulation and insertion controls in the simulator. The participants were first introduced to the simulator and the use of the gamepad and the Falcon to control the virtual probe demonstrated. Next, the participants spent approximately 45 minutes interacting with the simulator and getting used to the articulation controls. In addition to psychomotor skills training, we also provided good practices inspection training by having the participants inspect the engine model in a systematic fashion. Textures on the engine model emphasized this aspect of training by having numbered textures on the blades, with arrows pointing to the next stage of inspection feature. At the end of the familiarization phase, the participants were tested on their progress by performing a simulated task of inspecting 15 blades on the rotor for defects. Quantitative measures of time

to complete the task and the total number of probe tip intersections with the engine model were collected for offline analysis.

The training provided to the borescope training group consisted of introduction to the video borescope, a brief summary of controlling the probe tip with the articulation joystick and good practices in borescope inspection. On completion of these steps, the participants used the borescope and performed a 45 minute inspection on a PT-6 engine. The engine was pristine and did not have any defects, as we wanted the participants to become accustomed to the interface as opposed to the defect detection.

On day 2, the steps followed were similar to day 1 for all three groups with a few minor changes. In addition to providing good practices inspection for the simulator group, they were also provided training to detect common defects such as cracks and corrosion in the engine. Defect textures were developed and mapped to the engine model to provide a brief overview of different defects found in the engine. At the end of the simulator training, quantitative data was collected to compare the influence (if any) of longer training durations on participants' performance across the two days. There were no changes in the training process provided to the other two groups.

On day 3, all the three groups were tested on a PT-6 engine using the video borescope. The engine used in this study was different from the engine used for training the hands-on group in order to prevent learning effects. Instead of defects in the rotor, we marked random blades with distinguishing features (white X) to simulate defects in the rotor.

As the control group and the simulator groups were using the video borescope for the first time, the participants were provided a 10 minute introduction to the video borescope and the articulation controls. The inspection process consisted of the participants inserting the borescope probe into the engine through the guide tube and maneuvering the borescope probe through the engine stators to obtain a good view of the rotor. Once the participant had a clear view of the leading edge and the base of the rotor blades, the inspection task consisted of looking for the distinguishing markers on the blades. An accomplice manually rotated the engine to turn the rotor so that the participant could concentrate on borescope probe manipulation and controlling the camera articulation along with defect detection. Once the participant completed inspecting all 58 blades of the rotor, they were instructed to complete the inspection task by withdrawing the probe from the engine.

#### **8.1.4 Design and Data Collected**

A between-subjects completely random experimental design was used to study the transfer effects of simulator training. The twenty six participants were randomly assigned to one of the three training groups.



Training condition served as the independent variable. Performance data collected were time taken to complete the task and the number of defects correctly detected. The time taken to complete the inspection task was broken down into 4 intervals:

1. inserting the borescope probe through the guide tube into the engine,
2. maneuvering the probe through the stator to obtain a clear view of the rotor blades for inspection,
3. systematic inspection of the blades for simulated defects, and
4. withdrawal of the borescope probe from the engine.

The control group was expected to yield the the largest mean inspection times, compared to the simulator and hands-on training groups. The simulator and borescope training groups were expected to have similar performance due to improved skill levels compared to classroom-only training group.

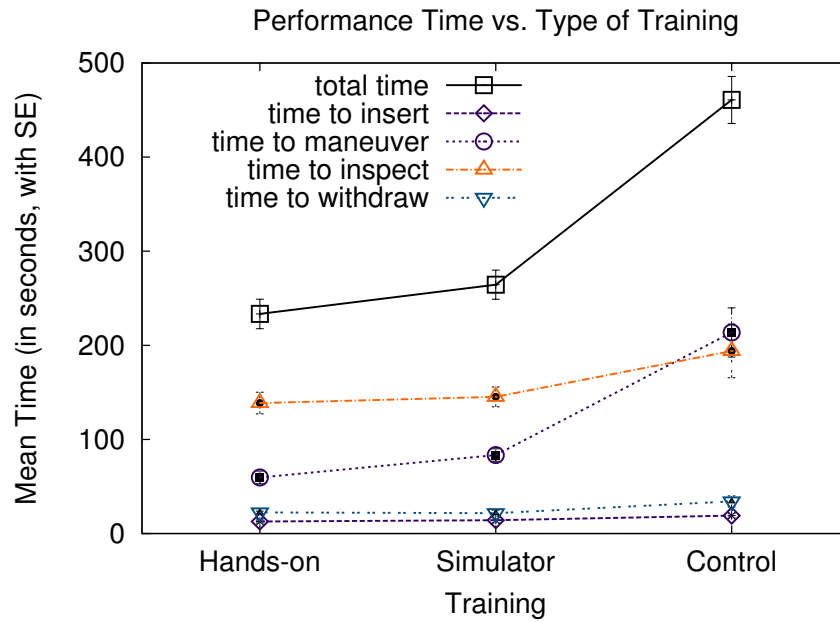
The virtual borescope group had additional performance and subjective data collected at the end of each individual training sessions. The total time to complete the simulator inspection and the number of intersections of the virtual camera with the engine model were collected and analyzed to determine the effects of repeated training on task performance in the simulator. On completion of the training, the participants filled out a modified Witmer-Singer Presence Questionnaire [72], with responses to the questionnaire on a 7-point Likert scale, with 1 being most negative, 4 neutral, and 7 most positive.

It was hypothesized that due to longer training, total inspection time and number of intersections with the engine model would decrease from day 1 to day 2.

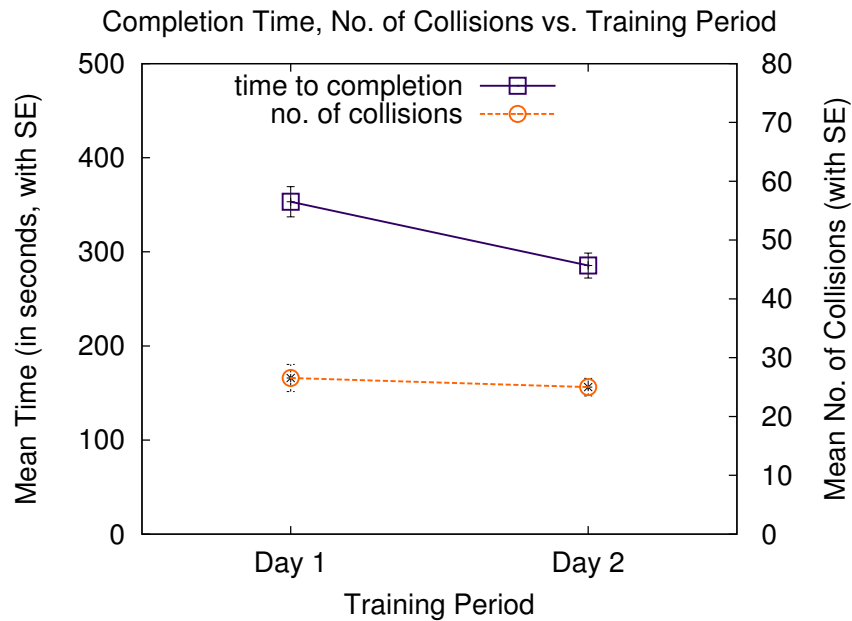
### **8.1.5 Results**

Figure 8.2 shows the mean completion times for all three training conditions, as well as the breakdown of the time taken to perform each of the four phases of the inspection task identified in the previous section. ANOVA of the mean completion times shows that there were significant differences among the three groups ( $F(2,23) = 40.3$ ,  $p < 0.01$ ), with the control group taking longer to complete the inspection task compared to the other two groups who received training. Pairwise t-tests (with Bonferroni correction) reveal no significant difference between the virtual borescope and real borescope group. However, there were significant differences in time to completion between the control group and the two training conditions ( $p < 0.01$  for both pairings).





**Figure 8.2:** Average time taken to insert, maneuver, inspect and withdraw the borescope from the test engine, grouped by type of training provided.



**Figure 8.3:** Time taken for simulated inspection and total number of virtual probe camera hits with the engine model evaluated at the end of training on day 1 and 2.

The Kruskal-Wallis test was used to analyze the time taken for each individual stage of the inspection, as Shapiro-Wilk's test revealed non-normal data distribution. There was no significant difference among the three groups for the average time taken to insert the borescope probe into the engine ( $\chi^2(2, N = 26) = 3.06, p > 0.05$ ), the time taken for inspection of the engine blades for defects ( $\chi^2(2, N = 26) = 0.85, p > 0.05$ ) and withdrawal of the borescope from the engine ( $\chi^2(2, N = 26) = 5.18, p > 0.05$ ). There was significant difference in the time taken to maneuver the borescope in the engine, ( $\chi^2(2, N = 26) = 18.61, p < 0.001$ ), with the control group taking an average of 213 seconds to maneuver the borescope probe through the stators compared to 83 s and 59 s taken by the simulator and borescope groups, respectively.

Figure 8.3 shows the mean completion time and the total number of hits of the virtual camera for the simulator training group across day 1 and 2. Repeated measures one-way ANOVA reveals significant difference in the total time taken for inspection  $F(1,8) = 35.09, p < 0.001$ . There was no significant difference in the number of hits across the two experiments,  $F(1,8) = 0.33, p > 0.05$ .

### 8.1.6 Discussion

Task completion results across the three groups indicates that the participants who received any form of training, either on the virtual simulator or the real borescope, completed the inspection task faster than the control group. From Figure 8.2, we see that the average time taken by the control group was approximately 460 seconds. This is almost double the time taken by participants in other groups with simulator or borescope training. Compared to traditional classroom-only teaching, we find that provision of even limited hands-on training with either the simulator or the real borescope drastically improves inspection performance.

The skills required to perform the borescope inspection, especially the hand eye coordination skills, are difficult to obtain except through hands-on training with the real borescope. As very few aircraft maintenance schools can afford the borescope, there are limited opportunities for novice students to gain experience using the borescope. The similar performance results of the group using the borescope simulator compared to hands-on borescope training provides an added opportunity for novice maintenance technicians to gain practical experience through repeated training with the simulator.

The similar performance of the simulator and the real borescope group could be attributed to the similar task profiles and skills needed for inspection. Similar to the video borescope, the simulator adopted a two handed interaction strategy by using the dominant hand for probe insertion and the non-dominant hand for camera articulation. The indirect manipulation and remote viewing of the component being inspected by the borescope had similar constraints as the virtual simulator.

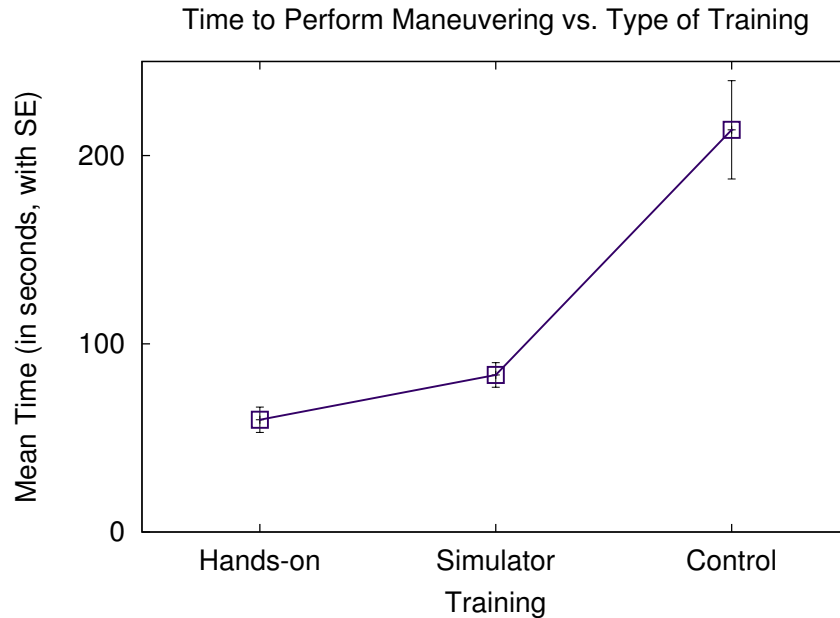


**Figure 8.4:** Average time taken for maneuvering the borescope through the engine between the stators.

Although the control group took longer to finish the inspection, a majority of the difference in the time could be attributed to the longer time taken by the participants in maneuvering the borescope through the engine. Figure 8.4 shows the average time taken by the three groups in maneuvering the borescope probe through the test engine. The participants in the control group took, on average, 2-3 times longer than the participants in groups that received training (213 seconds in control groups versus 59 seconds and 83 seconds for the borescope and simulator training group). Participants with no training were disoriented when using the borescope and had to repeatedly turn their attention away from the video screen to look at the hand-held articulation controls, as well as balance the borescope probe inserted into the engine. On the other hand, participants with simulator or borescope training were observed to be more comfortable interacting with the controls and the video screen.

There were no significant differences in the mean time taken by the participants in the three groups for the other stages of the inspection. Probe insertion and withdrawal are similar tasks and lend themselves to easy training in the classroom. The guide tube provides an easy outlet to insert the borescope through the different stages of the engine, and depending on the stage of the engine under inspection, novice inspectors can be instructed to choose the correct guide tube.

The task simulated is representative of borescope inspection performed on an aircraft engine. Once

inserted into the engine, the borescope is usually held steady in one place and the rotors being inspected manually rotated. Although defect identification is an important aspect of the simulation, the skills needed for inserting the probe through various stages of the engine are more critical to prevent damage to the probe. The provision of force feedback in the simulator may have helped the participants in transitioning from the simulator to the real world task. This is important as experienced inspectors rely on force feedback from the borescope probe to prevent accidental damage to the probe during insertion and withdrawal from the engine.

The results from the simulator evaluation on the two days when training was provided suggests potential for improved performance with longer durations of training. Unlike our previous evaluations where the pre-test familiarization phase was limited to about 15 minutes of hands-on learning with the simulator, in this study we provided longer duration of familiarization with the interface and the controls. Training effect may have played an important part in the participants taking less time to complete the inspection on day 2 compared to day 1. Despite the limited training time with the real and the virtual borescope, similar performance suggests that the skills needed for successful inspection can be obtained through repeated simulator training.

Although the number of intersections of the virtual camera with the engine model in the simulator did not significantly decrease during the training, provision of tip force feedback may have played a role in transferring skills to the real world. Unlike the simulator, there was no opportunity to collect the total number of intersections of the borescope with the engine during inspection. Informal discussions with the participants using the simulator suggested that they preferred the force feedback from the simulator as it aided them in interacting with the simulator, especially while maneuvering the virtual probe into the model.

There are a few ways in which we could improve the outcomes of simulator training. Unlike real inspection, we conducted the evaluation of simulator training by focusing on only the probe manipulation skills needed during the inspection. Unlike an actual engine with defects such as stress cracks, corrosion, and rust, the test engine was in relatively good shape. The focus of the study could be expanded to detect and identify defects (search and decision tasks) by continuing training with the simulator and comparing performance in the workforce. However, time constraints and limited resources available to perform the transfer effects evaluation led to a narrow focus of skills transfer from the simulator to the real world.

Due to the limited pool of participants needed for this study, unforeseen schedule and availability conflicts resulted in one of the participants in the borescope training group having to drop out of training after one session. This resulted in an unbalanced group of only eight participants in the borescope training group as opposed to nine participants in the other two groups. Preliminary analysis of the time taken for the inspection

by Shapiro-Wilk's test revealed that the distribution of data was not normal. Hence the Kruskal-Wallis test was chosen for analyzing non-normal data, as opposed to the more widely used ANOVA.

The results of this study are significant for two reasons. First, we provide evidence that any form of hands-on training is better than classroom-only learning. Participants were able to relate better to the inspection procedures through extended training with either the real borescope or the virtual simulator. Second, and more importantly, the results suggest that the skills needed to manipulate the borescope probe that are obtained through extended on-the-job training may possibly be acquired by novice aircraft maintenance inspectors through simulator training. Similar to pilots obtaining flight experience through simulator training, the virtual borescope could be a very useful aid in improving student outcomes from aviation maintenance schools.

## Chapter 9

# Conclusion

As we pointed out in the introduction to this dissertation, the visual inspection of aircraft engines with the video borescope is an important part of non-destructive testing. Presently, the skills required to operate the borescope are hard to acquire except through repeated and extensive hands-on training. Novice aircraft maintenance technicians graduating from aviation schools have limited hands on experience with the borescope, due to their prohibitive costs and limited time resources. As a result, they face a steep learning curve transitioning from the school to the workplace.

In this dissertation, we have presented one alternative to hands-on learning with a real borescope. We have described the development of a novel visuohaptic simulator for engine inspection using 3D models of engine components. Compared to the real device, our simulator uses commonly available off-the-shelf components for articulation control as well as force feedback. Unlike resource constraints in a real inspection, we are limited only by the availability of 3D models of various aircraft engines.

We described the development of the visual output of the simulator, as well as user evaluation of the visual and control interfaces of the simulator. We addressed the lack of force feedback in the simulator by developing a novel haptic interface to provide 1D force feedback of intersections of the virtual camera with the engine models. User evaluation of the haptic interface suggested a trend of improved performance and a reliance on intersection feedback.

To improve the behavior of the virtual camera, we developed a physically based model of the borescope camera. Modeled by a chained mass-spring system, the virtual probe provides a camera whose articulation is similar to the real borescope camera. Simulator evaluation with the enhanced camera and off-the-shelf haptic devices suggests that users perform the simulated inspection task best with the enhanced

camera combined with off-the-shelf haptic interfaces. Given the low cost and easy availability of the Novint Falcon, we recommend using the Falcon in tasks where force feedback forms an important part of sensory perception, but the task does not require high fidelity force feedback.

The probe model in the simulator was improved by using a simple algorithm to provide force feedback of intersections along the entire length of the virtual probe. We presented visual comparisons of the behavior of the real borescope intersecting with the rigid blades and simulated the same behavior through careful selection of parameters for the simulation. A skills transfer evaluation comparing the performance of students trained using the virtual borescope simulator with students who received training with the real borescope showed similar performance in terms of time taken to complete the inspection.

Directions for future work include evaluation of defect detection and identification using the simulator. Due to time and resource constraints, we concentrated only on determining the skills transfer from the simulator to the real world, with minimal attention to defect detection. Though control and interaction skills play an important part in the inspection process, defect determination and classification play an equally important role. Future evaluations should include acquiring engines with defects and evaluating the transfer effects of defect classification training on the simulator.

The training of the students was limited to a maximum of two hours on the simulator. A more thorough evaluation could consist of a semester long project mandating the use of the simulator for practical training for an extended period of time. It would be interesting to evaluate the skills acquired through such extensive training. Follow-up studies at the workplace with novice inspectors trained on the simulator would be useful in determining if the learning curve and challenges faced by the students in transitioning to the workforce could be ameliorated by simulator training.

Though the focus of this research was on aircraft engines, the concept of remote viewing and manipulation could be applied to a variety of related fields. Specifically, robotic teleoperation is similar in concept to this research. Minimally invasive surgery using catheters could benefit from the work presented in this dissertation, though unlike interaction of the flexible probe with rigid blades, the presence of elastic tissues would necessitate development of advanced force computation algorithms for realistic force feedback.

In summary, the results of this dissertation suggest that the psychomotor skills and the hand eye coordination required for a successful aircraft engine inspection using the video borescope can be (i) taught using hands-on training using the virtual borescope simulator (ii) that the training transfers to the real task and (iii) is comparable to hands-on training with the real borescope.

# Bibliography

- [1] Marco Agus, Andrea Giachetti, Enrico Gobbetti, Gianluigi Zanetti, Nigel W. John, and Robert J. Stone. Mastoidectomy simulation with combined visual and haptic feedback. In J. D. Westwood, H. M. Hoffmann, G. T. Mogel, and D. Stredney, editors, *Medicine Meets Virtual Reality 2002*, pages 17–23. IOS, Amsterdam, The Netherlands, January 2002.
- [2] Tanja Alderliesten, Maurits K. Konings, and Wiro J. Niessen. Simulation of minimally invasive vascular interventions for training purposes. *Computer Aided Surgery*, 9:3–15, 2004.
- [3] Object file format, 2009. URL: , <<http://local.wasp.uwa.edu.au/~pbourke/dataformats/obj/>> last accessed 11/20/09.
- [4] M. W. Allgaier and S. Ness, editors. *Visual and Optical Testing*. Number 8 in Nondestructive Testing Handbook. American Society for Nondestructive Testing, Columbus, OH, 1993.
- [5] American Society for Nondestructive Testing. Recommended Practices No. SNT TC-1A, 2001.
- [6] American Society for Nondestructive Testing. ASNT Level III Study Guide and Supplement on Visual and Optical Testing, 2005.
- [7] L. M. Auer, D. Auer, and J. F. Knoploch. Virtual Endoscopy for Planning and Simulation of Minimally Invasive Neurosurgery. *Lecture Notes in Computer Science*, 1205:315–318, 1997.
- [8] Federico Barbagli, Domenico Prattichizzo, and Kenneth Salisbury. *Multi-point Interaction with Real and Virtual Objects (Springer Tracts in Advanced Robotics)*. Springer-Verlag New York, Inc., Secaucus, NJ, USA, 2005.



- [9] Federico Barbagli, Ken Salisbury, Cristy Ho, Charles Spence, and Hong Z. Tan. Haptic Discrimination of Force Direction and the Influence of Visual Information. *ACM Transactions on Applied Perception*, 3(2):125–135, 2006.
- [10] Jonathan Baron and Yuelin Li. Notes on the use of R for psychology experiments and questionnaires. Online Notes, 09 November 2007. URL: <<http://www.psych.upenn.edu/~baron/rpsych/rpsych.html>> (last accessed December 2007).
- [11] Cagatay Basdogan, Chih-hao Ho, and M. A. Srinivasan. Virtual environments for medical training: Graphical and haptic simulation of laparoscopic common bile duct exploration. *IEEE/ASME Transactions on Mechatronics*, 6:269–285, 2001.
- [12] Nico Becherer, Jürgen Hesser, Ulrike Kornmesser, Dietmar Schranz, and Reinhard Männer. Interactive physical simulation of catheter motion within major vessel structures and cavities for asd/vsd treatment. volume 6509, page 65090U. SPIE, 2007.
- [13] S.N. Bobo and C.H. Puckett. *Visual Inspection for Aircraft, Draft Advisory Circular AC-43-XX*. Federal Aviation Administration, 1995.
- [14] Stephen N. Bobo. Visual inspection as an organized procedure. *Nondestructive Evaluation of Aging Aircraft, Airports, Aerospace Hardware, and Materials*, 2455(1):164–172, 1995.
- [15] Joel Brown, Jean-Claude Latombe, and Kevin Montgomery. Real-time knot-tying simulation. *The Visual Computer: International Journal of Computer Graphics*, 20(2):165–179, 2004.
- [16] Brookshire D. Conner, Scott S. Snibbe, Kenneth P. Herndon, Daniel C. Robbins, Robert C. Zeleznik, and Andries van Dam. Three-dimensional widgets. In *SI3D '92: Proceedings of the 1992 Symposium on Interactive 3D Graphics*, pages 183–188, New York, NY, USA, 1992. ACM.
- [17] F. Conti, O. Khatib, and C. Baur. Interactive Rendering Of Deformable Objects based on a Filling Sphere Modeling Approach. In *IEEE International Conference on Robotics and Automation*, volume 3, pages 3716–3721, 2003.
- [18] S. Cotin, C. Duriez, J. Lenoir, P. Neumann, and S. Dawson. New approaches to catheter navigation for interventional radiology simulation. In *Proceedings of medical image computing and computer assisted intervention (MICCAI)*, pages 300–308, 2005.

- [19] Steven L. Dawson, Stephane Cotin, Dwight Meglan, David W. Shaffer, and Margaret A. Ferrell. Designing a computer-based simulator for interventional cardiology training. *Catheterization and Cardiovascular Interventions*, 51(4):522–527, 2000.
- [20] Rajeev Dayal, Peter L. Faries, Stephanie C. Lin, Joshua Bernheim, Scott Hollenbeck, Brian DeRubertis, Susan Trocciola, Jason Rhee, James McKinsey, Nicholas J. Morrissey, and K. C. Kent. Computer simulation as a component of catheter-based training. *Journal of Vascular Surgery*, 40(6):1112–1117, 2004.
- [21] A. Ferlitsch, P. Glauninger, A. Gupper, M. Schillinger, M. Haefner, A. Gangl, and R. Schoefl. Evaluation of a Virtual Endoscopy Simulator for Training of Gastrointestinal Endoscopy. *Endoscopy*, 34(9):698–702, 2002.
- [22] A. Ferlitsch, P. Glauninger, A. Gupper, M. Schillinger, M. Haefner, A. Gangl, and R. Schoefl. Virtual endoscopy simulation for training of gastrointestinal endoscopy. *Endoscopy*, 34(9):698–702, 2002.
- [23] Gerald M. Fried, Liane S Feldman, Melina C Vassiliou, Shannon A Fraser, Donna Stanbridge, Gabriela Ghitulescu, and Andrew Christopher G. Proving the value of simulation in laparoscopic surgery. *Annals of Surgery*, 240(3):518–528, 2004.
- [24] Samir Garbaya and U. Zaldivar-Colado. The affect of contact force sensations on user performance in virtual assembly tasks. *Virtual Reality*, 11(4):287–299, 2007.
- [25] T. P. Grantcharov, V. B. Kristiansen, J. Bendix, L. Bardram, J. Rosenberg, and P. Funch-Jensen. Randomized clinical trial of virtual reality simulation for laparoscopic skills training. *British Journal of Surgery*, 91(2):146–150, 2004.
- [26] Saul Greenberg and Chester Fitchett. Phidgets: easy development of physical interfaces through physical widgets. In *UIST '01: Proceedings of the 14th annual ACM symposium on User Interface Software and Technology (UIST)*, pages 209–218, New York, NY, 2001. ACM.
- [27] S. G. Hart and L. E. Staveland. Development of a multi-dimensional workload rating scale: Results of empirical and theoretical research. In P. A. Hancock and N. Meshkati, editors, *Human Mental Workload*, pages 139–183. Elsevier, Amsterdam, Holland, 1988.
- [28] Brad M. Howard and Judy M. Vance. Desktop haptic virtual assembly using physically based modelling. *Virtual Reality*, 11(4):207–215, 2007.

- [29] Robert J. K. Jacob. Input devices and techniques. In *The Computer Science and Engineering Handbook*, pages 1494–1511, 1996.
- [30] Arjun D. Koch, Sonja N. Buzink, Jeroen Heemskerk, Sanne M. B. I. Botden, Roeland Veenendaal, Jack J. Jakimowicz, and Erik J. Schoonm. Expert and construct validity of the Simbionix GI Mentor II endoscopy simulator for colonoscopy. *Surgical Endoscopy*, 22(1):158–162, 2007.
- [31] Olaf Korner and Reinhard Manner. Implementation of a Haptic Interface for a Virtual Reality Simulator for Flexible Endoscopy. In *11th Symposium on Haptic Interfaces for Virtual Environment and Teleoperator Systems (HAPTICS'03)*, page 278, March 2003.
- [32] Blazej Kubiak, Nico Pietroni, Fabio Ganovelli, and Marco Fratarcangeli. A robust method for real-time thread simulation. In *VRST '07: Proceedings of the 2007 ACM symposium on Virtual reality software and technology*, pages 85–88, New York, NY, USA, 2007. ACM.
- [33] Pablo Lamata, Enrique J. Gomez, Fernando Bello, Roger L. Kneebone, Rajesh Aggarwal, and Felix Lamata. Conceptual framework for laparoscopic vr simulators. *IEEE Computer Graphics and Applications*, 26(6):69–79, 2006.
- [34] S. D. Laycock and A. M. Day. Incorporating haptic feedback for the simulation of a deformable tool in a rigid scene. *Computers and Graphics*, 29(3):341–351, 2005.
- [35] S.D. Laycock and A.M. Day. The haptic rendering of polygonal models involving deformable tools. In *EUROHAPTICS 2003*, pages 176–192, 2003.
- [36] S.D. Laycock and A.M. Day. Recent developments and applications of haptic devices. *Computer Graphics Forum*, 22(2):117–132, 2003.
- [37] S.D. Laycock and A.M. Day. Simulating deformable tools with haptic feedback in a virtual environment. In *WCSG Short Papers proceedings*, pages 75–81, 2003.
- [38] Julien Lenoir, Stephane Cotin, Christian Duriez, and Paul Neumann. Interactive physically-based simulation of catheter and guidewire. *Computers and Graphics*, 30(3):416–422, 2006.
- [39] Julien Lenoir, Stephane Cotin, Christian Duriez, and Paul Neumann. Physics-based models for catheter, guidewire and stent simulation. In *Medicine Meets Virtual Reality 14: Accelerating Change in Healthcare: Next Medical Toolkit*, volume Volume 119, pages 305–310. IOS Press, 2006.

- [40] T. Lim, J. M. Ritchie, R. G. Dewar, J. R. Corney, P. Wilkinson, M. Calis, M. Desmulliez, and J.-J. Fang. Factors affecting user performance in haptic assembly. *Virtual Reality*, 11(4):241–252, 2007.
- [41] S. Loncaric, T. Markovinovic, T. Petrovic, D. Ramljak, and E. Sorantin. Construction of Virtual Environment for Endoscopy. In *Proceedings of the IEEE International Conference on Multimedia Computing and Systems*, 1999.
- [42] Vincent Luboz, James Lai, Rafal Blazewski, Derek Gould, and Fernando Bello. A virtual environment for core skills training in vascular interventional radiology. In *ISBMS '08: Proceedings of the 4th International Symposium on Biomedical Simulation*, pages 215–220, 2008.
- [43] I. S. MacKenzie, Abigail Sellen, and William A. S. Buxton. A comparison of input devices in element pointing and dragging tasks. In *Proceedings of the SIGCHI conference on Human factors in computing systems*, pages 161–166, New York, NY, USA, 1991. ACM.
- [44] I. Scott MacKenzie. *Input devices and interaction techniques for advanced computing*, pages 437–470. Oxford University Press, Inc., New York, NY, USA, 1995.
- [45] Pascal Maillard, Lionel Flaction, Evren Samur, David Hellier, Josh Passenger, and Hannes Bleuler. Instrumentation of a clinical colonoscope for surgical simulation. *30th Annual International Conference of the IEEE Engineering in Medicine and Biology Society*, pages 70–73, Aug 2008.
- [46] T. H. Massie and J. K. Salisbury. The PHANToM haptic interface: A device for probing virtual objects. In *Proceedings of the ASME Winter Annual Meeting, Symposium on Haptic Interfaces for Virtual Environment and Teleoperator Systems*, pages 295–302, 1994.
- [47] Autodesk Maya. URL: <<http://www.autodesk.com/fo-products-maya/>> last accessed November, 2007.
- [48] Dan Morris, Christopher Sewell, Federico Barbagli, Kenneth Salisbury, Nikolas H. Blevins, and Sabine Girod. Visuohaptic Simulation of Bone Surgery for Training and Evaluation. *IEEE Computer Graphics and Applications*, 26(6):48–57, November/December 2006.
- [49] W.L. Nowinski and Chee-Kong Chui. Simulation of interventional neuroradiology procedures. *Proceedings of International Workshop on Medical Imaging and Augmented Reality*, pages 87–94, 2001.
- [50] Marcia K. O'Malley and Gina Upperman. A Study of Perceptual Performance in Haptic Virtual Environments. *Journal of Robotics and Mechatronics*, 18(4), 2006.

- [51] OpenSceneGraph. URL: <<http://www.openscenegraph.org/>> last accessed December, 2008.
- [52] Dinesh K. Pai. Strands: Interactive simulation of thin solids using cosserat models. *Computer Graphics Forum*, 21(3):347–352, 2002.
- [53] David S. Paik, Christopher F. Beaulieu, R. Brooke Jeffrey, Geoffrey D. Rubin, and Sandy Napel. Automated Path Planning for Virtual Endoscopy. *Medical Physics*, 25(5):629–637, May 1998.
- [54] Irvin Rock and Jack Victor. Vision and Touch: An Experimentally Created Conflict between the Two Senses. *Science*, 143(3606):594–596, 1964.
- [55] L. B. Rosenberg and B. D. Adelstein. Perceptual Decomposition of Virtual Haptic Surfaces. In *Proceedings of the IEEE 1993 Symposium on Research Frontiers in Virtual Reality*, pages 46–53, 1993.
- [56] Diego C. Ruspini, Krasimir Kolarov, and Oussama Khatib. The haptic display of complex graphical environments. In *SIGGRAPH '97: Proceedings of the 24th annual conference on Computer graphics and interactive techniques*, pages 345–352, New York, NY, USA, 1997. ACM Press/Addison-Wesley Publishing Co.
- [57] E. Samur, L. Flection, U. Spaelter, H. Bleuler, D. Hellier, and S. Ourselin. A Haptic Interface with Motor/Brake System for Colonoscopy Simulation. *Haptic Interfaces for Virtual Environment and Teleoperator Systems, 2008. Haptics 2008. Symposium on*, pages 477–478, March 2008.
- [58] Guillaume Saupin, Christian Duriez, and Stephane Cotin. Contact model for haptic medical simulations. 5104:157–165, 2008.
- [59] OpenGL Architectural Review Board. ARB\_FRAGMENT\_PROGRAM Specification. Revision: 26, August 22 2003. URL: <<http://oss.sgi.com/projects/ogl-sample/registry/>> (last accessed April 2004).
- [60] R. E. Sedlack, J. C. Kolars, and J. A. Alexander. Computer Simulation Training Enhances Patient Comfort During Endoscopy. *Clinical Gastroenterology and Hepatology*, 2(4):348–352, 2004.
- [61] Robert E. Sedlack and Joseph C. Kolars. Computer Simulator Training Enhances the Competency of Gastroenterology Fellows at Colonoscopy: Results of a Pilot Study. *American Journal of Gastroenterology*, 99(1):33–37, 2004.

- [62] Neal E. Seymour, Anthony G. Gallagher, Sanziana A. Roman, Michael K. O'Brien, Vipin K. Bansal, Dana K. Andersen, and Richard M. Satava. Virtual Reality Training Improves Operating Room Performance: Results of a Randomized, Double-Blinded Study. *Annals of Surgery*, 236(4):458–464, 2002.
- [63] Paris F. Stringfellow, Sajay Sadasivan, Deepak Vembar, Andrew T. Duchowski, and Anand K. Gramopadhye. Task Analysis of Video Borescope Operation for Use in a Virtual Training Tool. In *Proceedings of Institute of Industrial Engineers Annual Conference*, 2005.
- [64] P. Ström, L. Hedman, L. Särnå, A. Kjellin, T. Wredmark, and L. Felländer-Tsai. Early Exposure to Haptic Feedback Enhances Performance in Surgical Simulator Training: A Prospective Randomized Crossover Study in Surgical Residents. *Surgical Endoscopy*, 20(9):1383–1388, 2006.
- [65] Deepak Vembar, Andrew T. Duchowski, Anand K. Gramopadhye, and Carl Washburn. Improving Simulated Borescope Inspection with Constrained Camera Motion and Haptic Feedback. In *Proceedings of Graphics Interface*, 2009.
- [66] Deepak Vembar, Andrew T. Duchowski, Sajay Sadasivan, and Anand K. Gramopadhye. A Haptic Virtual Borescope for Visual Engine Inspection Training. In *Proceedings of IEEE 3DUI*, 2008.
- [67] Deepak Vembar, Sajay Sadasivan, Andrew T. Duchowski, Paris F. Stringfellow, and Anand K. Gramopadhye. Design of a Virtual Borescope: A Presence Study. In *Proceedings of the 11th International Conference on Human-Computer Interaction*, Reno, NV, USA, Jul 2005. Lawrence Erlbaum Associates, Inc.
- [68] Christopher R. Wagner, Robert D. Howe, and Nicholas Stylopoulos. The Role of Force Feedback in Surgery: Analysis of Blunt Dissection. In *10th Symposium on Haptic Interfaces for Virtual Environment and Teleoperator Systems*, page 73, 2002.
- [69] Christopher R. Wagner, Nicholas Stylopoulos, Patrick G. Jackson, and Robert D. Howe. The Benefit of Force Feedback in Surgery: Examination of Blunt Dissection. *Presence: Teleoperators and Virtual Environments*, 16(3):252–262, 2007.
- [70] F. Wang, E. Burdet, A. Dhanik, T. Poston, and C. L. Teo. Dynamic thread for real-time knot-tying. In *WHC '05: Proceedings of the First Joint Eurohaptics Conference and Symposium on Haptic Interfaces for Virtual Environment and Teleoperator Systems*, pages 507–508, Washington, DC, USA, 2005. IEEE Computer Society.

- [71] Fei Wang, Lindo Duratti, Evren Samur, Ulrich Spaelter, and Hannes Bleuler. A Computer-Based Real-Time Simulation of Interventional Radiology. In *29th Annual International Conference of the IEEE Engineering in Medicine and Biology Society (IEEE-EMBS)*, 2007.
- [72] Bob G. Witmer and Michael J. Singer. Measuring Presence in Virtual Environments: A Presence Questionnaire. *Presence*, 7(3):225–240, 1998.
- [73] Mason Woo, Jackie Neider, Tom Davis, and Dave Shreiner. *OpenGL Programming Guide: The Official Guide to Learning OpenGL, Version 1.2*. Addison-Wesley Longman Publishing Co., Inc., Boston, MA, USA, 1999.
- [74] Y. Zhang, T. Fernando, H. Xiao, and A. Travis. Evaluation of Auditory and Visual Feedback on Task Performance in a Virtual Assembly Environment. *Presence: Teleoperators and Virtual Environments*, 15(6):613–626, 2006.
- [75] C.B. Zilles and J.K. Salisbury. A constraint-based god-object method for haptic display. *Proceedings. 1995 IEEE/RSJ International Conference on Intelligent Robots and Systems 95, 'Human Robot Interaction and Cooperative Robots'*, 3:146–151, Aug 1995.